Study On Quantum Properties Of Non-Gaussian States

Thesis submitted for the degree of

Doctor of Philosophy (Sc.)

In Physics (Theoretical)

by

Name : Priyanka Chowdhury

Department of Physics

University of Calcutta

2016

Dedicated To My Family Members

Abstract

The difficulties in experimental realization of perfect Gaussian states makes the use of non-Gaussian states more practical. Non-Gaussian states have a lot of importance in quantum foundations and also in quantum information processing tasks. This thesis points towards the fact that non-Gaussian states can be more non-local than Gaussian states. In the second chapter, we have shown the violation of the gravitational weak equivalence principle through the mass dependence of the experimentally measurable quantities and the violation increases with the degree of non-Gaussianity. In the third chapter, we have studied the non-locality of non-Gaussian states in classical optics due to the existence of higher order correlation terms. In the next chapter, we have shown that to detect nonlocal correlations of non-Gaussian states, say, steerability, one needs to choose appropriate steering criteria that are sensitive to higher order terms of non-Gaussian states. In the fifth chapter, we have introduced fine-grained uncertainty relation for continuous-variable systems. With the help of our derived uncertainty relation, we have formulated stronger steering criterion for continuous-variable systems. Finally, in the concluding chapter, we have briefly summarized the important results of our works.

Acknowledgements

List of Publications

Publications by the candidate forming part of the thesis:

- P. Chowdhury, T. Pramanik, and A. S. Majumdar, '*Stronger steerability criterion for more uncertain continuous-variable systems*', Physical Review A **92**, 042317 (2015).

- P. Chowdhury, T. Pramanik, A. S. Majumdar, and G. S. Agarwal, '*Einstein-Podolsky-Rosen steering using quantum correlations in non-Gaussian entangled states*', Physical Review A **89**, 012104 (2014).

- P. Chowdhury, A. S. Majumdar, and G. S. Agarwal, ' *Nonlocal continuous-variable correlations and violation of Bell's inequality for light beams with topological singularities*', Physical Review A **88**, 013830 (2013).

- P. Chowdhury, D. Home, A. S. Majumdar, S. V. Mousavi, M. R. Mozaffari and S. Sinha, '*Strong quantum violation of the gravitational weak equivalence principle by a non-Gaussian wave packet*', Class. Quantum Grav. **29** 025010 (2012).

Additional publications by the candidate relevant to the thesis but not forming part of it:

- T. Pramanik, P. Chowdhury, and A. S. Majumdar, '*Fine-grained lower limit of quantum uncertainty in the presence of quantum memory*', Physical Review Letters **110**, 020402 (2013).

Contents

List of Figures

List of Tables

Chapter 1

General introduction

In physical systems, correlations describe the covariations of one variable with another on average across space and time, and can be categorized in two different forms : classical correlation and quantum correlation. Classical correlation can be explained by the laws of classical physics. The other part, which can not be explained by the laws of classical physics is quantum correlation. Quantum correlations may be inherently probabilistic and nonlocal, whereas classical correlations can be described by local deterministic theories. One possible way to detect the existence of quantum correlations is through the violation of the gravitational weak equivalence principle for quantum systems.

Although quantum theory works mainly for atomic or subatomic particles, i.e., in microscopic scale, it may be extended to the macroscopic scale under suitable circumstances. The weak equivalence principle which is a famous property of classical systems is shown to be violated in the quantum domain. In some cases, classical properties of a particle will emerge in the macroscopic limit of quantum mechanics. As for example, the compatibility between the weak equivalence principle and the quantum mechanics is recovered in the macroscopic limit of the latter [Ali et al., 2006; Chowdhury et al., 2012].

From the practical point of view, in information theory quantum correlations have been used as resource in performing tasks that are unable to be achieved using classical means, leading to many interesting and important information-theoretic applications, such as dense coding, the violation of local uncertainty relation by nonlocal correlations, the sending of unknown quantum states at a distant location using finite resources in quantum teleportation, the generation of secret key

in quantum cryptography, better playoff of nonlocal games, i.e., Bell-CHSH game, etc. The different forms of uncertainty relations are one aspect of the conceptual difference between classical and quantum physics. However, the understanding of the exact difference between these two worlds is vital in learning how to perform different information processing tasks. Developments in quantum information theory for both discrete [Horodecki et al., 2009] as well as continuous variables [Weedbrook et al., 2012] have brought about the realization of subtle differences in various categories of correlations.

Among all the properties, nonlocality plays a key role in quantum theory. These non-classical, more specifically, nonlocal correlations can be categorised by three different forms, i.e., entanglement, steering and Bell-noncal correlations. For bipartite systems, steering is a kind of correlation, in the formulation of which at least one of the systems is being trusted as quantum system. In case of entanglement, both of the systems are being trusted as quantum, whereas in Bell nonlocal correlations, none of them needs to be trusted as quantum system. This leads to a hierarchy, in which entanglement is the weakest and Bell nonlocality is the strongest of the three form of correlations, and steering takes the intermediate position [Cavalcanti et al., 2009; Jones, Wiseman, and Doherty, 2007; Wiseman, Jones, and Doherty, 2007]. Bell nonlocal states constitute a strict subset of steerable states which, in turn, are a strict subset of entangled states. For the case of pure entangled states of two qubits, the three classes overlap.

1.1 Gravitational Weak Equivalence Principle

Starting from Newton's version of the equivalence principle which includes the universality of free fall (UFF), the development of the statement of the weak equivalence principle is an important foundation of the general theory of relativity. Any violation of the weak equivalence principle for quantum systems would require the development of new theoretical physics, especially the attempts to connect gravity with quantum mechanics.

1.1.1 The Principle of Equivalence

The traditional equivalence principle is fundamentally both classical and local, and it is interesting to enquire how it is to be understood in quantum mechanics. In the famous gedanken experiment conceived by Galileo, the universality of the ratio between the gravitational and inertial masses had been studied with test bodies in free fall from the leaning tower of Pisa [Galilei, 1638]. The principle of equivalence states about this equivalence between the inertial mass and the gravitational mass : $m_i \equiv m_g \equiv m$. With respect to the mechanical motion of particles, Einstein concluded that a state of rest in a sufficiently weak, homogeneous gravitational field is physically indistinguishable from a state of uniform acceleration in a gravity-free space. Einstein elevated this concept to become the Principle of Equivalence which is the foundation of the General Theory of Relativity. Quantum mechanically, this statement becomes [Bonse and Wroblewski, 1983], ' The laws of physics are the same in a frame with gravitational potential $V = -mgz$ as in a corresponding frame lacking this potential but having a uniform acceleration g instead'.

Several tests have been performed to show the validity of the equivalence principle with classical test bodies such as very sensitive pendula or torsion balances. Even for quantum mechanical particles, the validity of the principle is also proved using gravity-induced interference experiments [Colella, Overhauser, and Werner, 1975; Peters, Chung, and Chu, 1999].

1.1.2 The Weak Equivalence Principle of quantum mechanics

The other alternative form of equivalence principle states that when all sufficiently small test bodies fall freely, they acquire an equal acceleration independent of their mass or constituent in a gravitational field. To obtain quantum analogue of this statement, it might be replaced by some principle such as [Holland, 1993], ' The results of experiments in an external potential comprising just a sufficiently weak, homogeneous gravitational field, as determined by the wave function, are independent of the mass of the system'. This statement is known as weak equivalence principle of quantum mechanics (WEQ).

The most familiar tests of the weak equivalence principle are experiments of the Eötvös-type [Eötvös, 1890; Eötvös, Pekar, and Fekete, 1922], which measure the gravitational acceleration of macroscopic objects.

1.1.3 Violation of the Weak Equivalence Principle of quantum mechanics

The evidence of existence of quantum correlations will be given by the violation of WEQ through the mass dependence of an experimentally measurable quantity in gravitational field. The violation of WEQ can be shown both experimentally and theoretically. Experimental evidence exists in the interference phenomenon associated with the gravitational potential in neutron and atomic interferometry experiments [Colella, Overhauser, and Werner, 1975; Peters, Chung, and Chu, 1999]. Theoretically, for a particle bound in an external gravitational potential, it is seen that the radii, frequencies and binding energy depend on the mass of the bound particle [Greenberger, 1968, 1983; Greenberger and Overhauser, 1979]. Viola and Onofrio [Viola and Onofrio, 1997] have studied the free fall of a quantum test particle in a uniform gravitational field. They have made a rough estimation of the fluctuations around the mean value of time of flight, which is shown to be dependent on the mass of the particle. Another quantum mechanical approach of the violation of WEQ was given by Davies [Davies, 2004] using a model quantum clock [Peres, 1980]. In other examples [Ali et al., 2006; Chowdhury et al., 2012], the violation of WEQ is shown for smaller mass particles due to the existence of quantum correlations. It can also be shown the emergence of WEQ for larger mass particles in the classical limit.

1.2 Uncertainty relations

Uncertainty principle is one of the most fundamental and important physical properties of quantum mechanics [Deutsch, 1983; Heisenberg, 1927; Kraus, 1987; Maassen and Uffink, 1988; Robertson, 1929]. It gives a fundamental limit to the precision of measurement outcomes for the measurement of two noncommuting observables, say, position and momentum on the observed quantum system, though there are several interpretations of this limit. Even with perfect instruments and

techniques, the uncertainty is inherent in the nature. In the derivation of uncertainty relation, the correlation of the observed system with the other system called quantum memory is not considered. If this correlation is considered, the precision of measurement outcome can be increased for the measurement of two noncommuting observables [Berta et al., 2010; Li et al., 2011; Pramanik, Chowdhury, and Majumdar, 2013; Prevedel et al., 2011]. For example, if the observed system is in maximally entangled state with the quantum memory, the uncertainty can be reduced to zero. Uncertainty relation is one of the aspects, which introduces a sharp distinction between classical and quantum physics in the sense that classical system can be assigned with its complete state without disturbing the system, whereas quantum mechanics denies this possibility due to the presence of uncertainty relation. There are several uncertainty relations on the basis of different methods of uncertainty measurement.

1.2.1 Heisenberg uncertainty relation and its generalization

In 1927, Werner Heisenberg first introduced the famous uncertainty relation [Heisenberg, 1927], where standard deviation is used as a measure of uncertainty. Heisenberg uncertainty relation (HUR) states that the position and momentum of a microscopic particle can not be measured simultaneously with arbitrary precision, i.e., the more precisely the position of some particle is determined, the less precisely its momentum can be known, and vice versa. The formal inequality relating the standard deviation of position x and the standard deviation of momentum p was derived later by Kennard [Kennard, 1927] and Weyl [Weyl, 1928]. They proved that the inherent fluctuations of position and momentum are bounded by the Plank constant, which is mathematically given as

$$\Delta x \, \Delta p \;\; \geq \;\; \frac{\hbar}{2} \, , \tag{1.1}$$

where Δx and Δp are the standard deviations of position and momentum respectively. $\hbar \, (= \, h/2\pi \,)$ is the reduced Plank constant. The relation (1.1) is known as the famous Heisenberg uncertainty relation.

In 1929, Robertson [Robertson, 1929] generalized the inequality (1.1) for arbitrary observables. For the measurement of any pair of arbitrary noncommuting Hermitian operators, say, $\hat{A}$ and $\hat{B}$ on the system $\mathcal{S}$, Robertson modified the Heisenberg uncertainty relation as

$$\Delta\hat{A}\,\Delta\hat{B} \;\geq\; \frac{1}{2}\left|\langle[\,\hat{A},\hat{B}\,]\rangle_{\rho_{\mathcal{S}}}\right|, \tag{1.2}$$

where the uncertainty of measurement outcomes for the measurement of an observable $\hat{\mathcal{O}} \in \{\hat{A},\hat{B}\}$ is given in terms of standard deviation as

$$\Delta\hat{\mathcal{O}} \;=\; \sqrt{\langle\,\hat{\mathcal{O}}^2\,\rangle - \langle\,\hat{\mathcal{O}}\,\rangle^2}\,, \tag{1.3}$$

and $\langle\,\hat{\mathcal{O}}\,\rangle = \mathrm{Tr}\,[\,\rho_{\mathcal{S}}\,\hat{\mathcal{O}}\,]$ is the expectation value of the observable $\hat{\mathcal{O}}$ for the density state $\rho_{\mathcal{S}}$ of the system $\mathcal{S}$. The commutation relation is given by $[\,\hat{A},\hat{B}\,] := \hat{A}\,\hat{B} - \hat{B}\,\hat{A}$.

In 1930, Schrödinger [Schrödinger, 1930] further generalized the modified inequality (1.2) given by Robertson by adding a new term for quantum states for which the covariance of the two operators is non-zero and the generalized uncertainty relation is given by

$$(\Delta\hat{A})^2\,(\Delta\hat{B})^2 \;\geq\; \frac{1}{2}\left|\langle[\,\hat{A},\hat{B}\,]\rangle_{\rho_{\mathcal{S}}}\right| + \left(\frac{1}{2}\left|\langle\{\,\hat{A},\hat{B}\,\}\rangle_{\rho_{\mathcal{S}}}\right| - \langle\,\hat{A}\,\rangle_{\rho_{\mathcal{S}}}\langle\,\hat{B}\,\rangle_{\rho_{\mathcal{S}}}\right), \tag{1.4}$$

where the anticommutator $\{\,\hat{A},\hat{B}\,\} := \hat{A}\,\hat{B} + \hat{B}\,\hat{A}$. For quantum states with zero covariance of $\hat{A}$ and $\hat{B}$, this relation (1.4) reduces to Robertson's inequality (1.2). In this sense, it is more general and can be applied to any two observables of a large class of states of quantum systems.

Drawbacks :

The uncertainty relations, defined on the basis of standard deviations of the corresponding conjugate pair of dynamical variables are meaningful, only if both the standard deviations are finite. There are a number of interesting statefunctions, whose standard deviation diverges. In fact, the use of variance as a measure of uncertainty is quite limited. Uncertainty in terms of variance of an observable gives the average uncertainty, where the average is taken over all possible measurement outcomes of the observable. Another and most important drawback is

that both the lower limits of the inequalities (1.2) and (1.4) depend on he state of the quantum system.

1.2.2 Entropic uncertainty relations

To improve the drawbacks of the variance-based uncertainty relations and also to connect uncertainty with information-theoretic concepts, the uncertainty relating to the outcomes of observables has been reformulated by Everett [Everett, 1973] on the basis of information entropy. From the perspective of information theory, uncertainty is nothing but the deficiency of information. He concluded that the new relation is stronger than the variance-based relation, since it implies the former but is not implied by the former. The entropic uncertainty relation (EUR) involves sum of uncertainties measured in terms of Shannon entropy [Bialynicki-Birula and Mycielski, 1975] of noncommuting observables.

Deutsch [Deutsch, 1983] first introduced the entropic uncertainty relation for two observables. Later, the uncertainty relation was improved and the improved version is given by

$$\mathcal{H}(R) + \mathcal{H}(S) \;\geq\; \log_2 \frac{1}{c}, \tag{1.5}$$

which was first conjectured by Kraus [Kraus, 1987], and then proved by Maassen and Uffink [Maassen and Uffink, 1988]. Here, $\mathcal{H}(X) \, (= -\sum_i p_i \ln p_i)$ denotes the Shannon entropy of the probability distribution $\{p_i\}$ of the measurement outcomes of observable X ($X \in \{R, S\}$), p_i is the probability of the ith outcome of the observable, and $\frac{1}{c}$ quantifies the complementarity of the observable. For nondegenerate observables,

$$c = \max_{i,j} |\langle a_i | b_j \rangle|^2, \tag{1.6}$$

where $|a_i\rangle$ and $|b_j\rangle$ are eigenvectors of R and S respectively. The inequality (1.5) is a more general form of the uncertainty relation containing correlations in all orders of two observables of a discrete variable quantum system. In case of continuous variable systems for example using the position and momentum distribution of a quantum system, the entropic uncertainty principle first proposed by Bialynicki-Birula and Mycielski is given by [Bialynicki-Birula and Mycielski,

1975]

$$\mathcal{H}(X) + \mathcal{H}(P) \;\geq\; \ln \pi e \,. \tag{1.7}$$

The advantage of these uncertainty relations over the variance-based relations is that both the lower bounds of the inequalities (1.5) and (1.7) are independent of the state of the system.

Recently, Berta et al. [Berta et al., 2010] have shown that the lower bound of entropic uncertainty relation (1.5) can be improved in the presence of quantum memory. They generalized the uncertainty relation as

$$\mathcal{S}(R \,|\, B) + \mathcal{S}(S \,|\, B) \;\geq\; \log_2 \frac{1}{c} + \mathcal{S}(A \,|\, B) \,, \tag{1.8}$$

where $\mathcal{S}(R \,|\, B) = \mathcal{S}(\rho_{RB}) - \mathcal{S}(\rho_B) \,[\,\mathcal{S}(S \,|\, B)\,]$ is the conditional von Neumann entropy, which quantifies the uncertainty corresponding to the measurement $R\,(S)$ on the system A given information stored in the system B (i.e., quantum memory). $\mathcal{S}(\rho)$ is the von Neumann entropy with ρ_{RB} denoting the state after R measurement on subsystem A of ρ_{AB} and ρ_B denoting the reduced state of ρ_{RB}. $\mathcal{S}(A \,|\, B)$ quantifies the lower bound of the one-way distillable entanglement between Alice's system and Bob's system [Devetak and Winter, 2005].

Drawbacks :

As a measure of uncertainty, entropy gives average uncertainty of observables, where the average is again taken over all possible measurement outcomes of an observable similar to variance-based uncertainty. Entropic functions do not distinguish the uncertainty inherent in obtaining any combination of outcomes for different measurements.

1.2.3   Fine-grained uncertainty relation

To overcome the drawbacks of the uncertainty relations obtained in coarse-grained way, where all the measurement outcomes of an observable are considered and to capture the full nonlocal strength by quantum physics, Oppenheim and Wehner [Oppenheim and Wehner, 2010] have introduced a completely different and new form of the uncertainty relation known as fine-grained uncertainty relation (FUR). Here, uncertainty is measured for a particular measurement outcome or some

combination of outcomes to win a particular nonlocal game. The winning condition is the essence of fine graining and every game gives rise to an uncertainty relation, and vice versa. In discrete-variable systems, fine-grained uncertainty relation is the strongest one.

In Ref.[Oppenheim and Wehner, 2010], Oppenheim and Wehner have considered games for both the single qubit case and the bipartite case. In the single-qubit system, a FUR can be described by the following game, where Alice is considered to receive a binary question $s \in \{0, 1\}$ with the probability $p(s) = \frac{1}{2}$. When she receives the question $s = 0$ ($s = 1$), Alice measures σ_z (σ_x) observable on her state ρ_A. She gets outcome a_s, where $a_s \in \{0, 1\}$. Alice wins the game if she gets a particular outcome a_s for both the questions $s = 0$ and $s = 1$. The winning probability of the above game is given by

$$
\begin{aligned}
P^{\text{game}} &= \sum_s p(s)\, p(a_s)_{\rho_A} \\
&\leq P^{\text{game}}_{\text{max}} = \max_{\rho_A} P^{\text{game}},
\end{aligned}
\tag{1.9}
$$

where $p(a_s)$ is the probability of obtaining a particular outcome a_s for the measurement corresponding to the question s on the state ρ_A. $P^{\text{game}}_{\text{max}}$ is the maximum winning probability over all possible strategies, i.e., the choice of the single-qubit state ρ_A in this game. For spin-up outcome (i.e., $a_s = 0$), $P^{\text{game}}_{\text{max}} = \frac{1}{2} + \frac{1}{2\sqrt{2}}$ occurs for the eigenstates of $(\sigma_x + \sigma_z)/\sqrt{2}$. For the spin-down winning condition (i.e., $a_s = 1$), we achieve the same maximum winning probability using eigenstates of $(\sigma_x - \sigma_z)/\sqrt{2}$. These are known as maximally certain states.

For the bipartite case, authors have considered a game according to which Alice and Bob both receive binary questions, i.e., projective spin measurements along two different directions at each side. For this case if ρ_{AB} is a bipartite state shared between Alice and Bob, the winning probability is given by the relation

$$
\begin{aligned}
P^{\text{game}}(\mathcal{T}_A, \mathcal{T}_B, \rho_{AB}) &= \sum_{t_A, t_B} p(t_A, t_B) \sum_{a,b} V(a, b\,|\, t_A, t_B)\, \langle (A^a_{t_A} \otimes B^b_{t_B}) \rangle_{\rho_{AB}} \\
&\leq P^{\text{game}}_{\text{max}},
\end{aligned}
\tag{1.10}
$$

where $\mathcal{T}_A$ and $\mathcal{T}_B$ represent the set of measurement settings $\{t_A\}$ and $\{t_B\}$ chosen by Alice and Bob, respectively, with probability $p(t_A, t_B)$. Alice and Bob receive their binary question t_A and t_B, and their outcomes are a and b,

respectively, with

$$
\begin{aligned}
A^a_{t_A} &= \frac{1}{2}\left[I + (-1)^a A_{t_A}\right], \\
B^b_{t_B} &= \frac{1}{2}\left[I + (-1)^b B_{t_B}\right]
\end{aligned}
\tag{1.11}
$$

being a measurement of the observable A_{t_A} and B_{t_B}, respectively. Here, $V(a, b \,|\, t_A, t_B)$ is some function determining the winning condition of the game. The winning condition corresponding to a special class of nonlocal retrieval games (CHSH game) for which there exists only one winning answer for one of the two parties, is given by $V(a, b \,|\, t_A, t_B) = 1$, if and only if $a \oplus b = t_A \cdot t_B$, and 0 otherwise. $P^{\text{game}}_{\text{max}}$ is the maximum winning probability of the game, i.e.,

$$
P^{\text{game}}_{\text{max}} = \max_{\mathcal{T}_A, \mathcal{T}_B, \rho_{AB}} P^{\text{game}}(\mathcal{T}_A, \mathcal{T}_B, \rho_{AB}).
\tag{1.12}
$$

Using the maximum winning probability it is possible to discriminate among classical theory, quantum theory, and no-signaling theory with the help of the degree of nonlocality [Oppenheim and Wehner, 2010]. Later, it has been generalized for the tripartite systems [Pramanik and Majumdar, 2012]. Fine-grained uncertainty relation also provides an optimal lower bound of entropic uncertainty in presence of quantum memory [Pramanik, Chowdhury, and Majumdar, 2013]. Recently, fine-grained uncertainty relation is derived for continuous variable systems [Chowdhury, Pramanik, and Majumdar, 2015] and is demonstrated in the Chapter 5.

1.2.4   Applications

The presence of uncertainty relations endows quantum mechanics with significant advantages over classical mechanics for performing different information processing tasks. Various versions of uncertainty relations have been used to detect entanglement [Biswas and Agarwal, 2005; Gillet, Bastin, and Agarwal, 2008; Nha, 2007; Simon, 2000; Wehner and Winter, 2010], to classify mixedness of states [Mal, Pramanik, and Majumdar, 2013], to categorize different physical theories according to their strength of nonlocality [Dey, Pramanik, and Majumdar, 2013; Oppenheim and Wehner, 2010; Pramanik and Majumdar, 2012], and to bound information leakage in key distribution [Berta et al., 2010; Branciard et al., 2012; Devetak and Winter, 2005; Furrer et al., 2012; Grosshans and Grangier, 2002; Pramanik,

Chowdhury, and Majumdar, 2013; Pramanik, Kaplan, and Majumdar, 2014; Renes and Boileau, 2009; Tomamichel and Renner, 2011].

1.3 EPR paradox

At the advent of quantum mechanics, a point of view of quantum mechanics arose differentiating it from the classical view point. According to this view point [Nielsen and Chuang, 2000], an unobserved particle does not possess physical properties that exist independent of observation, unless otherwise an appropriate measurement is performed upon the system. For example, according to quantum mechanics a qubit does not possess definite properties of σ_z and σ_x observables, the spins in the z and x directions respectively, each of which can be revealed with certain probabilities for the possible measurement outcomes after performing the appropriate measurement on the observables. The most prominent objector was Albert Einstein. In 1935, Einstein in his famous 'EPR paper' [Einstein, Podolsky, and Rosen, 1935], in collaboration with Boris Podolsky and Nathan Rosen, proposed a thought experiment demonstrating that quantum mechanics is not a complete theory of Nature. They emphasized that any physical theory of nature must be complete if it includes 'elements of reality'. The way they attempted to do the thought experiment was by introducing two assumptions,

1. *Reality : If it is possible to predict with certainty (i.e., with probability 1) the value of a physical quantity of a system, without in any way disturbing the system, i.e., without performng any actual measurements, then there exists an element of reality corresponding to that physical quantity.*

2. *Locality : Performing a measurement on one system can not have any influence on the result of measurements on the other.*

These two assumptions together are known as the assumptions of *local realism.*

For example, a singlet state is shared between an entangled pair of qubits belonging to Alice and Bob, respectively. The singlet state is given by

$$| \psi \rangle = \frac{| 01 \rangle - | 10 \rangle}{\sqrt{2}} . \tag{1.13}$$

They are assumed to be far enough apart from each other and they perform their measurements simultaneously. Now, if Alice measures σ_z observable on her qubit and gets spin up outcome, then she can predict with certainty (probability 1) what

will be the Bob's measurement outcome if he would measure the same observable on his qubit. So, Alice can predict that Bob will get spin down outcome. Again, if she obtains spin down outcome, Bob's outcome will be spin up. Therefore, σ_z is the element of reality as it is possible to predict the certain value of this observable, immediately before the measurement on Bob's qubit. Similarly, σ_x is also an element of reality, for which both the observables σ_z and σ_x can be measured simultaneously with arbitrary precision for Bob's system. This phenomenon, which contradicts the uncertainty relation given by Heisenberg [Heisenberg, 1927], appears as a paradox. According to the uncertainty relation, σ_z and σ_x are two noncommuting observables. So, they can not be measured simultaneously with arbitrary precision. This paradox is known as EPR paradox. But Einstein did not challenge the uncertainty relation. EPR wanted to show that the quantum mechanical description of physical reality given by wave functions is incomplete, by demonstrating that quantum mechanics lacked some essential element of reality, by their criterion.

EPR explained the paradox as the information about the outcome of all possible measurements was already present in both particles. Also the more complete theory contains variables corresponding to all the elements of reality. So, there were some 'hidden variables', which encoded that information. Then they concluded that quantum mechanics was incomplete since its formalism does not permit hidden variables. In 1964, John Bell [Bell, 1964] showed that quantum mechanics and the class of hidden variable theories Einstein favoured (local hidden variable theory) would lead to different experimental results. There are many experiments to test Bell's theorem, e.g., those of A. Aspect and others [Aspect, Dalibard, and Roger, 1982; Aspect, Grangier, and Roger, 1981, 1982]. They support the predictions of quantum mechanics rather than the local hidden variable theories supported by Einstein. Realist interpretation of quantum mechanics must reject either locality or realism.

1.4 Classification of entanglement

In EPR paradox [Einstein, Podolsky, and Rosen, 1935], it appears that one particle somehow knows what measurement has been performed on the other particle, and with what outcome, even though there is no known means for communication of such information between the particles. The word 'entanglement' was first

coined by Schrödinger [Schrödinger, 1935, 1936] to describe the property of such spatially separated but quantum mechanically correlated particles. Entanglement is a physical phenomenon which occurs in quantum domain. If a pairs or groups of particles are entangled, then each particle can not be fully described by quantum mechanics without considering the other.

Quantum systems can become entangled through various types of interactions such as using spontaneous parametric down conversion, fiber coupler, quantum dots, entanglement swapping etc. Even though two particles are presently not interacting (interacted once before) and also remote from one another, then they still may be entangled if their shared state can not be written as the mixture of product of the states of individual subsystems. Entanglement is broken through the interaction of the entangled particles with the environment (decoherence).

There are two types of entangled states : pure entangled and mixed entangled. For the bipartite case, let us consider two particles A and B associated with finite dimensional Hilbert spaces H_A and H_B, respectively. The state space of the composite system is given by the tensor product $H = H_A \otimes H_B$.

1.4.1 Pure entangled states

Consider, $|\psi\rangle\,(\in H_A \otimes H_B)$ be the pure state of the composite system, and $|\psi\rangle_A$ and $|\psi\rangle_B$ are that of the subsystems A and B, respectively. $|\psi\rangle$ is said to be separable state, if it can be written in the form

$$|\psi\rangle = |\psi\rangle_A \otimes |\psi\rangle_B. \tag{1.14}$$

When the composite pure state can not be written in this form, i.e., in the form of the product of individual states of subsystems, it is called entangled state. When a pair of systems share an entangled pure state, it is not possible to assign states to individual systems. In general, a bipartite pure state is entangled if and only if its reduced states are mixed rather than pure. The more uncertainty statistically will cause larger entropy. So, the zero entropy of a composite pure state indicates that there is no uncertainty about a system in pure state, whereas the entropy of each subsystem of the composite system gives maximum entropy for 2×2 mixed states.

For the case of multipartite system, let a composite system, consisting of n subsystems has state space $H = H_1 \otimes .... \otimes H_n$. A pure state $|\psi\rangle\,(\in H)$ is said to be entangled if

$$|\psi\rangle \;\neq\; |\psi\rangle_1 \otimes .... \otimes |\psi\rangle_n\,, \tag{1.15}$$

where $|\psi\rangle_i$ is a pure state of the i-th subsystem.

1.4.2 Mixed entangled states

Let us consider bipartite mixed state case. A mixed state of the composite system is described by density matrix ρ acting on the Hilbert space of the composite system, $H = H_A \otimes H_B$. When there is less than total information about the state of a quantum system, we need density matrices to represent the state. The density matrix of a pure state $|\phi\rangle$ is described by the outer product, $\rho_\phi = |\phi\rangle\langle\phi|$. For separable mixed states, ρ can be written as

$$\rho \;=\; \sum_k p_k\, \rho_A^k \otimes \rho_B^k\,, \tag{1.16}$$

where $p_k \geq 0$ and $\sum_k p_k = 1$, $\{\rho_A^k\}$ and $\{\rho_B^k\}$ are the pure ensembles of the respective subsystems. It is clear from the definition that the family of separable states is a convex set. ρ is said to be entangled if it can not be written in the form given above, i.e., it can not be written as the mixture of product states of individual systems. A mixed state with rank 1 describes a pure ensemble.

For a multipartite system consisting of n subsystems, a mixed state ρ acting on the state space $H\,(= H_1 \otimes .... \otimes H_n)$ of the composite system is said to be entangled if

$$\rho \;\neq\; \sum_k p_k\, \rho_1^k \otimes .... \otimes \rho_n^k\,, \tag{1.17}$$

where ρ_i^k is the pure ensemble of i-th subsystem.

1.4.3   Applications

Entanglement has many applications in quantum information-processing tasks that can not be achieved by any other means. Superdense coding and quantum teleportation are two important applications of entanglement. Technologies relying on quantum entanglement are now being developed. In quantum cryptography, entangled particles are used to transmit signals that can not be eavesdropped upon without leaving a trace. In quantum computation, entangled quantum states are used to perform computations in parallel, which may allow certain calculations to be performed much more quickly than they ever could be with classical computers.

1.5   Classification of steering

In the pioneering work of Einstein, Podolsky and Rosen (EPR) [Einstein, Podolsky, and Rosen, 1935], EPR argued that the quantum mechanical description of the state of a particle is not complete, when one considers a position-momentum correlated state of two particles, and assumes the notions of spatial separability, locality, and reality to hold true at the level of quantum particles. This is arguably a paradoxical feature of quantum mechanics and is well known as EPR paradox. An immediate consequence of correlations between spatially separated particles was then noted by Schrödinger [Schrödinger, 1935, 1936] in that it allowed for the control of the state on one side merely by the choice of the measurement basis on the other side without in any way having direct access to the affected particle. So, the EPR paradox was reexpressed as the possibility of steering by Schrödinger. This is also known as EPR steering.

Uncertainty relations are linked directly to the ability of quantum states to enable steering. Starting with the Heisenberg uncertainty relation, a number of improved uncertainty relations have been provided [Bialynicki-Birula and Mycielski, 1975; Maassen and Uffink, 1988; Oppenheim and Wehner, 2010; Robertson, 1929; Schrödinger, 1930; Wehner and Winter, 2010]. Again, stronger steering criteria are built up with the help of stronger uncertainty relations. To capture steering of an entangled state, one needs to built up some steering inequalities using uncertainty relations.

1.5.1 The Reid criterion for steering

The phenomenon of quantum steering [Schrödinger, 1935, 1936] emerging from the EPR paradox [Einstein, Podolsky, and Rosen, 1935] was first formulated by Reid for experimental realization [Reid, 1989]. She proposed the EPR steering criterion for continuous variable systems based on the position-momentum Heisenberg uncertainty relation, in terms of an inequality involving products of inferred variances of incompatible observables. For two conjugate observables $\hat{X}_1$ and $\hat{X}_2$, which are noncommuting, the Reid inequality is given by

$$(\Delta_{\text{inf}} \hat{X}_1)^2 (\Delta_{\text{inf}} \hat{X}_2)^2 \geq 1 , \tag{1.18}$$

where $\Delta_{\text{inf}} \hat{X}_i$ is the variance of the inferred observables $\hat{X}_i$ $[i \in \{1, 2\}]$. For a given bipartite entangled state, the violation of the above inequality will give the EPR steering of that state. Ou et al. [Ou et al., 1992] gave an experimental demonstration of the EPR paradox for the case of two spatially separated and correlated light modes. The EPR criterion has been used to demonstrate the steerability of two mode squeezed vacuum states [Steinlechner et al., 2013] experimentally and entanglement in Bose-Einstein condensates, as well [He et al., 2012, 2011; Opanchuk et al., 2012]. Other works have shown that the Reid inequality is effective in giving demonstration of the EPR paradox for systems in which correlations appear at the level of variances.

Drawback :

The steerability of the states having correlations higher than the second order remains unable to be captured by the Reid criterion for EPR steering, although the Bell nonlocal correlation for that states may be exhibited [Chowdhury et al., 2014; Walborn et al., 2011]. In Chapter 4, the failure of the Reid criterion is demonstrated for some non-Gaussian states.

1.5.2 The entropic steering criterion

To improve the situation produced by the Reid criterion for EPR steering and to derive more stronger steering inequality, in terms of an information-theoretic task Walborn et al. [Walborn et al., 2011] have introduced a new steering criterion

on the basis of more general entropic uncertainty relation proposed by Bialynicki-Birula and Mycielski [Bialynicki-Birula and Mycielski, 1975]. Entropic functions by definition incorporate correlations up to all orders. They have considered that the measurements correspond to either position or momentum. For steerable states, correlations between the measurement outcomes of Alice and Bob can not be explained by a local hidden state (LHS) model. So, for continuous variable systems, the entropic steering inequality can be written as the sum of conditional Shannon entropies [Walborn et al., 2011]

$$h\left(X_B \,|\, X_A\right) + h\left(P_B \,|\, P_A\right) \;\geq\; \ln \pi e \,, \tag{1.19}$$

where X_A, X_B are the correlated positions and P_A, P_B are the correlated momenta of the particles possessed by Alice and Bob, respectively. The EPR steering criterion (1.18) derived by Reid [Reid, 1989] can be obtained as a limiting case of the entropic steering criterion (1.19). The new criterion can be used to show steerability not only for Gaussian states having correlations upto second order but also for pure entangled non-Gaussian states [Walborn et al., 2011], for which Reid criterion fails to detect steerability. Since entanglement is a weaker form of correlations compared to steering [Cavalcanti et al., 2009; Wiseman, Jones, and Doherty, 2007], it is clear that for such entangled non-Gaussian states the steering correlations appear at the level of higher than the second order (variances). Therefore, the criterion (1.19) is more sensitive than the Reid criterion (1.18). Chapter 4 includes the steerability of some class of entangled non-Gaussian states through the entropic steering criterion [Chowdhury et al., 2014].

For discrete variable systems, the lower bound of the entropic steering inequality (1.19) will be changed according to the discrete version of the entropic uncertainty relation given by the inequality (1.5). In terms of conjugate pairs of discrete variables $\{R_A, S_A\}$ and $\{R_B, S_B\}$, the entropic steering inequality can be written as [Schneeloch et al., 2013]

$$\mathcal{H}\left(R_B \,|\, R_A\right) + \mathcal{H}\left(S_B \,|\, S_A\right) \;\geq\; \log_2 \frac{1}{c \,|\, _B} \,, \tag{1.20}$$

Here, the correlations exist between R_A and R_B (S_A and S_B), and $c \,|\, _B$ is the value of c given by the Eq.(1.6) associated with the observables of Bob's system. The steerability is to be shown through the violation of the steering inequalities (1.19) and (1.20).

Drawback :

Although entropic steering criterion overcomes the drawbacks of Reid criterion for steering, it has also some drawbacks itself. In continuous variable systems, there are some non-Gaussian states like NOON states, for which entropic steering criterion detects steerability only with $N = 1$ [Chowdhury et al., 2014]. But for $N \geq 2$, these states are not steerable through the entropic criterion in spite of violating Bell-type inequalities for all N [Bell, 1964; Clauser et al., 1969; Wildfeuer, Lund, and Dowling, 2007]. So, NOON states should be steerable for all values of N since steering lies between entanglement and nonlocality in the hierarchy [Wiseman, Jones, and Doherty, 2007] of quantum correlations.

1.5.3 The fine-grained steering criterion

The tightest steering inequality in discrete variable systems is obtained [Pramanik, Kaplan, and Majumdar, 2014] through the application of the fine-grained uncertainty relation (FUR), first proposed by Oppenheim and Wehner [Oppenheim and Wehner, 2010]. Fine-graining makes it possible to distinguish the uncertainty inherent in obtaining any particular combination of outcomes for different measurements. They bound an event corresponding to win a nonlocal retrieval game considered between Alice and Bob by its minimum possible uncertainty, or maximum possible certainty, for two incompatible observables. In discrete variable systems, fine-grained uncertainty relation given by the inequality (5.3) is the strongest uncertainty relation. If the combined state between Alice and Bob is steerable, Alice's measurement outcome a for the measurement chosen randomly from the set $\mathbb{A} \in \{\mathcal{S}, \mathcal{T}\}$ and Bob's measurement outcome b for the measurement chosen randomly from the set $\mathbb{B} \in \{\mathcal{P}, \mathcal{Q}\}$ can not be written in terms of local hidden state (LHS) model. So, For discrete variable systems, the fine-grained steering inequality is given by the sum of conditional probabilities [Pramanik, Kaplan, and Majumdar, 2014]

$$P\left(b_{\mathcal{P}} \,|\, a_{\mathcal{S}}\right) + P\left(b_{\mathcal{Q}} \,|\, a_{\mathcal{T}}\right) \;\; > \;\; 1 + \frac{1}{\sqrt{2}}, \qquad\qquad (1.21)$$

where Alice has prior knowledge of Bob's measurement settings. The steerable states must satisfy the inequality (1.21). The new steering inequality (1.21) improves over previous ones since it can experimentally detect all steerable two-qubit

Werner state considering only two measurement settings on each side and it is also able to show that pure entangled states are maximally steerable as well [Pramanik, Kaplan, and Majumdar, 2014] .

For continuous variable systems, the improved version of steering criterion over the inability of the entropic criterion to show the steerability of NOON states for $N \geq 2$ is introduced in Chapter 5 based on newly derived fine-grained uncertainty relation using continuous variables [Chowdhury, Pramanik, and Majumdar, 2015].

1.6   Bell nonlocality

Inspired by the early works of EPR and Schrödinger, Bell was the first who proposed a new formalism [Bell, 1964; Clauser et al., 1969] for quantifying the correlations in terms of joint measurements of observables corresponding to two spatially separated particles for the case of any general theory obeying the tenets of locality and realism, and derived Bell's inequality. Bell's theorem brings a compelling example of an essential difference between quantum and classical physics. It states that any physical theory of local hidden variables can not reproduce all the predictions of quantum mechanical theory.

To obtain Bell's inequality, it is considered that Charlie prepares a pair of particles A and B in a combined state ρ_{AB}. He sends particle A to Alice and particle B to Bob. He repeats this process many times. After receiving her particle, Alice could choose to measure randomly one of two different observables labelled by $\mathcal{A}_1$ and $\mathcal{A}_2$. Similarly, Bob is capable of measuring randomly one of two different observables $\mathcal{B}_1$ and $\mathcal{B}_2$. The measurement of each observable has dichotomic outcomes yielding either the value $+1$ or -1. It is assumed that Alice and Bob are far enough apart from each other and perform their measurements simultaneously. Therefore, performing a measurement on one system can not have an influence on the result of measurements on the other system since any physical influence can not propagate faster than light. Considering these, Bell's inequality is given by

$$|\langle \mathcal{A}_1 \otimes \mathcal{B}_1 \rangle + \langle \mathcal{A}_1 \otimes \mathcal{B}_2 \rangle + \langle \mathcal{A}_2 \otimes \mathcal{B}_1 \rangle - \langle \mathcal{A}_2 \otimes \mathcal{B}_2 \rangle| \; \leq \; 2 \, . \quad (1.22)$$

This is also known as Bell-CHSH inequality [Clauser et al., 1969]. The above inequality is upper bounded by 2 under local hidden variable (LHV) theory. Bell-nonlocal correlations are those for which at least any Bell's inequality is violated

indicating nonexistence of LHV model. In deriving Bell's inequality, quantum mechanics is not considered at all, only probability theory is invoked. So, Bell-nonlocal correlations are the strongest one in quantum mechanics. As for example [Nielsen and Chuang, 2000], we consider that Alice and Bob share singlet state given by the Eq.(1.13), which is maximally entangled state. If they perform measurements of the following observables :

$$\mathcal{A}_1 = Z_1 \qquad\qquad \mathcal{A}_2 = X_1$$

$$\mathcal{B}_1 = \frac{-Z_2 - X_2}{\sqrt{2}} \qquad\qquad \mathcal{B}_2 = \frac{Z_2 - X_2}{\sqrt{2}}, \qquad (1.23)$$

the value of the Bell sum will become $2\sqrt{2}$, which is the maximum Bell violation in quantum mechanics. So, quantum mechanics does not allow LHV theory. It turns out that Nature experimentally agrees with quantum mechanics. To derive his famous inequality, Bell considered two assumptions, which are 1) Reality and 2) Locality. Therefore, at least one of the assumptions is violated by quantum mechanics. It is possible to infer that violation of Bell's inequality is due to the presence of nonlocal character of quantum mechanics known as "quantum entanglement". Bell's inequality was shown to be violated in quantum mechanics in several subsequent experiments [Aspect, Dalibard, and Roger, 1982; Aspect, Grangier, and Roger, 1981, 1982].

1.7 The utility of the Wigner function in continuous-variable systems

Quasiprobability distributions are mathematical objects, which satisfy several general features of ordinary probability distributions. Quasiprobability distributions arise naturally to study the phase space representation of quantum mechanics on top of the operator mechanics and are commonly used in quantum optics, time-frequency analysis [Cohen, 1995], and elsewhere. In this representation, the expectation values and probabilities of physical quantities are evaluated by rules of the classical statistics. In contradiction to the ordinary probabilities, some quasiprobability distributions have regions of negative probability density. When

the density operator is represented in a diagonal form, i.e., with respect to an over-complete basis, then it can be written in a way more like an ordinary function, at the expense that the function has the features of a quasiprobability distribution, evolution of which completely determines the evolution of the system.

There exists a family of different quasiprobability distributions, depending on different operator orderings. The most important of these in the general physics literature is the Wigner quasiprobability distribution [Wigner, 1932] introduced by E. P. Wigner in 1932, which is related to symmetric operator ordering given by the Weyl transform. In constructing the possible phase-space distribution, he had to give up the positivity property of the distribution for states, which have no classical model. Thus the Wigner distribution could be negative, which is a convenient indicator of quantum mechanical interference. The formalism of Wigner theory demonstrates an autonomous description of the quantum world. The Wigner function, which yields the correct marginal distributions for a quantum system, is in one hand the phase space counterpart of the density matrix and the quantum counterpart of the classical distribution function on the other hand. Both states and observables are represented by functions of the phase space coordinates. This function is very useful in a variety of fields as it always exists but remarkably used in quantum optics, particularly in the characterization and visualization of nonclassical fields.

The fully symmetric Weyl order contains some of the basic properties of a characteristic function of a probability distribution [Tatarskii, 1983]. So, the Wigner quasiprobability distribution can be written in terms of characteristic function, from which all quantum mechanical expectation values can be derived. Also, it is well known that a probability distribution is nothing but the Fourier transform of the characteristic function. Therefore, the Wigner function is defined as

$$W(\alpha) \;=\; \frac{1}{\pi^2} \int d^2\beta \; \mathrm{Tr}\,[\,\rho\,D(\beta)\,]\,\exp\,[-(\,\beta\,\alpha^* - \beta^*\,\alpha\,)\,], \qquad (1.24)$$

which is a two-dimensional Fourier transform of the quantum mechanical characteristic function

$$\mathrm{Tr}\,[\,\rho\,D(\beta)\,] \;=\; \langle\,D(\beta)\,\rangle,$$
$$D(\beta) \;=\; \exp\,[\,\beta\,a^\dagger - \beta^*\,a\,]. \qquad (1.25)$$

Here, $D(\beta)$ is the displacement operator for the complex phase-space displacement β, and a and $a^\dagger$ are the annihilation and creation operators, respectively with the commutation relation $[a, a^\dagger] = 1$. ρ is the density matrix of the respective quantum system. The Wigner function should be normalised, i.e.,

$$\int W(\alpha)\, d^2\alpha \;=\; 1\,. \tag{1.26}$$

This is a real, square integrable function and also remains bounded.

Banaszek and Wodkiewicz [Banaszek and Wodkiewicz, 1998, 1999] have used the two mode Wigner function instead of joint probability to derive the Bell like inequality in continuous variable systems. This becomes possible because they were able to express the Wigner function as an expectation value of a product of displaced parity operators and the parity plays the same role as spin-1/2 observables in discrete variable systems due to the property of getting dichotomic outcomes of both the observables.

In addition to the Wigner representation of phase-space defined above, there are many other quasiprobability distributions that arise in alternative representations of the phase space distribution, e.g., Glauber P, Husimi Q distributions. These representations are all interrelated to each other.

1.8 Quantum cryptography and quantum key distribution protocols

Quantum cryptography is the study to perform cryptographic tasks, i.e., the techniques for secure communication of encrypted messages in presence of third party by exploiting quantum mechanical properties. The advantage of quantum cryptography lies in the fact that it allows the completion of various cryptographic tasks that are impossible to be performed using only classical communication. The best known and developed application of this is quantum key distribution, which offers an information-theoretic secure solution to the key exchange problem.

Quantum key distribution (QKD) uses quantum mechanics to guarantee secure communication. In quantum key distribution protocol, the two communicating users, Alice and Bob share a random secret key, which remains unknown to any

third party, say, Eve trying to gain the knowledge of the key. This is achieved by Alice encoding the bits of the key as quantum data and sending them to Bob. The fundamental aspect of quantum mechanics says that the measurement on a quantum state in general changes the state except for the eigenstates of a system. Therefore, the very act of reading the data encoded in a quantum state by Eve must in some way measure it, introducing detectable anomalies. This will make Alice and Bob able to detect the presence of an eavesdropper. This is an important and unique property of QKD. The secret key can be used to encrypt messages by the sender (Alice) and decrypt messages by the receiver (Bob).

If the level of eavesdropping is below a certain threshold, a key can be produced that is guaranteed to be secure, i.e., the eavesdropper has no information about it, otherwise no secure key is possible and communication is aborted. In contradiction with the classical key distribution, the security of QKD can be proven mathematically without imposing any restrictions on the abilities of an eavesdropper. This is usually described as unconditional security, although there are some minimal assumptions required including that the laws of quantum mechanics apply and that Alice and Bob are able to authenticate each other.

Quantum key distribution is only used to produce and distribute a key, not to transmit any message data. This key can then be used with any chosen encryption algorithm to encrypt (and decrypt) a message, which can then be transmitted over a standard communication channel.

QKD exploits certain properties of information-encoded quantum states to ensure its security. There are two main categories of QKD depending on which property they exploit : prepare and measure protocols, and entanglement based protocols. The examples of both the protocols described below use discrete variable coding. Each of these two approaches can be further divided into three families of protocols: discrete variable, continuous variable and distributed phase reference coding. Among them, discrete variable protocols are the most widely implemented. The other two families are mainly concerned with overcoming practical limitations of experiments.

1.8.1   Prepare and measure protocols

This is based on quantum indeterminacy (i.e., measuring an unknown quantum state changes that state in some way), which underlies the results of Heisenberg uncertainty principle, information-disturbance theorem and no cloning theorem. This property can be used as a resource to detect eavesdropping if any and to calculate the amount of information that has been intercepted. The example of this type of protocols is BB84 protocol, which is first proposed by Bennet and Brassard in 1984 [Bennett and Brassard, 1984], and which is described below.

BB84 Protocol :

Assume that Alice and Bob wish to exchange a message securely. Alice initiates the message by sending Bob a secret key, which will be the mode for encrypting the message data. Eve has the objective to obtain some information about this secret key. Consider that Alice and Bob have access to a noiseless quantum channel and also a classical authenticated channel. Eve can act freely on the quantum channel as she has total access to the quantum channel, keeping in mind that she would be able neither to duplicate the quantum information (No-Cloning theorem) nor to measure a quantum state completely (Heisenberg uncertainty relation). But she can only listen to what happens on the classical channel, which makes her impossible to modify the information sent through the classical channel.

Alice chooses a random measurement basis from $\mathcal{B}_0$ and $\mathcal{B}_1$ given by

$$\mathcal{B}_0 = \{\,|0\rangle, |1\rangle\,\} \quad \text{and} \quad \mathcal{B}_1 = \left\{ \frac{|0\rangle + |1\rangle}{\sqrt{2}}, \frac{|0\rangle - |1\rangle}{\sqrt{2}} \right\}, \qquad (1.27)$$

which are σ_z and σ_x bases, respectively and also chooses a bit at random from $\{0, 1\}$. If the bit is 0, she sends the first state of her bases to Bob, if it is 1 she sends the second state of her bases. She repeats this procedure N times and sends the N resulting states to Bob.

After receiving all the states, Bob measures them randomly either in $\mathcal{B}_0$ or in $\mathcal{B}_1$ basis. He obtains N bits string, known as raw key after performing measurements on N states. Next, Alice and Bob announce their individual measurement basis through the classical communication channel but not the results they obtained.

When both the bases match with each other, they keep the corresponding bit of their string. When they differ, they discard the corresponding bit. Therefore, they obtain a string of n bits, which is smaller than N ($n < N$) that they agree on (called the sifted key). This is the secret key shared between Alice and Bob. Whenever Eve introduces errors to know about the key, Alice and Bob can notice it easily as their respective sifted key would differ, so that any subsequent communication making use of it to encrypt and decrypt messages would fail.

The goal of this protocol is to make sure that the knowledge of Eve about a secret key shared between Alice and Bob is very small. So, with high probability, either Alice and Bob will agree on a key about which Eve's knowledge is very small, or Alice and Bob will decide to abort the key and try again, possibly with a different quantum channel as the security of the key can not be guaranteed. In order to bound Eve's knowledge about their secret key, Alice and Bob can apply a Privacy Amplification scheme [Bennett et al., 1995; Deutsch et al., 1996].

1.8.2 Entanglement based protocols

For an entangled state, measurement on one object affects the other. If Alice and Bob share an entangled state, anyone intercepting either object alters the overall system, revealing the presence of the third party and the amount of intercepted information. Here, entanglement can be used as a resource. The example of this type of protocols is E91 protocol, which is described below.

E91 Protocol :

In 1991, Ekert [Ekert, 1991] first proposed that quantum key distribution be implemented using the quantum states. This protocol is a modification of original Bennet-Brassard protocol and takes into consideration of EPR states. Let us consider that after preparing an entangled pair of spin-1/2 particles by a source, one particle is sent to Alice and other is sent to Bob. The state shared between Alice and Bob is maximally entangled, e.g., spin-singlet state given by the Eq.(1.13).

If the particles are travelling along the z-direction, the measurement basis vectors of Alice and Bob are defined as being located in the $x - y$ plane perpendicular to the trajectory of the particles. Alice randomly chooses to measure the spin

of incoming particles from the set of basis $\left\{ \mathcal{A}_1 = \sigma_x, \mathcal{A}_2 = \frac{\sigma_x + \sigma_y}{\sqrt{2}}, \mathcal{A}_3 = \sigma_y \right\}$ and similarly, Bob measures randomly chosen from the set $\left\{ \mathcal{B}_1 = \frac{\sigma_x + \sigma_y}{\sqrt{2}}, \mathcal{B}_2 = \sigma_y, \mathcal{B}_3 = \frac{-\sigma_x + \sigma_y}{\sqrt{2}} \right\}$. All the steps of this process is repeated for N times. After performing N measurements by both Alice and Bob, they publicly discuss about their measurement basis chosen for each particular measurement. They separate the measurements in two groups. In the first group, they accumulate the measurements performing in incompatible bases and the second group consist of measurements performing with compatible bases.

The correlation coefficient of joint measurements for the choice of Alice's basis $\mathcal{A}_i$ and Bob's basis $\mathcal{B}_j$ is given by

$$C\left(\mathcal{A}_i, \mathcal{B}_j\right) = P_{++}\left(\mathcal{A}_i, \mathcal{B}_j\right) + P_{--}\left(\mathcal{A}_i, \mathcal{B}_j\right) - P_{+-}\left(\mathcal{A}_i, \mathcal{B}_j\right) - P_{-+}\left(\mathcal{A}_i, \mathcal{B}_j\right),$$

$$(1.28)$$

where $i, j = 1, 2, 3$. $P_{\pm\pm}\left(\mathcal{A}_i, \mathcal{B}_j\right)$ is the joint probability of getting the result ± 1 for Alice's choice of spin measurement $\mathcal{A}_i$ and of getting the result ± 1 for Bob's choice of spin measurement $\mathcal{B}_j$. If Alice and Bob choose incompatible bases to measure their respective particles, only then they publicly announce the actual measurement results they obtained and can figure out the value of the Bell sum, which can be written in terms of correlation coefficients of joint measurements as

$$B = C\left(\mathcal{A}_1, \mathcal{B}_1\right) - C\left(\mathcal{A}_1, \mathcal{B}_3\right) + C\left(\mathcal{A}_3, \mathcal{B}_1\right) + C\left(\mathcal{A}_3, \mathcal{B}_3\right). \qquad (1.29)$$

Using local realism, Bell proved that $|B| \leq 2$. For maximally entangled states [Eq.(1.13)], $|B| = 2\sqrt{2}$, i.e., violation of Bell's theorem occurs. In absence of an eavesdropper, $|B|$ should be equal to $2\sqrt{2}$. This assures Alice and Bob that when Alice and Bob choose compatible bases, their measurement results will be anti-correlated and can be converted into a secret string of bits, i.e., the key. The $1/3$ chance that Alice and Bob will choose compatible bases to measure the incoming particles can shrink the key down to 30% of its original size, leaving them with a sifted key, which may be used in a conventional cryptographic communication between Alice and Bob. Within the sifted secret key, the spin up and spin down states of the particles correspond to bit values 0 and 1, respectively.

The entanglement present between Alice and Bob makes an eavesdropper, say, Eve hard to gain information about the key. The information about a system does not exist until an actual measurement has been performed on the system and

then communicated publicly. To know the key, Eve can provide a state, which is entangled with Alice's and Bob's system but Alice and Bob do not receive their expected value of B. So, in presence of an eavesdropper, $|B| < 2\sqrt{2}$. Future real life situations is more accurately indicated by the Ekert protocol as a practical implementation of quantum cryptography would involve a central source to overcome the distance limitations.

1.9 Non-Gaussian states and their usefulness

There exist both the theoretical and experimental demonstrations of all the quantum properties using Gaussian states. But it is realized that Gaussian states are a rather special class of states and it is quite difficult to achieve such special states experimentally. Gaussian states are defined as those states described by a Gaussian Wigner function, which differs from the non-Gaussian nature of the Wigner function of non-Gaussian states. The non-Gaussian states can be generated in different procedures, e.g., by truncating the Gaussian distribution or by the processes of photon subtraction and addition [Agarwal, 2013], and these states generally have a higher degree of entanglement than the Gaussian states. Also, non-Gaussian state can be constructed by the superposition of the Gaussian states. As for example, entangled non-Gaussian states can be constructed by the superposition of the energy eigenstates of the two-dimensional harmonic oscillator. Schrödinger's cat states, some mixtures of squeezed or coherent states etc. are also the examples of non-Gaussian states.

As the non-Gaussian states are rich in entanglement than the Gaussian states, the former have applications in tests of Bell inequalities, quantum teleportation and other quantum information protocols [Lee et al., 2011; Lloyd and Braunstein, 1999; Opatrny, Kurizki, and Welsch, 2000; Seshadreesan, Dowling, and Agarwal, 2015; Takahashi et al., 2010]. Extensions of the entanglement criteria for non-Gaussian states have been proposed recently [Ivan et al., 2011; Roncaglia, Montorsi, and Genovese, 2014]. Non-Gaussianity is needed for entanglement distillation and quantum computation. Since the steering of correlated systems has started being studied only recently, and EPR steering for Gaussian states has been studied extensively both theoretically and experimentally, now it becomes important to understand the steering of systems with non-Gaussian correlations. A particular example of a non-Gaussian state was considered by Walborn et al. [Walborn

et al., 2011] revealing steering through the entropic inequality. Non-Gaussian entanglement and steering have also been recently studied in the context of Kerr-squeezed optical beams [Olsen and Corney, 2013].

1.10 Outline of thesis

In this thesis, some properties of quantum mechanics are studied using several classes of important non-Gaussian states for continuous variable systems. The outline of this thesis, which actually points towards the fact that non-Gaussian states are more nonlocal, is briefly given below.

In *Chapter-2*, we have studied the mass dependence of both the position detection probabilities for quantum particles projected upwards against gravity around the classical turning point and the point of initial projection, and also the mean arrival time of freely falling particles, using a class of non-Gaussian wave packets, which depart from the Gaussian wave packet by a continuous and tunable parameter. We have shown the stronger violation of the WEQ by increasing the non-Gaussian parameter of the wave packet through the mass dependence of the probabilities and the mean arrival time [Chowdhury et al., 2012]. Then, we have used a selection of Bohm trajectories to illustrate these features in the free fall case.

In *Chapter-3*, we have considered Laguerre-Gaussian beam, which is a classical optical beam with topological singularities and possesses Schmidt decomposition. We have shown that such classical beams share many features of two mode entanglement in quantum optics. We have demonstrated the coherence properties of such beams through the violations of Bell's inequality for continuous variables using Wigner function formalism due to the presence of correlations between two different modes of the beam. The magnitude of the Bell violation is shown to be increased with higher orbital angular momenta of the vortex beam [Chowdhury, Majumdar, and Agarwal, 2013]. So, we have shown the mathematical reinterpretation of quantum nonlocality in classical theory.

In *Chapter-4*, we have demonstrated the steerability of several classes of currently important non-Gaussian entangled states [Chowdhury et al., 2014], such as the two-dimensional harmonic oscillator, the photon-annihilated two mode squeezed vacuum, and the NOON states for $N = 1$ only, through the violation of the entropic steering inequality. We have shown that the steerability of those states remains

unable to be captured by the Reid criterion, whereas that of Gaussian states is demonstrated using the Reid criterion. We have also provided a comparative study of violation of the Bell inequality for these states, from which it is shown that the entanglement present is more easily revealed through steering compared to Bell violation for several such states.

In *Chapter-5*, we have derived a fine-grained uncertainty relation for the measurement of two incompatible observables on a single quantum system of continuous variables, and have shown that continuous variable systems are more uncertain than discrete variable systems. Using the derived fine-grained uncertainty relation, we have formulated a stronger steering criterion, which has the ability to reveal the steering property of NOON states for all $N \geq 2$, which remains unable to be captured by any other previously derived steering criterion. We have also shown that the newly derived uncertainty relation has improved the lower bound on the secret key rate of a one-sided device independent quantum key distribution protocol for continuous variable systems [Chowdhury, Pramanik, and Majumdar, 2015] than that obtained in discrete variable systems.

In the last chapter, i.e., in *Chapter-6*, we have summarized the important results obtained in this thesis. We have also discussed about some future directions of study in this connection.

Chapter 2

Violation of Weak Equivalence Principle in quantum mechanics

The Equivalence Principle which is a consequence of the equality of gravitational and inertial masses [Galilei, 1638], was tested experimentally for classical test bodies to high precision. The validity of the Equivalence Principle for quantum mechanical particles has been tested through the gravity-induced interference experiments [Colella, Overhauser, and Werner, 1975; Peters, Chung, and Chu, 1999]. The possibility of violation of the weak equivalence principle in quantum mechanics (WEQ), which is the weak version of the equivalence principle adopted to the quantum mechanical framework, is discussed in a number of papers, for instance using neutrino mass oscillations in a gravitational potential [Adunas, Milla, and Ahluwalia, 2001; Gago, Nunokawa, and Funchal, 2000; Gasperini, 1988; Halprin and Leung, 1996; Krauss and Tremaine, 1988; Mureika, 1997]. The WEQ can be shown to be violated in quantum mechanics both theoretically [Greenberger, 1968, 1983; Greenberger and Overhauser, 1979] and experimentally [Colella, Overhauser, and Werner, 1975; Peters, Chung, and Chu, 1999]. One of the quantum mechanical approach of the violation of WEQ was given by Davies [Davies, 2004] for a quantum particle in a uniform gravitational field using a model quantum clock [Peres, 1980] as shown through the mass dependence of the tunnelling depth of the particle in the classically forbidden region.

In another way, Ali et al. have given the example of violation of WEQ for quantum particles represented by Gaussian wave packets projected upwards against gravity

[Ali et al., 2006]. They have shown the violation through the explicit mass de-
pendence of the position detection probabilities around both the classical turning
point and the point of initial projection and of the mean arrival time of freely
falling particles at an arbitrary detector location using Gaussian wave packet.

It is now interesting to know how WEQ works for quantum particles represented
by parametrized non-Gaussian wave packets. In real experiments, realization of
exactly Gaussian wave packets is rather difficult . One of the aims of our study
is to enable relaxation of the wave packet to be Gaussian. Therefore, the non-
Gaussian nature of the wave packet can facilitate the experimental observation of
the violation of WEQ, as well as enable a quantitative verification of the way the
violation of WEQ depends on the departure from the Gaussian nature of the wave
packet.

2.1   Initial wave function and it's time evolution

Let us consider an ensemble of quantum particles in an external gravitational
potential. The initial state of each particle is represented by a one-dimensional
non-Gaussian wave function, given as

$$\psi(z, t = 0) \;\; = \;\; N \left[1 + \alpha \, \sin \left(\frac{\pi}{4 \, \sigma_0} z \right) \right] \, e^{-\frac{z^2}{4 \, \sigma_0^2} + i \, k_0 \, z}. \tag{2.1}$$

Here, α is the tuneable parameter varying from 0 to 1. N is the normalisation
factor given by

$$N \;\; = \;\; \left(\sqrt{2 \, \pi} \, \sigma_0 \left[1 + \frac{\alpha^2}{2} \, (1 - e^{-\pi^2/8}) \right] \right)^{-1/2}. \tag{2.2}$$

The salient features corresponding to the above wave packet are its asymmetry due
to the presence of sine function, its infinite tail, and its reduciblity to a Gaussian
wave packet upon a continuous decrement of the parameter α to zero. The property
of an infinite tail of the above wave function is not associated with non-Gaussian
forms that are generated by truncating the Gaussian distribution. For $\alpha = 0$,
we get the Gaussian wave function. Here, we have restricted ourselves to a one-
dimensional representation along the vertical z direction.

The initial group velocity is given by $u = \frac{\hbar k_0}{m}$, where m is the mass of the particle and k_0 is the wave number. In the Schrödinger picture, the mean initial conditions for the initial wave functions ψ_1 and ψ_2 representing particles 1 and 2 respectively are

$$
\begin{aligned}
\langle \hat{z} \rangle_{\psi_1} &= \langle \hat{z} \rangle_{\psi_2} = \langle \hat{z}(0) \rangle \,, \\
\frac{\langle \hat{p}_z \rangle_{\psi_1}}{m_1} &= \frac{\langle \hat{p}_z \rangle_{\psi_2}}{m_2} = u \,,
\end{aligned}
\tag{2.3}
$$

where $\langle \hat{z} \rangle_{\psi}$ and $\langle \hat{p}_z \rangle_{\psi}$ represent the expectation values for position and momentum operators respectively. The propagator of a particle in the linear gravitational potential $V = mgz$ is given below

$$
G(z, t \,|\, y, 0) = \sqrt{\frac{m}{2\pi i \hbar t}}\, e^{\frac{i m}{2 \hbar t}(z-y)^2 - \frac{i m g t}{2 \hbar}(z+y) - \frac{i m g^2 t^3}{24 \hbar}}
\tag{2.4}
$$

Using this propagator in the relation

$$
\psi(z, t) = \int dy\, G(z, t \,|\, y, 0)\, \psi(y, 0) \,,
\tag{2.5}
$$

one can obtain the Schrödinger time evolved wave function $\psi(z, t)$ at any subsequent time t as

$$
\begin{aligned}
\psi(z, t) \;=\; & N \sqrt{\frac{\sigma_0}{s_t}}\, e^{\frac{i m}{2 \hbar t}[z^2 - g t^2 z - \frac{g^2 t^4}{12}]} \\
& \times \left[e^{-\frac{i m}{2 \hbar t}\frac{\sigma_0}{s_t}[z - \frac{\hbar t}{m} k_0 + \frac{g t^2}{2}]^2} + \frac{\alpha}{2 i} e^{-\frac{i m}{2 \hbar t}\frac{\sigma_0}{s_t}[z - \frac{\hbar t}{m}(k_0 + \beta) + \frac{g t^2}{2}]^2} \right. \\
& \left. \qquad - \frac{\alpha}{2 i} e^{-\frac{i m}{2 \hbar t}\frac{\sigma_0}{s_t}[z - \frac{\hbar t}{m}(k_0 - \beta) + \frac{g t^2}{2}]^2} \right] \,,
\end{aligned}
\tag{2.6}
$$

where $s_t = \sigma_0 \left(1 + i \frac{\hbar t}{2 m \sigma_0^2}\right)$ and $\beta = \frac{\pi}{4 \sigma_0}$. The probability density $(|\psi(z, t)|^2)$ is given by

$$
\begin{aligned}
\rho(z, t) \;=\; & N^2 \frac{\sigma_0}{\sigma_G}\, e^{E_1} \left[e^{E_2} + \alpha \left(e^{E_3} \sin A_1 + e^{E_4} \sin A_2 \right) \right. \\
& \left. \qquad + \frac{\alpha^2}{4} \left(1 + e^{E_5} - 2\, e^{E_6} \cos A_3 \right) \right] \,,
\end{aligned}
\tag{2.7}
$$

where

$$E_1 = -\frac{\left[\pi\,\hbar\,t + 4\,m\,\sigma_0\left(z - u\,t + \frac{1}{2}\,g\,t^2\right)\right]^2}{32\,m^2\,\sigma_G^2\,\sigma_0^2} \ ,$$

$$E_2 = \frac{\pi\,\hbar\,t\left[\pi\,\hbar\,t + 8\,m\,\sigma_0\left(z - u\,t + \frac{1}{2}\,g\,t^2\right)\right]}{32\,m^2\,\sigma_G^2\,\sigma_0^2} \ ,$$

$$E_3 = \frac{\pi\,\hbar\,t\left[\pi\,\hbar\,t + 24\,m\,\sigma_0\left(z - u\,t + \frac{1}{2}\,g\,t^2\right)\right]}{64\,m^2\,\sigma_G^2\,\sigma_0^2} \ ,$$

$$E_4 = \frac{\pi\,\hbar\,t\left[\pi\,\hbar\,t + 8\,m\,\sigma_0\left(z - u\,t + \frac{1}{2}\,g\,t^2\right)\right]}{64\,m^2\,\sigma_G^2\,\sigma_0^2} \ ,$$

$$E_5 = \frac{\pi\,\hbar\,t\left(z - u\,t + \frac{1}{2}\,g\,t^2\right)}{2\,m\,\sigma_G^2\,\sigma_0} \ ,$$

$$E_6 = \frac{E_5}{2} \ ,$$

$$A_1 = \frac{\pi\left[-\pi\,\hbar\,t + 8\,m\,\sigma_0\left(z - u\,t + \frac{1}{2}\,g\,t^2\right)\right]}{32\,m\,\sigma_G^2} \ ,$$

$$A_2 = \frac{\pi\left[\pi\,\hbar\,t + 8\,m\,\sigma_0\left(z - u\,t + \frac{1}{2}g\,t^2\right)\right]}{32\,m\,\sigma_G^2} \ ,$$

$$A_3 = \frac{\pi\,\sigma_0\left(z - u\,t + \frac{1}{2}\,g\,t^2\right)}{2\,\sigma_G^2} \ ,$$

and

$$\sigma_G = |s_t| = \sigma_0\left(1 + \frac{\hbar^2\,t^2}{4\,m^2\,\sigma_0^4}\right)^{\frac{1}{2}} \tag{2.8}$$

is the spreading of the Gaussian wave packet. The probability density is explicitly mass dependent. Here, the spreading of the wave packet is given by

$$\sigma_{NG} = \frac{\sqrt{\lambda^{(0)} + \lambda^{(2)}\,\alpha^2 + \lambda^{(4)}\,\alpha^4}}{4\,m\,\sigma_0\left[2\,e^{\frac{\pi^2}{8}} + \alpha^2\left(e^{\frac{\pi^2}{8}} - 1\right)\right]} \ , \tag{2.9}$$

where

$$\lambda^{(0)} = 64\,e^{\frac{\pi^2}{4}}\,m^2\,\sigma_0^2\,\sigma_G^2 \ ,$$

$$\lambda^{(2)} = 8\,e^{\frac{\pi^2}{8}}\,\pi^2\,m^2\,\sigma_0^4\left(1 - 2\,e^{\frac{\pi^2}{16}}\right) + 64\,e^{\frac{\pi^2}{8}}\,m^2\,\sigma_0^2\,\sigma_G^2\left(e^{\frac{\pi^2}{8}} - 1\right) + 2\,e^{\frac{\pi^2}{4}}\,\pi^2\,\hbar^2\,t^2 \ ,$$

$$\lambda^{(4)} = \left(e^{\frac{\pi^2}{8}} - 1\right)\left[16\,m^2\,\sigma_0^2\,\sigma_G^2\left(e^{\frac{\pi^2}{8}} - 1\right) + 4\,\pi^2\,m^2\,\sigma_0^4 + e^{\frac{\pi^2}{8}}\,\pi^2\,\hbar^2\,t^2\right] \ , \tag{2.10}$$

which is also mass dependent. From Fig. 2.1, we can see that for large masses, σ_{NG} becomes almost constant with α. For a particular value of α, σ_{NG} decreases with increasing value of mass m.
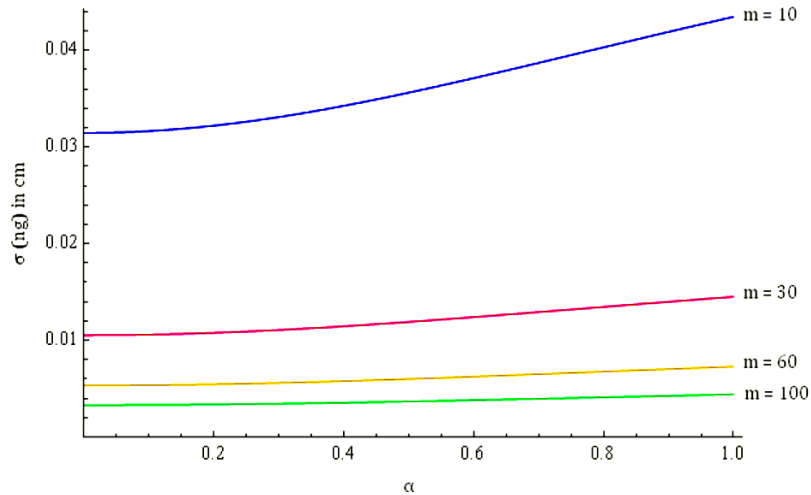
FIGURE 2.1: The variation of the width of the wave packet with α for different values of m (in a.m.u.). We take $\sigma_0 = 10^{-3}$ cm, $t = 1$ sec and $u = 10^3$ cm s^{-1}.

Using the time evolved wave function $\psi(z, t)$, the expressions for expectation value of position z and momentum p are calculated and are given by

$$
\begin{aligned}
\langle z \rangle &= \frac{\pi \, \alpha \, \sigma_0}{2 + \alpha^2 \left(1 - e^{-\frac{\pi^2}{8}} \right)} \, e^{-\frac{\pi^2}{32}} + u\,t - \frac{1}{2}\,g\,t^2, \\
\langle p \rangle &= m\,(u - g\,t).
\end{aligned}
\tag{2.11}
$$

Here, $\langle z \rangle$ is α-dependent but mass independent. The value of z_{peak} is obtained from the numerical solution of the equation $\frac{d|\psi|^2}{dz} = 0$, for which $|\psi|^2$ is maximum. In Table 2.1 and Table 2.2, it is shown numerically how z_{peak} and $\langle z \rangle$ vary with α for $0 \le \alpha \le 1$ and mass m respectively. It is clear that $z_{peak} \ne \langle z \rangle$ and z_{peak} increases with α and mass m, whereas $\langle z \rangle$ increases with α only and remains constant for all masses. Here, the difference between mean and peak occurs due to the presence of the asymmetry of the wave packet. In the Gaussian limit (i.e., $\alpha \to 0$), $\langle z \rangle = z_{peak}$.

Fig. 2.2 shows the time variation of z_{peak} and $\langle z \rangle$. Dotted curve shows the motion of z_{peak} whereas the continuous curve shows the motion of $\langle z \rangle$. As we take

α	z_{peak} in cm	$\langle z \rangle$ in cm
0	38.59999999999815	38.599999999999910
0.1	38.61540633397262	38.611498366598200
0.2	38.62925626009014	38.622755653868810
0.3	38.64090000000000	38.633500000000000
0.4	38.65026513575232	38.643679695976970
0.5	38.65786585282045	38.652999876917650
0.6	38.66400000000000	38.661400000000000
0.7	38.66910000000000	38.668800000000000
0.8	38.67337906376510	38.675246198243485
0.9	38.67696171641449	38.680689435211890
1.0	38.68002216630916	38.685197660661515

TABLE 2.1: The variation of $\langle z \rangle$ and z_{peak} in cm with α for mass $m = 10$ a.m.u. $t = 2$ sec and $\sigma_0 = 0.1$ cm.

Mass (m) in a.m.u.	z_{peak} in cm	$\langle z \rangle$ in cm
30	38.657865898827980	38.65299987691765
60	38.657865903136155	38.65299987691765
90	38.657865903934166	38.65299987691765
120	38.657865904213070	38.65299987691765
150	38.657865904342295	38.65299987691765

TABLE 2.2: The variation of $\langle z \rangle$ and z_{peak} in cm with mass m in a.m.u. for $\alpha = 0.5$, $t = 2$ sec and $\sigma_0 = 0.1$ cm.

$\sigma_0 = 10^{-7}$ cm, the α-dependence of $\langle z \rangle$ and z_{peak} becomes vanishingly small. So, this α-dependence can not be shown graphically. As a result, the curves for z_{peak} and $\langle z \rangle$ coincide totally in this graph.
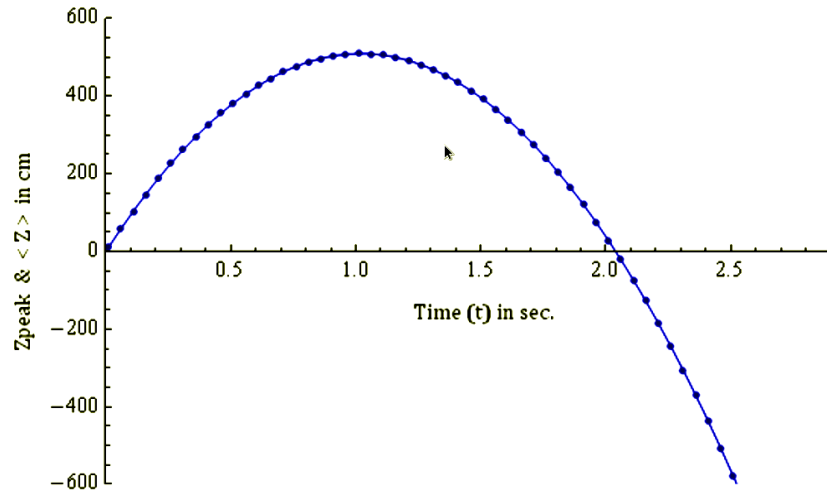
FIGURE 2.2: The variation of z_{peak} and $\langle z \rangle$ with time t. We take $\sigma_0 = 10^{-7}$ cm, $u = 10^3$ cm s^{-1}, $m = 50$ a.m.u. and $\alpha = 0.5$.

2.2 Quantum mechanics in terms of classical concepts

When a wave packet satisfies Ehrenfest's theorem and classical Liouville's equation using Wigner distribution, then one can conclude that the dynamics of $\langle z \rangle$ is like a classical point particle.

2.2.1 Ehrenfest's theorem

According to Ehrenfest's theorem, the expectation value of quantum mechanical operators obey classical laws of motion, the instances of which are given below

$$
\begin{aligned}
\frac{d\langle z \rangle}{dt} &= \frac{\langle p \rangle}{m}, \\
\frac{d\langle p \rangle}{dt} &= \left\langle -\frac{\partial V}{\partial z} \right\rangle .
\end{aligned}
\tag{2.12}
$$

From Eq. (2.11), it is possible to check that Ehrenfest's theorem is satisfied for our non-Gaussian wave packet.

2.2.2 Wigner distribution function

If a full classical description is to emerge from quantum mechanics, we must be able to describe quantum systems in phase-space. To observe the expression of $\langle z \rangle$ in the classical limit, we use the Wigner distribution function [Ford and O'Connell, 2002; Robinett, Doncheski, and Bassett, 2005; Wigner, 1932], which is one of the important phase space distributions.

From the non-Gaussian wave function $\psi(z,t)$ (Eq. (2.6)), we have calculated the Wigner distribution function $D_w(z,p,t)$ as

$$
D_w(z,p,t) \;=\; \frac{1}{\pi\,\hbar} \int_{-\infty}^{\infty} \psi^*(z+y,t)\,\psi(z-y,t)\,e^{\frac{2\,i\,p\,y}{\hbar}}\,dy\,, \tag{2.13}
$$

the marginals of which yield the correct quantum probabilities for position and momentum separately. $D_w(z,p,t)$ satisfies the classical Liouville's equation [Das and Sengupta, 2002] given by

$$
\frac{\partial D_w(z,p,t)}{\partial t} + \dot{z}\,\frac{\partial D_w(z,p,t)}{\partial z} + \dot{p}\,\frac{\partial D_w(z,p,t)}{\partial p} \;=\; 0\,. \tag{2.14}
$$

Here, $H = p^2/2m + mgz$ is the Hamiltonian of the system and from Hamilton's equation of motion, we get

$$
\dot{z} \;=\; \frac{\partial H}{\partial p} \;=\; p/m\,,
$$

$$
\dot{p} \;=\; -\frac{\partial H}{\partial z} \;=\; -\,m\,g\,.
$$

The corresponding position distribution function is given by

$$
\rho_C(z,t) \;=\; \int_{-\infty}^{\infty} D_w(z,p,t)\,dp\,. \tag{2.15}
$$

So, the expression for the average value of z using Wigner distribution function in the classical limit is given by

$$
\begin{aligned}
\langle z \rangle &= \frac{\int_{-\infty}^{\infty} z\,\rho_C(z,t)\,dz}{\int_{-\infty}^{\infty} \rho_C(z,t)\,dz} \\[2mm]
&= \frac{\pi\,\alpha\,\sigma_0}{2 + \alpha^2\left(1 - e^{-\frac{\pi^2}{8}}\right)}\,e^{-\frac{\pi^2}{32}} + u\,t - \frac{1}{2}\,g\,t^2 \\[2mm]
&\equiv z_0 + u\,t - \frac{1}{2}\,g\,t^2\,,
\end{aligned} \tag{2.16}
$$
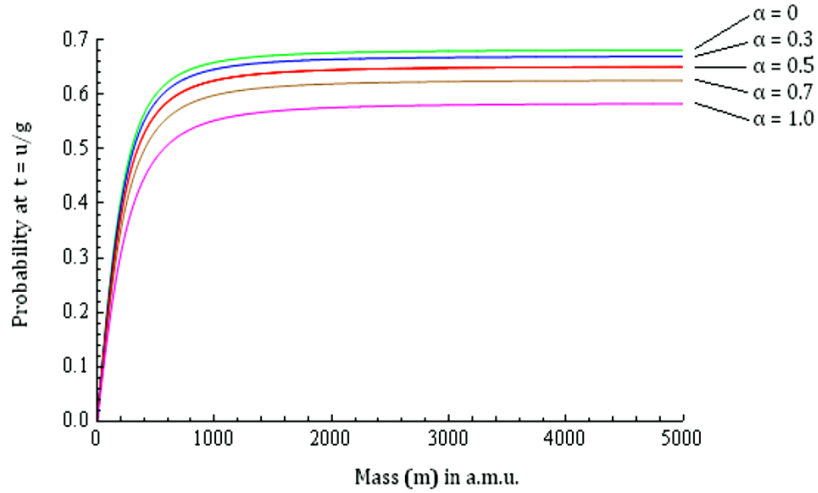
FIGURE 2.3: The variation of probability $P_1(m)$ with mass (in a.m.u.) for different constant values of α. We take $u = 10^3$ cm s^{-1}, $\sigma_0 = 10^{-3}$ cm and $\epsilon = \sigma_0$.

which is exactly equal to the quantum mechanical expectation value of z [Chowdhury et al., 2012].

2.3 Position detection probabilities

Now, we consider an ensemble of quantum particles projected upwards against gravity with a given initial mean position and mean velocity. Classically, the particle moving upwards from the reference point at $z = 0$ reaches the maximum height $z = z_{\max} = u\,t_1 - \frac{1}{2}\,g\,t_1^2$ at time $t_1 = u/g$ and returns to its initial projection point at $z = 0$ at time $t_2 = 2\,u/g$. Let, $P_1(m)$ and $P_2(m)$ be the probabilities of finding the particles within a very narrow detector region $(-\epsilon$ to $+\epsilon)$ around $z_{\max}$ and around $z = 0$ respectively, and are given by

$$
\begin{aligned}
P_1(m) &= \int_{z_{\max}-\epsilon}^{z_{\max}+\epsilon} |\,\psi(z,t_1)\,|^2\, dz\,, \\
P_2(m) &= \int_{-\epsilon}^{+\epsilon} |\,\psi(z,t_2)\,|^2\, dz\,.
\end{aligned}
\tag{2.17}
$$

From both the Fig. 2.3 and Fig. 2.4, it can be seen that both the probabilities $P_1(m)$ and $P_2(m)$ show the violation of WEQ [Chowdhury et al., 2012] through
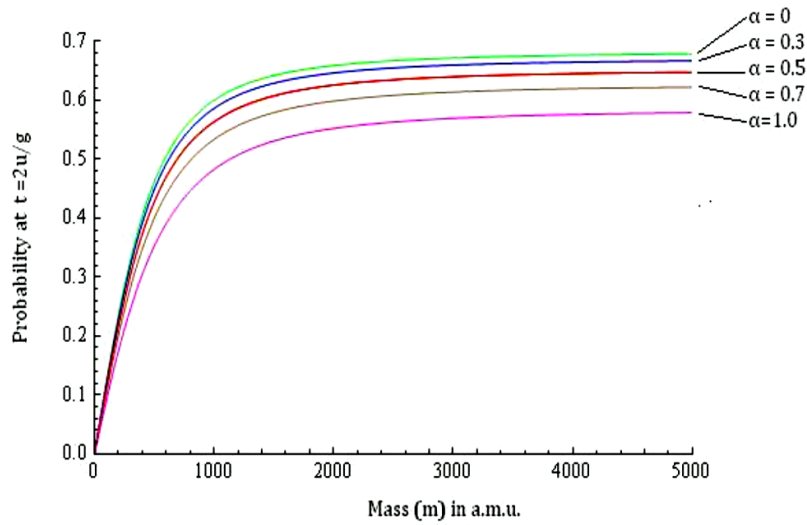
FIGURE 2.4: The variation of probability $P_2(m)$ with mass (in a.m.u.) for different constant values of α. We take $u = 10^3$ cm s^{-1}, $\sigma_0 = 10^{-3}$ cm and $\epsilon = \sigma_0$.

their mass dependence for smaller masses using an initial non-Gaussian wave packet. This effect of mass dependence of the probabilities occur essentially as the spreading of the wave packet under linear gravitational potential depends on the mass of the particles. These probabilities become saturated in the limit of large mass. Again, it is seen that both the probabilities decrease for a particular value of m but the violation increases with the non-Gaussian parameter α, signifying a stronger violation of the weak equivalence principle.

2.4   Mean arrival time

Next, we consider quantum particles falling freely from the initial position at $z = 0$ under gravity with the initial state given by the Eq. (2.1) and with the initial velocity $u = 0$. Using the probability current approach [Dumont and Marchioro, 1993; Leavens, 1993], the mean arrival time of the particles to reach a detector location at $z = Z$ is given by

$$\bar{\tau} = \frac{\int_0^\infty |J(z = Z, t)| \, t \, dt}{\int_0^\infty |J(z = Z, t)| \, dt} , \qquad (2.18)$$

where $J(z,t)$ is the quantum probability current density. $J(z,t)$ can be negative, so we take the modulus sign here. From Eq. (2.18), it can be seen that the integral of the denominator converges whereas the integral of the numerator diverges formally. To converge the numerator, among the available several techniques [Damborenea, Egusquiza, and Muga, 2002; Hahne, 2003] here we use the simple technique of getting a cut-off at $t = T$ in the upper limit of the time integral with $T = \sqrt{2\,(\,|\,Z\,| + 3\,\sigma_T\,)/g}$. σ_T is the width of the wave packet at time T. Thus, our calculations of the arrival time are valid upto the $3\,\sigma_T$ level of spread in the wave function.

We have calculated $J(z,t)$ with the initial non-Gaussian position distribution as

$$
\begin{aligned}
J(z,t) &= \frac{\hbar}{m}\,\Im\,(\psi^*\,\nabla\,\psi) \\
&= N^2\,\frac{e^{E_1}}{32\,m^2\,\sigma_0\,\sigma_G^3}\,\big(\eta^{(0)} + \alpha\,\eta^{(1)} + \alpha^2\,\eta^{(2)}\big)\,,
\end{aligned} \tag{2.19}
$$

where

$$
\begin{aligned}
\eta^{(0)} &= 8\,e^{E_2}\left[\hbar^2\,t\left(z - \frac{1}{2}\,g\,t^2\right) + 4\,m^2\,\sigma_0^4\,(u - g\,t)\right]\,, \\
\eta^{(1)} &= \eta^{(0)}\,e^{-E_2}\left(e^{E_3}\,\sin A_1 + e^{E_4}\,\sin A_2\right) - 2\,\pi\,\hbar^2\,t\,\sigma_0\left(e^{E_3}\,\cos A_1 + e^{E_4}\,\cos A_2\right) \\
&\qquad\qquad + 4\,\pi\,m\,\hbar\,\sigma_0^3\left(e^{E_3}\,\sin A_1 - e^{E_4}\,\sin A_2\right)\,, \\
\eta^{(2)} &= \left[2\,\hbar^2\,t\left(z - \frac{1}{2}\,g\,t^2\right) + 8\,m^2\,\sigma_0^4\,(u - g\,t)\right]\left(1 + e^{E_5} - 2\,e^{E_6}\,\cos A_3\right) \\
&\qquad\qquad - 2\,\pi\,\hbar^2\,t\,\sigma_0\,e^{E_6}\,\sin A_3 + 2\,\pi\,m\,\hbar\,\sigma_0^3\,(e^{E_5} - 1)\,,
\end{aligned}
$$

and where the E_i's are defined below Eq. (2.7).

$\bar{\tau}$ is also mass dependent through the explicit mass dependence of $J(z,t)$. From Fig. 2.5, it is clear that for smaller masses $\bar{\tau}$ is mass dependent. Fig. 2.6 shows that for large masses, $\bar{\tau}$ becomes almost constant with α. For a particular value of α, $\bar{\tau}$ decreases with increasing value of mass m. This mass-dependence of the mean arrival time gradually vanishes as the mass is increased. Thus, compatibility with the equivalence principle emerges in the limit of large mass, or classical limit [Chowdhury et al., 2012]. For a particular value of mass, $\bar{\tau}$ increases with α. The increment of $\bar{\tau}$ with α from the result of Gaussian case (i.e., with $\alpha = 0$) signifies the stronger violation of WEQ [Chowdhury et al., 2012]. A non-Gaussian wave packet can exhibit non-classical features in a mass range where its Gaussian counterpart behaves classically.
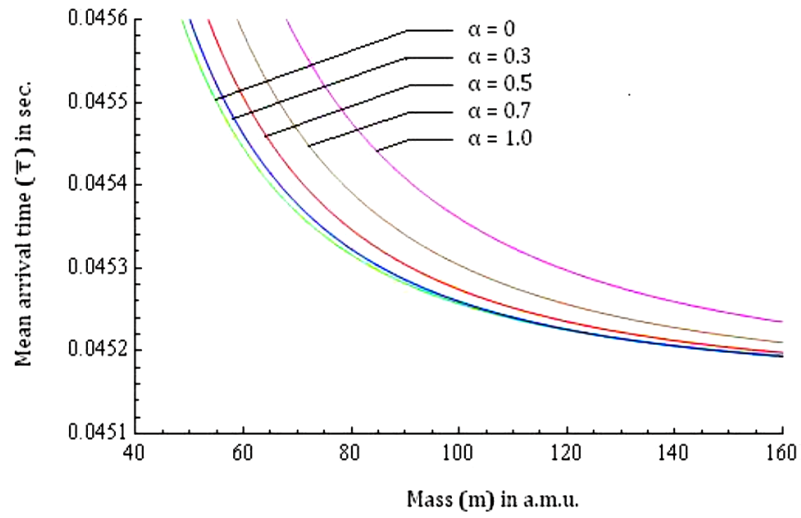
FIGURE 2.5: The variation of mean arrival time with mass (in a.m.u.) for different constant values of α. We take $\sigma_0 = 10^{-6}$ cm, $Z = -1$ cm and $u = 0$.
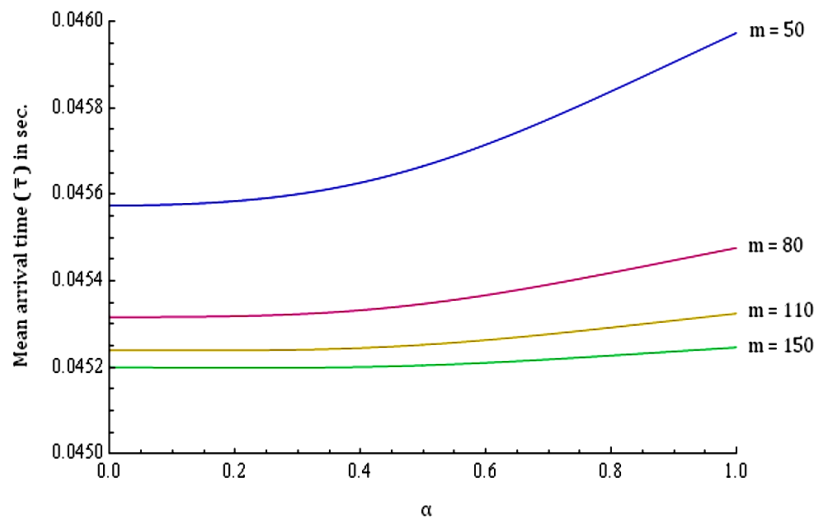
FIGURE 2.6: The variation of mean arrival time with α for different constant values of m (in a.m.u.).We take $\sigma_0 = 10^{-6}$ cm, $Z = -1$ cm and $u = 0$.

2.5   Bohmian interpretation

In the Bohmian model of quantum mechanics [Bohm, 1952, 1953], each individual particle is assumed to have a definite position, irrespective of any measurement. The pre-measured value of position is revealed when an actual measurement is done. If each of an ensemble of particles have the same wave function ψ, which evolves with time according to the Schrödinger equation, these ontological positions are distributed according to the probability density $\rho = |\psi|^2$. If v is the Bohmian velocity of the particle and J is the probability current density, then the equation of motion of any individual particle is determined by the guidance equation $v = J/\rho$. Solving the guidance equation, one gets the trajectory of the particle.

The violation of WEQ arises as a consequence of the spread of wave packets, the magnitude of which itself depends on the mass. In order to illustrate this effect we present an analysis in terms of Bohmian trajectories in the free fall case. Within the context of Bohmian interpretation of quantum mechanics [Bohm, 1952, 1953], each individual particle is assumed to have a definite position, irrespective of any measurement. The equation of motion of the particle is,

$$m\,\ddot{\vec{x}} = -\nabla\left(V + Q\right)|_{\vec{x} = \vec{x}(t)}, \qquad (2.20)$$

where $Q = -\frac{\hbar^2}{2\,m}\frac{\nabla^2\sqrt{\rho}}{\sqrt{\rho}}$ is called 'quantum potential energy' and it is explicitly mass-dependent and $\vec{x}(t)$ determines the path of the particle. In the gravitational potential $V = mgz$, the quantum version of Newton's second law is given by

$$\ddot{z} = g - \frac{1}{m}\frac{\partial Q}{\partial z}\bigg|_{z = z(t)}. \qquad (2.21)$$

According to Holland [Holland, 1993], due to the intervention of the mass-dependent quantum force term, WEQ is violated. The arrival-time problem is unambiguously solved in the Bohmian mechanics, where for an arbitrary scattering potential $V(\vec{x})$, the arrival-time distribution of particles [Leavens, 1993, 1996, 1998, 2002] that actually reach $\vec{x} = \vec{X}$, is given by the modulus of the probability current density, i.e., $|J(\vec{X}, T)|$.

The effect of nonlocal nature and the mass-dependence of the quantum potential Q on the violation of WEQ is manifested in a similar way like the violation observed
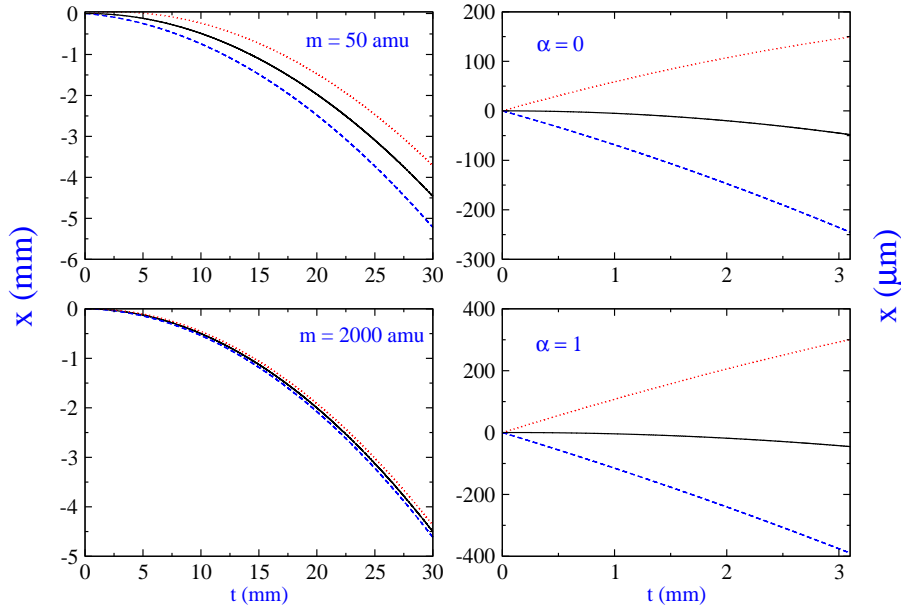
FIGURE 2.7: A selection of Bohmian trajectories for $u = 0$ (free fall) and $\sigma_0 = 10^{-6}$ cm. In the left column tunable parameter α has the fixed value $\alpha = 0.5$ and in the right one mass is constant and equal to $m = 100$ amu. The solid black trajectory starts at $\langle z \rangle(0)$, the dashed blue one at $\langle z \rangle(0) - 2\sigma_0$ and the dotted red one at $\langle z \rangle(0) + 2\sigma_0$.

due to the spread of the wave packet. We have computed a set of Bohmian trajectories corresponding to the free fall of our non-Gaussian wave packet with the tunable parameter α. Fig. 2.7 shows a selection of Bohmian trajectories exhibiting their mass and α dependent spread. One can see that for small mass, the trajectories with initial positions on the left and right of the center of the wave packet (mean $\langle z \rangle$) spread out with time evolution, indicating violation of WEQ. The magnitude of spread increases with α, signifying stronger violation of WEQ [Chowdhury et al., 2012] with increased departure from Gaussianity. The spread of the trajectories decreases as mass is increased, leading to the emergence of WEQ in the classical limit.

2.6 Summary

To summarize, in this chapter we have studied the violation of the gravitational weak equivalence principle in quantum mechanics using a non-Gaussian wave packet. The wave packet is constructed in such a way that its departure from Gaussianity is represented by a continuous and tunable parameter α. The asymmetry of the wave packet entails a difference between its mean and peak, and causes the peak to evolve differently from a classical point particle, whereas the mean evolves like a classical point particle modulo a constant depending upon the parameter α. Such a result is consistent with the Ehrenfest therorem, as we have shown, and re-confirmed using the Wigner distribution. The correspondence with the results following from a Gaussian wave packet is achieved in the limit of $\alpha \to 0$.

First, we have shown the violation of the weak equivalence principle through the dependence on mass of the position detection probabilities of an ensemble of particles projected upwards against gravity. We next compute the mean arrival time of freely falling wave packets through the probability current distribution corresponding to the non-Gaussian wave packet. The mass dependence of the arrival time again causes the violation of WEQ. In both the cases, the magnitude of violation increases with the increase of the non-Gaussian parameter α, signifying stronger violation of WEQ with larger deviation from Gaussianity. It is observed that in the limit of large mass the classical value for the mean arrival time is approached, thereby indicating the emergence of the WEQ in the classical limit. In this context, it is worthwhile mentioning that though our work follows as a natural consequence of quantum mechanics or quantum theory in the non-relativistic limit, it does not imply a violation of general covariance in the relativistic domain. An interesting connection between the non-relativistic limit of quantum theory and the principle of equivalence has recently been discussed [Padmanabhan and Padmanabhan, 2011]. Finally, a computation of Bohmian trajectories further establishes the stronger violation of the WEQ by a non-Gaussian wave packet.

Chapter 3

Violation of Bell's inequality for classical beam

Vortex beams provide another interesting example of non-Gaussian character. Vortex beams can encode large amounts of information due to the absence of an upper limit on their topological charge [Nye and Berry, 1974], a feature which is endowed due to the twisting of light like a corkscrew around its axis of propagation. This feature associated with a corresponding number of allowed states have lead their applicability in quantum information processing tasks [Molina-Terriza, Torres, and Torner, 2007]. Vortex beams have interesting coherence properties [Agarwal and Banerji, 2002; Simon and Agarwal, 2000], and such beams with large values of orbital angular momenta have been experimentally realized both in the optical domain [Fickler et al., 2012] as well as using electrons [McMorran, 2011; Verbeeck, Tian, and Schattschneider, 2010].

Due to the presence of the mathematical isomorphism of correlations between discrete degrees of freedom in classical optics with quantum entanglement in two-qubit systems, a common framework to study correlations in discretized degrees of freedom in both classical and quantum optics has been proposed [Aiello and Woerdman, 2005; Ghose and Mukherjee, 2014; Qian, Broadbent, and Eberly, 2014; Qian and Eberly, 2011; Simon et al., 2010; Spreeuw, 1998]. Schmidt decomposition has been known much before the advent of quantum mechanics and it plays a key role in defining quantum entanglement, when one uses the wave function. In classical theory the Schmidt decomposition is in terms of the electromagnetic fields, and the coherence function is directly related to the Schmidt spectrum

[Jha, Agarwal, and Boyd, 2011]. The well known classical Laguerre-Gaussian (LG) beams that have optical vortices with topological singularities [Agarwal, 2013] have a Schmidt decomposition [Agarwal and Banerji, 2002]. Therefore, one would expect that they may have the capability of showing many of the features developed within the context of quantum mechanics.

After the derivation of Bell's inequality, the violation of Bell's inequality in quantum mechanics has been shown in several subsequent experiments [Aspect, Dalibard, and Roger, 1982; Aspect, Grangier, and Roger, 1981, 1982]. The derivation of the inequality does not involve the concept of quantum mechanics. Recently, Bell's measure, which is the amount of violation of a Bell inequality [Bell, 1964; Clauser et al., 1969], has been suggested as a measure to quantify the magnitude of correlation between different degrees of freedom of a classical beam through joint measurements [Borges et al., 2010; Kagalwala et al., 2013]. Now, we want to demonstrate the coherence properties of LG beams through the violations of Bell's inequality for continuous variables.

3.1   Schmidt decomposition and classical fields

Let us consider, Alice and Bob possess two particles A and B respectively. In quantum mechanics, there is a possibility that these particles are entangled. This is a consequence of the superposition principle, which allows us to write the two particle wave function $\psi(x, y)$ as a superposition of the product of the single particle wave functions $\Phi_i(x)$ and $\chi_i(y)$,

$$\psi(x, y) \;\; = \;\; \sum_i c_i \, \Phi_i(x) \, \chi_i(y), \tag{3.1}$$

where c_i's are some constants. As long as there are at least two nonzero c_i's, the above state will remain nonseparable, i.e., entangled. In fact, the state (3.1) is in the form of a Schmidt decomposition which has been extensively used in studying quantum entanglement [Grobe, Rzazewski, and Eberly, 1994; Law, Walmsley, and Eberly, 2000; Sperling and Vogel, 2011]. A way to study entanglement is to study the nonpositivity of the quasiprobabilities [Sperling and Vogel, 2009].

Presently, we consider the classical fields with topological singularities. For these classical fields, there is a close parallel to the development in quantum mechanics.

It is well known that in paraxial optics, the beam propagation in free space is described by [Saleh and Teich, 2007]

$$E\left(\vec{r},t\right) = \varepsilon\left(x,y,z\right)e^{i\omega z/c - i\omega t}, \tag{3.2}$$

$$i\frac{\partial\varepsilon}{\partial z} = -\frac{\lambda_c}{2}\left(\frac{\partial^2}{\partial x^2} + \frac{\partial^2}{\partial y^2}\right)\varepsilon, \tag{3.3}$$

with $\lambda_c = \lambda/2\pi$, $2\pi/\lambda = \omega/c$. The Eq.(3.3) has exactly the same form as the Schrodinger equation for a free particle in two dimensions with $t \to z$, $\psi \to \varepsilon$, $\hbar \to \lambda_c$. Thus, an optical beam in two dimensions can be expressed as a superposition of fundamental solutions of Eq.(3.3). For an example, we consider the classical Laguerre-Gaussian (LG) beams.

3.2   Classical Laguerre-Gaussian (LG) beams

The well known LG beam in two dimensions is a physically realizable field distribution containing optical vortices with topological singularities and is given by [Agarwal, 2013]

$$\Phi_{nm}\left(\rho,\theta\right) = e^{i\left(n-m\right)\theta}e^{-\rho^2/w^2}\left(-1\right)^{\min\left(n,m\right)}\left(\frac{\rho\sqrt{2}}{w}\right)^{|n-m|}$$

$$\times\sqrt{\frac{2}{\pi\,n!\,m!\,w^2}}\,L_{\min\left(n,m\right)}^{|n-m|}\left(\frac{2\,\rho^2}{w^2}\right)\left[\min\left(n,m\right)\right]!, \tag{3.4}$$

where ρ and θ are the polar coordinates in two dimensions $\rho = \sqrt{x^2 + y^2}$, $\tan\theta = y/x$. This is a normalized wave function as $\int |\Phi_{nm}(\rho,\theta)|^2\,dx\,dy = 1$. Here, the integers n,m representing the two modes of the beam satisfy $0 \le n,m \le \infty$, w is the beam waist, and $L_p^l(x)$ is the generalized Laguerre polynomial. $N = n + m$ is called the order of the mode, $l = n - m$ is the azimuthal index, and $p = \min(n,m)$ is called the radial index. These LG beams can be written as superpositions of Hermite-Gaussian (HG) beams [Beigersbergen et al., 1993; Danakas and Aravind, 1992]

$$\Phi_{nm}\left(\rho,\theta\right) = \sum_{k=0}^{n+m}u_{n+m-k,k}\left(x,y\right)\frac{f_k^{(n,m)}}{k!}\left(\sqrt{-1}\right)^k\sqrt{\frac{k!\left(n+m-k\right)!}{n!\,m!\,2^{n+m}}}, \tag{3.5}$$

$$f_k^{(n,m)} \;\;=\;\; \frac{d^k}{dt^k}\left\{(1-t)^n\,(1+t)^m\right\}|_{t=0}\,, \tag{3.6}$$

and the HG beam is defined by

$$u_{nm}(x,y) \;\;=\;\; \sqrt{\frac{2}{\pi}}\left(\frac{1}{2^{n+m}\,w^2\,n!\,m!}\right)^{1/2} H_n\!\left(\frac{\sqrt{2}\,x}{w}\right) H_m\!\left(\frac{\sqrt{2}\,y}{w}\right) e^{-(x^2+y^2)/w^2}\,. \tag{3.7}$$

This wave function of HG beam is also normalized as $\int |u_{nm}(x,y)|^2\,dx\,dy = 1$. The superposition (4.26) is like a Schmidt decomposition. In the special case

$$\Phi_{10} \;\;=\;\; \frac{2}{\sqrt{\pi}\,w^2}\,(x+i\,y)\,e^{-(x^2+y^2)/w^2}\,,$$

$$\Phi_{01} \;\;=\;\; \frac{2}{\sqrt{\pi}\,w^2}\,(x-i\,y)\,e^{-(x^2+y^2)/w^2}\,. \tag{3.8}$$

Motivated by the structural similarities between Eq.(3.1) for a quantum system and Eq.(4.26) for optical beams, we examine the possibilities of violations of Bell like inequalities for classical optical LG beams. For this, one needs to construct some Bell-like inequalities for continuous variable systems. The approach of using the Wigner function for demonstrating the violation of Bell inequalities for continuous variables in quantum optics has gained popularity in recent years [Jeong et al., 2003; Olivares and Paris, 2004; Zhang and Mukamel, 2007; Zhang et al., 2007]. Therefore, in the present work, we shall use the framework of obtaining Bell inequalities for continuous variable systems using the Wigner function.

3.3   Wigner function

The entanglement between continuous variable quantum systems (i.e., non-"qubit" quantum systems) is usually characterized in terms of the quasiprobabilities. It is well known that Wigner function is one of the important quasiprobabilities. For example, Banaszek and Wodkiewicz [Banaszek and Wodkiewicz, 1998, 1999] have shown that the Wigner function, expressed as an expectation value of a product of displaced parity operators, can be used to derive an analog of Bell inequalities in continuous variable systems. There exists an analogy between the measurement of spin-1/2 projectors and the parity operator, since the outcome of a measurement of the latter is also dichotomic. The solid angle defining the direction of the spin

in the former case, is replaced by the coherent displacement describing the shift in phase space in the latter. For a radiation field with two modes a and b, the Wigner function can be written as

$$W(\alpha, \beta) \;=\; \frac{4}{\pi^2} \left\langle D_1(\alpha)\,(-1)^{a^\dagger a}\,D_1^\dagger(\alpha) \,\otimes\, D_2(\beta)\,(-1)^{b^\dagger b}\,D_2^\dagger(\beta) \right\rangle, \quad (3.9)$$

where $D(\alpha)\left(= \exp\left\{a^\dagger \alpha - a\,\alpha^*\right\}\right)$ is the displacement operator for the coherent displacement α, and $\left[a, a^\dagger\right] = 1 = \left[b, b^\dagger\right]$ are the commutation relations.

3.4   Bell inequalities for continuous variable systems

In local hidden variable theories, the correlations between the outcomes of measurements on two spatially separated systems possessed by Alice and Bob with detector settings labeled by $\mathbf{a}$ and $\mathbf{b}$, respectively, may be written as a statistical average over hidden variables τ, of the functions $p\left(\mathbf{a}, \tau\right) = \pm 1$, and $p\left(\mathbf{b}, \tau\right) = \pm 1$, viz.

$$S\left(\mathbf{a}, \mathbf{b}\right) \;=\; \int d\tau\, \rho\left(\tau\right) p\left(\mathbf{a}, \tau\right) p\left(\mathbf{b}, \tau\right), \qquad (3.10)$$

where $\rho\left(\tau\right)$ is a local and positive distribution of the hidden variables τ. Using the choice of two different settings $(\mathbf{a}, \mathbf{a}', \mathbf{b}, \mathbf{b}')$ on either side, the Bell-CHSH inequality [Bell, 1964; Clauser et al., 1969], viz.

$$B \;\equiv\; \left|\, S\left(\mathbf{a}, \mathbf{b}\right) + S\left(\mathbf{a}, \mathbf{b}'\right) + S\left(\mathbf{a}', \mathbf{b}\right) - S\left(\mathbf{a}', \mathbf{b}'\right) \,\right| \;<\; 2 \qquad (3.11)$$

may be derived, which has been shown to be violated experimentally for quantum systems with correlations in discrete variables [Aspect, Dalibard, and Roger, 1982; Aspect, Grangier, and Roger, 1981, 1982]. A Bell inequality involving correlations between the discrete variables of polarization and parity has been shown to be violated in classical optics [Borges et al., 2010; Kagalwala et al., 2013].

For a radiation field with two modes a and b, we replace $S(\mathbf{a}, b)$ in Eq.(3.10) by the Wigner function given by the Eq.(3.9). Thus, for continuous variable systems,

one can test the violations of the inequality

$$B \;=\; \frac{\pi^2}{4} \, | \, W(\alpha,\beta) + W(\alpha,\beta') + W(\alpha',\beta) - W(\alpha',\beta') \, | \; < \; 2 \,. \quad (3.12)$$

Here, α's and β's are coherent displacements. We shall use the inequality (3.12) for classical light beams with topological singularities to find the features of quantum inspired optical entanglement. For this, in the next section we examine the violation of the Bell's inequality (3.12) for classical LG beams. Moreover, the Schmidt decomposition for LG beams contains many more terms for larger values of the orbital angular momentum [Agarwal and Banerji, 2002], and hence, one can expect a rise in the Bell measure for higher orbital angular momentum.

3.5   Violation of Bell's inequality through the Wigner function

We now apply the above framework to the case of LG beams. Defining the Wigner function as the Fourier transform of the electric field amplitude E, viz.

$$W(\mathbf{X},\mathbf{P}) \;=\; \frac{1}{\pi^2} \int d^2\xi \, e^{2 i \mathbf{P} \xi} \, \langle \, E^*(\mathbf{X} - \xi) \, E\,(\mathbf{X} - \xi) \, \rangle \,, \qquad (3.13)$$

has facilitated the experimental measurement of the Wigner function in terms of the two-point field correlations [Iaconis and Walmsley, 1996; Zhang and Mukamel, 2007]. The Wigner function has been calculated for LG beams [Simon and Agarwal, 2000] :

$$\begin{aligned}
W_{nm}(x,p_x;y,p_y) \;=\;& (-1)^{n+m} \, (\pi)^{-2} \, L_n \, [\, 4 \, (Q_0 + Q_2)] \\
& \times L_m \, [\, 4 \, (Q_0 - Q_2)] \, \exp \, (-\, 4 \, Q_0) \,,
\end{aligned}$$

$$(3.14)$$

where the expressions for Q_0 and Q_2 are given as follows :

$$\begin{aligned}
Q_0 \;&=\; \frac{1}{2} \left[\frac{x^2 + y^2}{w^2} + \frac{w^2}{4 \, \lambda_c^2} \, (p_x^2 + p_y^2 \,) \right] \,, \\
Q_2 \;&=\; \frac{x \, p_y - y \, p_x}{2 \, \lambda_c} \,.
\end{aligned} \qquad (3.15)$$

We shall make the following variable transformations,

$$x(y) \rightarrow \frac{w}{\sqrt{2}} \, X(Y), \quad p_x(p_y) \rightarrow \frac{\sqrt{2}\,\lambda_c}{w} \, P_X(P_Y), \tag{3.16}$$

where $\{X, \, P_X\}$ and $\{Y, \, P_Y\}$ are conjugate pairs of dimensionless quadratures. With the above transformations, $[\hat{x}, \hat{p}_x] = i\,\lambda_c$; $[\hat{y}, \hat{p}_y] = i\,\lambda_c$ becomes $[\hat{X}, \hat{P}_X] = i$; $[\hat{Y}, \hat{P}_Y] = i$, and the operators $\hat{P}_X$ and $\hat{P}_Y$ are given by

$$\hat{P}_X = -i\frac{\partial}{\partial X}, \quad \hat{P}_Y = -i\frac{\partial}{\partial Y}. \tag{3.17}$$

The Wigner function is rewritten in terms of the scaled variables as

$$\begin{aligned}
W_{nm}(X, P_X; Y, P_Y) &= (-1)^{n+m}\,(\pi)^{-2}\,L_n\left[4\,(Q_0 + Q_2)\right] \\
&\quad \times L_m\left[4\,(Q_0 - Q_2)\right]\exp\left(-4\,Q_0\right), \\
Q_0 &= \frac{1}{4}\left[X^2 + Y^2 + P_X^2 + P_Y^2\right], \\
Q_2 &= \frac{X\,P_Y - Y\,P_X}{2},
\end{aligned} \tag{3.18}$$

with the normalization

$$\int W_{nm}(X, P_X; Y, P_Y)\,dX\,dY\,dP_X\,dP_Y = 1. \tag{3.19}$$

For further proceedings of this work, we shall use this Wigner function of dimensionless quadratures. In terms of the Wigner function for the LG beam, we would search violations of the analog of Eq.(3.12) given by

$$\begin{aligned}
B &= \Pi_{nm}(X=0, P_X=0; Y=0, P_Y=0) + \Pi_{nm}(X, 0; 0, 0) \\
&\quad + \Pi_{nm}(0, 0; 0, P_Y) - \Pi_{nm}(X, 0; 0, P_Y) < 2,
\end{aligned} \tag{3.20}$$

where the Wigner transform Π_{nm} [Zhang et al., 2007] associated with the Wigner function $W_{nm}(X, P_X; Y, P_Y)$ is given by

$$\Pi_{nm}(X, P_X; Y, P_Y) = (\pi)^2\,W_{nm}(X, P_X; Y, P_Y). \tag{3.21}$$

We again emphasize that since the expression for correlations in joint measurement of separated observables given by Eq.(3.10) is not exclusive to the quantum domain, the above formulation of Bell inequalities through the Wigner function

may also be applied in classical theory.

3.5.1   Bell violation for n = 1, m = 0

First, we consider the state $\Phi_{10}(x, y)$ (given by Eq. (4.29)). In terms of the dimensionless variables (X, Y), $\Phi_{10}(X, Y)$ can be written as

$$\Phi_{10}(X, Y) \; = \; \frac{1}{\sqrt{\pi}} \, (X + i\, Y) \, \exp\left[-\frac{X^2 + Y^2}{2} \right]. \tag{3.22}$$

The corresponding normalized Wigner function is given by

$$W_{10}(X, P_X; Y, P_Y) \; = \; e^{-P_X^2 - P_Y^2 - X^2 - Y^2} \, \frac{\left[(P_X - Y)^2 + (P_Y + X)^2 - 1 \right]}{\pi^2}. \tag{3.23}$$

In order to obtain the Bell sum, we consider the Wigner transform [Zhang et al., 2007] $\Pi_{10}(X, P_X; Y, P_Y) = \pi^2 W_{10}(X, P_X; Y, P_Y)$. The two measurement settings on one side are chosen to be $\{X_1 = 0, P_{X_1} = 0\}$ or $\{X_2 = X, P_{X_2} = 0\}$, and the corresponding settings on the other side are $\{Y_1 = 0, P_{Y_1} = 0\}$ or $\{Y_2 = 0, P_{Y_2} = P_Y\}$ [Zhang et al., 2007]. Hence, the Bell sum associated with $\Pi_{10}(X, P_X; Y, P_Y)$ for the bimodal state $\Phi_{10}(X, Y)$ is given by

$$\begin{aligned}
B \; &= \; \Pi_{10}(X = 0, P_X = 0; Y = 0, P_Y = 0) \\
&\quad + \Pi_{10}(X, 0; 0, 0) + \Pi_{10}(0, 0; 0, P_Y) - \Pi_{10}(X, 0; 0, P_Y) \\
&= \; e^{-P_Y^2} \left(P_Y^2 - 1 \right) + e^{-X^2} \left(X^2 - 1 \right) \\
&\quad - e^{-P_Y^2 - X^2} \left[(P_Y + X)^2 - 1 \right] - 1. \tag{3.24}
\end{aligned}$$

Upon maximization of the Bell sum B with respect to parameters X and P_Y, we obtain the maximum Bell violation, $|B_{\max}| \sim 2.17$ which occurs for the choices of parameters $X \sim 0.45$, $P_Y \sim 0.45$ [Chowdhury, Majumdar, and Agarwal, 2013]. If one would like to compare this result with the result obtained in quantum mechanics, then the two-mode squeezed vacuum state can be considered for continuous variable systems. Because, this state gives the maximum Bell violation for any measurement settings in CV quantum systems and the increasing violation with the squeezing parameter reaches the maximum value $2\sqrt{2}$ of quantum mechanics for infinite squeezing. The maximum Bell violation through the Wigner function

for this state using similar settings (Eq. (3.24)) is given by $|B_{\max}|_{QM} \sim 2.19$ [Banaszek and Wodkiewicz, 1998, 1999].

3.5.2   Bell violation for higher values of n, m

Next, we consider the above analysis for higher values of n and m for the LG field amplitude. We use Eq. (4.31) and Eq. (3.21) to calculate the Bell sum. In the Fig. 3.1, we plot $|B|$ against X and P_Y for three different values of n keeping $m = 0$. From this figure, it is clear that the maximum violation of the Bell's inequality increases with higher orbital angular momentum [Chowdhury, Majumdar, and Agarwal, 2013]. The increase of Bell violations with n is analogous to the enhancement of nonlocality in quantum mechanics for many particle Greenberger-Horne-Zeilinger states or for higher spins [Gisin and Peres, 1992; Home and Majumdar, 1995; Mermin, 1990; Roy and Singh, 1991], an effect which may also be manifested in physical situations [Majumdar and Nayak, 2001]. Here, we have been able to demonstrate such an effect within the realm of classical theory.
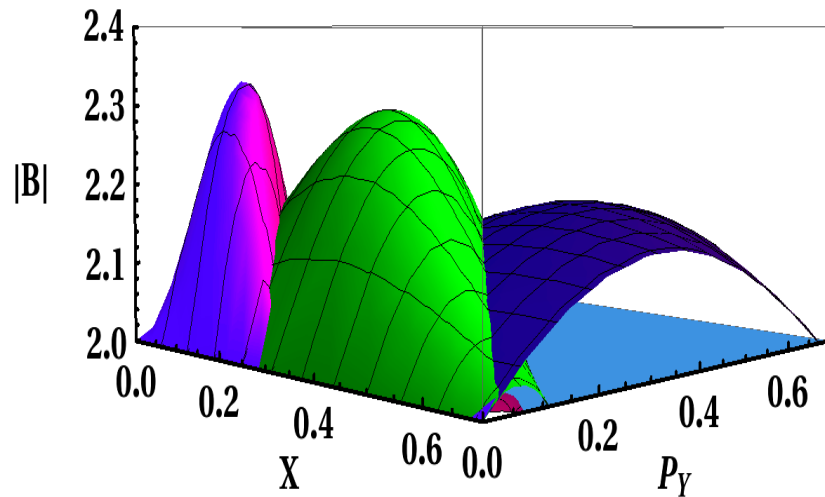
FIGURE 3.1: The plot shows the variation of the Bell sum $|B|$ with respect to dimensionless variables X and P_Y for different values of n, where $m = 0$. The indigo (right) curve is for $n = 1$, the green (centre) curve is for $n = 5$, and the magenta (left) curve is for $n = 30$.

For the purpose of experimental realization of the violation of Bell inequalities in classical optical systems with topological singularities, it may be worthwhile to

n	$|B_{\max}|$	n	$|B_{\max}|$
0	2.0	7	2.4833
1	2.23868	8	2.49236
2	2.34874	9	2.49964
3	2.40256	10	2.50561
4	2.43475	16	2.52683
5	2.45626	20	2.5343
6	2.47168	30	2.5446

TABLE 3.1: Maximum Violation of Bell-CHSH inequality by LG beam for different values of n keeping m=0.

employ techniques for enhancing the Bell violation. This is indeed possible using several approaches, and we would here like to point out two such schemes.

First, it has been observed [Jeong et al., 2003; Olivares and Paris, 2004] that the Bell violation may be further optimized by considering more general choice of settings than those used in the inequality (3.20), i.e.,

$$
\begin{aligned}
B &= \Pi_{n,m}(X_1, P_{X_1}; Y_1, P_{Y_1}) + \Pi_{n,m}(X_2, P_{X_2}; Y_1, P_{Y_1}) \\
&\quad + \Pi_{n,m}(X_1, P_{X_1}; Y_2, P_{Y_2}) - \Pi_{n,m}(X_2, P_{X_2}; Y_2, P_{Y_2}).
\end{aligned} \tag{3.25}
$$

Considering the $n = 1, m = 0$ case, and maximizing the Bell violation with respect to the parameters $X_1, P_{X_1}, X_2, P_{X_2}, Y_1, P_{Y_1}, Y_2, P_{Y_2}$, one obtains the maximum Bell violation, $|B_{\max}| = 2.24$ [Chowdhury, Majumdar, and Agarwal, 2013] which exceeds the maximum violation obtained through our earlier choice of settings given by the Eq. (3.24), and occurs for the choices of parameters $X_1 \sim -0.07$, $P_{X_1} \sim 0.05$, $X_2 \sim 0.4$, $P_{X_2} \sim -0.26$, $Y_1 \sim -0.05$, $P_{Y_1} \sim -0.07$, $Y_2 \sim 0.26$, $P_{Y_2} \sim 0.4$. Similarly, a corresponding increase of the Bell sum occurs for higher values of n too, which has demonstrated in the Table 3.1 [Chowdhury, Majumdar, and Agarwal, 2013]. For $n \to \infty$, the value of $|B_{\max}|$ approaches to the value $2\sqrt{2}$ of quantum mechanics.

Secondly, another method of obtaining a higher violation of Bell inequalities may be through elliptical transformation of LG beams. Such transformations are easily achievable in practice [Bandres and Gutierrez-Vega, 2008; Verrier et al., 2008], viz.

a Gaussian elliptical beam of the sort

$$\Phi \;=\; \frac{1}{\sqrt{\pi}}\,\exp\left[-\frac{X^2+Y^2}{2}\,\cosh(2t) \pm XY\,\sinh(2t)\right] \qquad (3.26)$$

is observed to increase the Bell violation for the $n=1, m=0$ case to 2.32.

3.6   Nonlocal correlations and Bell violations in vortex beams

The violation of the Bell's inequality which we have shown previously, is obtained as a result of the presence of nonvanishing nonlocal correlations between two separate modes or variables in separate directions of the type $\langle X, P_Y \rangle \neq 0$, which originates due to the finite and nonvanishing wavelength λ_c, resulting in the lack of precision in the simultaneous measurement of two observables corresponding to two different modes of light. In wave optics, the wavelength λ_c plays a role analogous to the Planck's constant $\hbar$ in quantum mechanics. Here, $\lambda_c \to 0$ leads to the limit of geometrical optics, again analogously to the quantum case where $\hbar \to 0$ gives the classical limit.

Let us now consider the quadrature phase components of two correlated and spatially separated light fields, $E_\alpha = C\left[\hat{\alpha}\,e^{-i\,\omega_\alpha t} + \hat{\alpha}^\dagger\,e^{i\,\omega_\alpha t}\right]$ (where, $\alpha \in \{a, b\}$, are the bosonic operators for two different modes, ω_α is the frequency, and C is a constant incorporating spatial factors taken to be equal for each mode). The quadrature amplitudes associated with these fields are given by

$$\hat{X}_\theta \;=\; \frac{\hat{a}\,e^{-i\,\theta} + \hat{a}^\dagger\,e^{i\,\theta}}{\sqrt{2}}\,, \quad \hat{Y}_\phi \;=\; \frac{\hat{b}\,e^{-i\,\phi} + \hat{b}^\dagger\,e^{i\,\phi}}{\sqrt{2}}\,, \qquad (3.27)$$

where

$$\begin{aligned}
\hat{a} &= \frac{X + i\,P_x}{\sqrt{2}}\,, \quad \hat{a}^\dagger = \frac{X - i\,P_x}{\sqrt{2}}\,, \\
\hat{b} &= \frac{Y + i\,P_y}{\sqrt{2}}\,, \quad \hat{b}^\dagger = \frac{Y - i\,P_y}{\sqrt{2}}\,,
\end{aligned} \qquad (3.28)$$

and the commutation relations of the bosonic operators are given by $[\hat{a}, \hat{a}^\dagger] = 1 = [\hat{b}, \hat{b}^\dagger]$. Now, using the Eq. (4.3) the expression for the quadratures can be

rewritten as

$$\hat{X}_\theta = \cos[\theta]\,\hat{X} + \sin[\theta]\,\hat{P}_x\,, \qquad \hat{Y}_\phi = \cos[\phi]\,\hat{Y} + \sin[\phi]\,\hat{P}_y\,. \qquad (3.29)$$

The correlations between the quadrature amplitudes $\hat{X}_\theta$ and $\hat{Y}_\phi$ are captured by the correlation coefficient, $C_{\theta,\phi}$ defined as [Ou et al., 1992; Reid, 1989; Tara and Agarwal, 1994]

$$C_{\theta,\phi} = \frac{\langle \hat{X}_\theta\,\hat{Y}_\phi \rangle}{\sqrt{\langle \hat{X}_\theta^2 \rangle\,\langle \hat{Y}_\phi^2 \rangle}}\,, \qquad (3.30)$$

where $\langle \hat{X}_\theta \rangle = 0 = \langle \hat{Y}_\phi \rangle$. The correlation is perfect for some values of θ and ϕ, if $|C_{\theta,\phi}| = 1$. Clearly, $|C_{\theta,\phi}| = 0$ for uncorrelated variables. For the case of LG beams with $n = 1, m = 0$, the correlation function is given by

$$C_{\theta,\phi}(\Phi_{10}(X,Y)) = \frac{1}{2}\sin[\phi - \theta]\,. \qquad (3.31)$$

Here, the maximum correlation strength $|C_{\theta,\phi}^{\max}| = \frac{1}{2}$ occurs for $\phi - \theta = \frac{k\pi}{2}$ (where k is an odd integer). For arbitrary values of n and m, it can be shown [Chowdhury, Majumdar, and Agarwal, 2013] that the expression for the maximum correlation function is given by

$$C_{\theta,\phi}^{\max} = \frac{\langle \hat{X}\,\hat{P}_Y \rangle}{\sqrt{\langle \hat{X}^2 \rangle\,\langle \hat{P}_Y^2 \rangle}} = -\frac{\langle \hat{P}_X\,\hat{Y} \rangle}{\sqrt{\langle \hat{P}_X^2 \rangle\,\langle \hat{Y}^2 \rangle}}\,. \qquad (3.32)$$

In Fig. 3.2, we provide a plot of the maximum correlation function for several values of n and m. The strength of the correlations increases with $n\,(m)$ [Chowdhury, Majumdar, and Agarwal, 2013], asymptotically reaching the limit of perfect correlations as n becomes very large, as is expected to be the case due to the presence of more and more terms in the Schmidt decomposition of LG beams [Agarwal and Banerji, 2002]. This feature thus further corroborates our earlier results of an increase in Bell violations for larger orbital angular momentum of LG beams.
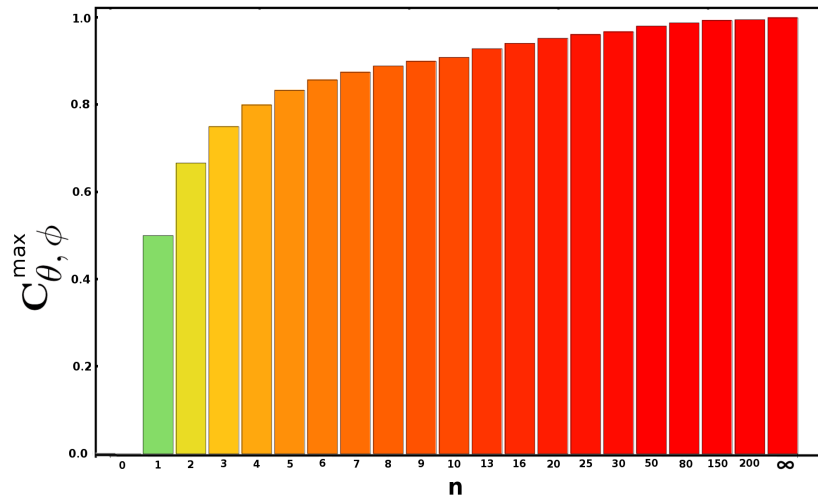
FIGURE 3.2: The plot shows the values of the maximum correlation function $C_{\theta,\phi}^{\max}$ for various values of n, where $m = 0$. Similar results are obtained by choosing $n = 0$ and varying m. Note that $C_{\theta,\phi} = 0$ for $n = m = 0$.

3.7   Conclusions

In this chapter, we have presented a study of nonlocal correlations in classical optical beams with topological singularities. These nonlocal correlations between two different light modes of LG beams are manifested through the violation of a Bell inequality using the Wigner function of this system. Here, we need to use the Wigner function as we are dealing with two continuous variables. The magnitude of the violation of the Bell inequality is shown to increase with the value of orbital angular momentum of the beam, an effect that is analogous to the enhancement of nonlocality for many particle Greenberger-Horne-Zeilinger states or for higher spins [Gisin and Peres, 1992; Home and Majumdar, 1995; Mermin, 1990; Roy and Singh, 1991]. We have also shown that the maximum of the correlation function between two correlated and spatially separated light modes increases with the orbital angular momentum of the beam. This feature thus further supports our earlier result of increase in Bell violations for larger orbital angular momentum of classical LG beams. Therefore, quantum nonlocality is reinterpreted in classical theory, where a violation of Bell's inequality corresponding to a particular light beam possessing classical entanglement signifies the impossibility of constructing such a beam using other beams with uncoupled degrees of freedom.

Our predicted values of the correlation function as a function of the beam parameters should be not difficult to realize experimentally, since production of such vortex beams has been achieved not only in the optical domain [Fickler et al., 2012; Singh et al., 2006], but recently has also been implemented for electron beams [McMorran, 2011; Verbeeck, Tian, and Schattschneider, 2010] having far-reaching applications. We conclude by noting that the feasibility of direct measurement of the two-point correlation function through shear Sagnac interferometry [Iaconis and Walmsley, 1996; Singh et al., 2006; Zhang and Mukamel, 2007] is a potentially promising avenue for experimental verification of our predicted Bell violation and its enhancement for vortex beams with higher angular momentum. We expect that these results hold also for other types of beams with no azimuthal symmetry. An example would be Bessel beams [Durnin, Miceli, Jr., and Eberly, 1987; Garces-Chavez et al., 2002; Mitri, 2008] of higher order $\left[J_l(\rho) \, e^{i l \theta}; \, l \neq 0 \right]$.

Chapter 4

Quantum steering for non-Gaussian entangled states

The understanding of the precise nature of correlations that lead to the EPR paradox had to wait for a number of years beyond Bell's derivation of his inequality, and further advances in quantum information theory. In this direction, a testable formulation of the EPR paradox was proposed by Reid [Reid, 1989] in the realm of continuous variable systems using the famous position-momentum Heisenberg uncertainty relation. To test the EPR paradox, Reid gave an inequality involving products of inferred variances of incompatible observables [Drummond and Reid, 1990; Tara and Agarwal, 1994]. The realization of the EPR paradox was observed in some subsequent experimental works [Ou et al., 1992]. For two mode squeezed vacuum states, recently a much stronger violation of the Reid inequality has been experimentally demonstrated [Steinlechner et al., 2013]. However, in systems with correlations manifesting in higher than the second moment, the Reid formulation generally fails to show occurrence of the EPR paradox, even though Bell nonlocality may be exhibited [Chowdhury, Majumdar, and Agarwal, 2013; Walborn et al., 2011].

After Reid's formulation of EPR paradox, Wiseman et al. have proposed a more direct manifestation of EPR-type correlations in terms of an information-theoretic task [Cavalcanti et al., 2009; Wiseman, Jones, and Doherty, 2007]. Using similar formulations for all the three types of correlations, they have shown that entanglement is the weakest, Bell violation is the strongest form of correlation, and steering

takes the intermediate position between them. These differences have been demonstrated experimentally for mixed entangled states of two qubits [Saunders et al., 2010]. The case of continuous variable states however poses an additional difficulty, since there exist several pure entangled states, which do not display steering through the Reid criterion based on variances of observables [Reid, 1989]. In order to exploit higher order correlation in such states, Walborn et al. [Walborn et al., 2011] proposed a new steering condition, which is derived using the more stronger entropic uncertainty principle [Bialynicki-Birula and Mycielski, 1975]. The Reid criterion can be seen to follow as a limiting case of the entropic steering relation [Walborn et al., 2011]. Generalizations of entropic steering inequalities to the case of symmetric steering [Schneeloch et al., 2013], loss-tolerant steering [Evans, Cavalcanti, and Wiseman, 2013], as well as to the case of steering with quantum memories [Schneeloch, Broadbent, and Howell, 2014] has also been proposed recently.

EPR steering for Gaussian states has been studied extensively both theoretically and experimentally. It is realized though that Gaussian states are a rather special class of states, and there exist very common examples of states, such as the superposition of two oscillators in Fock states that are far from Gaussian in nature. The non-Gaussian states generally have a higher degree of entanglement than the Gaussian states. Since the steering of correlated systems has started to be studied only recently, it is important to understand the steering of systems with non-Gaussian correlations. Recently, Walborn et al. Walborn et al. [2011] have shown the steerability for a particular example of non-Gaussian state through the entropic steering inequality. In this chapter, we shall consider several categories of non-Gaussian states with the motivation of investigating EPR steering of such states.

4.1 The EPR paradox and steering

Here, we consider two parties Alice and Bob, who possess systems A and B respectively. Now, to understand the EPR paradox, we have to consider a bipartite entangled state shared between the systems A and B. This state may be expressed

in two different ways, as

$$|\Psi\rangle \;=\; \sum_{n=1}^{\infty} c_n \,|\psi_n\rangle \,|u_n\rangle \;=\; \sum_{n=1}^{\infty} d_n \,|\phi_n\rangle \,|v_n\rangle\,, \tag{4.1}$$

where $\{|u_n\rangle\}$ and $\{|v_n\rangle\}$ are two orthonormal bases for one of the parties (say, Alice). If Alice's choice is to measure in the $\{|u_n\rangle\}$ basis, then Bob's system is projected instantaneously into one of the states $|\psi_n\rangle$. Similarly, if Alice measures in the $\{|v_n\rangle\}$ basis, she instantaneously projects Bob's system into one of the states $|\phi_n\rangle$. This ability of Alice to affect Bob's state through her choice of the measurement basis was dubbed "steering" by Schrödinger [Schrödinger, 1935, 1936]. Since there is no direct physical interaction between Alice and Bob, it is paradoxical that the ensemble of $|\psi_n\rangle$'s is different from the ensemble of $|\phi_n\rangle$'s.

The EPR paradox stems from the correlations between two noncommuting observables of a subsystem with those of the other subsystem, i.e., $\langle x, p_y\rangle \neq 0$, with $\langle x\rangle = 0 = \langle p_y\rangle$ individually. In the original formulation of the paradox, correlations between the measurement outcomes of positions and momenta for two separated particles were considered. Due to the presence of correlations, the measurement of the position of, say, the first particle leads one to infer the correlated value of the position for the second particle (say, x_{inf}). Now, if the momentum of the second particle is measured giving the outcome, say p, the value of the product of uncertainties $(\Delta x_{\mathrm{inf}})^2\,(\Delta p_{\mathrm{inf}})^2$ may turn out to be less than that allowed by the uncertainty principle, viz. $(\Delta x)^2\,(\Delta p)^2 \geq 1$, thus leading to the paradox. In the following section, we shall try primarily to fix the setting for our work on non-Gaussian entangled states.

4.2 The Reid inequality and its validation

The possibility of demonstrating the EPR paradox in the context of continuous variable correlations was first proposed by Reid [Reid, 1989]. Such an idea has been experimentally realized [Ou et al., 1992] through quadrature phase measurements performed on the two output beams of a nondegenerate parametric amplifier. This technique of demonstrating the product of variances of the inferred values of correlated observables to be less than that allowed by the uncertainty principle, has since gained popularity [Drummond and Reid, 1990; Tara and Agarwal, 1994], and

has been employed recently for variables other than position and momentum, e.g., for correlations between optical and orbital angular momentum of light emitted through spontaneous parametric down-conversion [Leach et al., 2010].

4.2.1 Formulation of the Reid inequality

Let us now consider the situation where the quadrature phase components of two correlated and spatially separated light fields are measured. Here, we consider the light fields like $E_\gamma = C\left[\hat{\gamma}\, e^{-i\,\omega_\gamma\, t} + \hat{\gamma}^\dagger e^{i\,\omega_\gamma\, t}\right]$, where $\gamma \in \{a, b\}$ are the bosonic operators for two different modes, ω_γ is the frequency, and C is a constant incorporating spatial factors taken to be equal for each mode. The quadrature amplitudes associated with these fields are given by

$$\hat{X}_\theta = \frac{\hat{a}\, e^{-i\,\theta} + \hat{a}^\dagger e^{i\,\theta}}{\sqrt{2}}, \quad \hat{Y}_\phi = \frac{\hat{b}\, e^{-i\,\phi} + \hat{b}^\dagger e^{i\,\phi}}{\sqrt{2}}, \tag{4.2}$$

where

$$\begin{aligned} \hat{a} &= \frac{X + i\, P_x}{\sqrt{2}}, & \hat{a}^\dagger &= \frac{X - i\, P_x}{\sqrt{2}}, \\ \hat{b} &= \frac{Y + i\, P_y}{\sqrt{2}}, & \hat{b}^\dagger &= \frac{Y - i\, P_y}{\sqrt{2}}. \end{aligned} \tag{4.3}$$

Here, the commutation relations of the bosonic operators are given by $[\hat{a}, \hat{a}^\dagger] = 1 = [\hat{b}, \hat{b}^\dagger]$. Now, using Eq. (4.3) the expression for the quadratures can be rewritten as

$$\hat{X}_\theta = \cos[\theta]\, \hat{X} + \sin[\theta]\, \hat{P}_x, \qquad \hat{Y}_\phi = \cos[\phi]\, \hat{Y} + \sin[\phi]\, \hat{P}_y. \tag{4.4}$$

The amplitudes, $\hat{X}_\theta$ and $\hat{Y}_\phi$ are correlated to each other. The correlations between these quadrature amplitudes can be captured by the correlation coefficient, $C_{\theta,\phi}$. The correlation coefficient is defined as [Drummond and Reid, 1990; Ou et al., 1992; Reid, 1989; Tara and Agarwal, 1994]

$$C_{\theta,\phi} = \frac{\langle \hat{X}_\theta\, \hat{Y}_\phi \rangle}{\sqrt{\langle \hat{X}_\theta^2 \rangle\, \langle \hat{Y}_\phi^2 \rangle}}, \tag{4.5}$$

where $\langle \hat{X}_\theta \rangle = 0 = \langle \hat{Y}_\phi \rangle$. The correlation will be perfect, i.e., $|C_{\theta,\phi}| = 1$ for some values of θ and ϕ. Clearly, for uncorrelated quadrature amplitudes $|C_{\theta,\phi}| = 0$.

Due to the presence of correlations between the quadrature amplitudes $\hat{X}_\theta$ and $\hat{Y}_\phi$, the quadrature amplitude $\hat{X}_\theta$ can be inferred by measuring the corresponding amplitude $\hat{Y}_\phi$. The EPR paradox arises due to the ability to infer an observable of one system from the result of measurement performed on a spatially separated second system. In realistic situations, the correlations can not be perfect because of the interaction with the environment, finite detector efficiency, etc. Hence, the estimated amplitudes $\hat{X}_{\theta_1}$ and $\hat{X}_{\theta_2}$ with the help of the measurement results of $\hat{Y}_{\phi_1}$ and $\hat{Y}_{\phi_2}$, respectively, are given by [Reid, 1989]

$$\hat{X}^e_{\theta_1} \,=\, g_1\,\hat{Y}_{\phi_1}\,, \quad \hat{X}^e_{\theta_2} \,=\, g_2\,\hat{Y}_{\phi_2}\,, \tag{4.6}$$

where g_1 and g_2 are scaling parameters. Now, one may choose g_1, g_2, ϕ_1, and ϕ_2 in such a way that $\hat{X}_{\theta_1}$ and $\hat{X}_{\theta_2}$ are inferred with the highest possible accuracy. The estimated amplitudes are subject to inference errors, which arise due to the deviation of the estimated amplitudes from the true amplitudes $\hat{X}_{\theta_1}$ and $\hat{X}_{\theta_2}$, and are captured by $(\hat{X}_{\theta_1} - \hat{X}^e_{\theta_1})$ and $(\hat{X}_{\theta_2} - \hat{X}^e_{\theta_2})$, respectively. The average errors of the inferences are given by

$$
\begin{aligned}
(\Delta_{\mathrm{inf}}\hat{X}_{\theta_1})^2 &\,=\, \langle(\hat{X}_{\theta_1} - \hat{X}^e_{\theta_1})^2\rangle \,=\, \langle(\hat{X}_{\theta_1} - g_1\,\hat{Y}_{\phi_1})^2\rangle\,, \\
(\Delta_{\mathrm{inf}}\hat{X}_{\theta_2})^2 &\,=\, \langle(\hat{X}_{\theta_2} - \hat{X}^e_{\theta_2})^2\rangle \,=\, \langle(\hat{X}_{\theta_2} - g_2\,\hat{Y}_{\phi_2})^2\rangle\,.
\end{aligned}
\tag{4.7}
$$

The values of the scaling parameters g_1 and g_2 are chosen such that $\frac{\partial(\Delta_{\mathrm{inf}}\hat{X}_{\theta_1})^2}{\partial g_1} = 0 = \frac{\partial(\Delta_{\mathrm{inf}}\hat{X}_{\theta_2})^2}{\partial g_2}$, from which it follows that

$$g_1 = \frac{\langle\hat{X}_{\theta_1}\,\hat{Y}_{\phi_1}\rangle}{\langle\hat{Y}^2_{\phi_1}\rangle}\,, \quad g_2 = \frac{\langle\hat{X}_{\theta_2}\,\hat{Y}_{\phi_2}\rangle}{\langle\hat{Y}^2_{\phi_2}\rangle}\,. \tag{4.8}$$

The values of ϕ_1 (ϕ_2) are obtained by maximizing C_{θ_1,ϕ_1} (C_{θ_2,ϕ_2}). Now, due to the commutation relations $[\hat{X},\hat{P}_X] = i\,;\ [\hat{Y},\hat{P}_Y] = i$, it is required that the product of the variances of the above inferences $(\Delta_{\mathrm{inf}}\hat{X}_{\theta_1})^2\,(\Delta_{\mathrm{inf}}\hat{X}_{\theta_2})^2 \geq 1/4$. Hence, the EPR paradox occurs if the correlations in the field quadratures lead to the condition

$$\mathcal{S}_{\mathrm{EPR}} \equiv (\Delta_{\mathrm{inf}}\hat{X}_{\theta_1})^2\,(\Delta_{\mathrm{inf}}\hat{X}_{\theta_2})^2 \,<\, \frac{1}{4}\,. \tag{4.9}$$

4.2.2 Example of steerability of two mode squeezed vacuum state

Let us consider a two mode squeezed vacuum state $|\text{NOPA}\rangle$, produced in non-degenerate optical parametric amplifier. This is actually a two mode entangled Gaussian state. The mathematical expression of this state is given by [Agarwal, 2013]

$$| \text{NOPA} \rangle = |\xi\rangle = S(\xi)|0,0\rangle = \sqrt{1-\lambda^2} \sum_{n=0}^{\infty} \lambda^n |n,n\rangle, \qquad (4.10)$$

where $\lambda = \tanh(r) \in [0,1]$, the squeezing parameter $r > 0$ and $|m,n\rangle = |m\rangle_A \otimes |n\rangle_B$ (where $|m\rangle$ and $|n\rangle$ are the usual Fock states). $S(\xi)$ $(= e^{\xi \hat{a}_1^\dagger \hat{a}_2^\dagger - \xi^* a_1 a_2}$, where $\xi = r\,e^{i\phi})$ is the squeezing operator (unitary). A and B are the two involved modes for Alice and Bob respectively.

For the NOPA state given by Eq. (4.10), the inferred uncertainties is given by

$$(\Delta_{\text{inf}} X_\theta)^2 = \frac{1}{2}\cosh[2r] - \frac{1}{2}\tanh[2r]\sinh[2r]\cos^2[\theta + \phi], \qquad (4.11)$$

where the quadrature amplitude X_θ is inferred by measuring the corresponding amplitude Y_ϕ. For two different values of θ, i.e., $\theta_1 = 0$ and $\theta_2 = \pi/2$, the minimum values of $(\Delta_{\text{inf}} X_\theta)^2$ are

$$(\Delta_{\text{inf}} X_{\theta_1})^2 = (\Delta_{\text{inf}} X_{\theta_2})^2 = \frac{1}{2\cosh[2r]}, \qquad (4.12)$$

which occur for $\phi_1 = 0$ and $\phi_2 = \pi/2$, respectively. The product of uncertainties is thus $\frac{1}{4\cosh^2[2r]}$, which has the value $1/4$ for $r \to 0$, and asymptotically reaches the value 0 for $r \to \infty$. This shows that the Reid condition (4.9) for occurrence of the EPR paradox holds. Hence, the two mode squeezed vacuum state shows EPR steering for all values of r except at $r = 0$.

4.3 Limitations of the Reid inequality

The Reid inequality is effective in demonstrating the EPR paradox for systems in which correlations appear at the level of variances, i.e., the Reid criterion can detect steerability of Gaussian states. However, this criterion fails to demonstrate

steering by more general non-Gaussian states, for example, the two-dimensional harmonic oscillator, as we will show later in this chapter [Chowdhury et al., 2014].

4.4   Steering as an information-processing task

A modern formulation of EPR steering was presented by Wiseman et al. [Cavalcanti et al., 2009; Wiseman, Jones, and Doherty, 2007] as an information-processing task. They considered that one of the two parties (say, Alice) prepares system A and system B in a combined state ρ_{AB}, and sends system B to Bob. The procedure is repeated as many times as required. Bob's particle is assumed to possess a definite state, even if it is unknown to him (local hidden state). Bob also believes that his particle is quantum and he will make quantum measurements on his particle. No such assumptions are made for Alice, and hence this formulation of steering is an asymmetric task. Alice and Bob make measurements on their respective particles, and communicate classically. Alice's task is to convince Bob that the state they share is entangled. If correlations between Bob's measurement results and Alice's declared results can be explained by a local hidden state (LHS) model for Bob, he is not convinced. This is because Alice may cheat him in a way that she could have drawn a pure state at random from some ensemble and sent it to Bob, and then chosen her result based on her knowledge of this LHS. Conversely, if the correlations cannot be so explained, then the state must be entangled. Alice will be successful in her task of steering if she can create genuinely different ensembles for Bob by steering Bob's state. It may be noted that a similar formulation of Bell nonlocality as an information-theoretic task is also possible [Wiseman, Jones, and Doherty, 2007], where Alice and Bob, both will not be restricted to possess quantum particles, and the correlations between Alice and Bob may be described in terms of a local hidden variable (LHV) model.

In the above situation, an EPR steering inequality [Cavalcanti et al., 2009] may be derived involving an experimental situation for qubits with n measurement settings for each side. Bob's k-th measurement setting is taken to correspond with the observable $\hat{\sigma}_k$, and Alice's declared result is denoted by the random variable $A_k \to \{-1, 1\}$. Violation of the inequality

$$\frac{1}{n} \sum_{k=1}^{n} \langle A_k \hat{\sigma}_k \rangle \ \leq \ C_n \tag{4.13}$$

reveals the occurrence of steering, where

$$C_n \equiv \max_{\{A_k\}} \left(\frac{\lambda_{\max}}{n} \sum_{k=1}^{n} A_k \, \hat{\sigma}_k \right) .$$

C_n is the maximum value of the left-hand side of the inequality (4.13) if Bob has a preexisting state known to Alice, with $\lambda_{\max}$ being the largest eigenvalue of the operator $\frac{1}{n} \sum_{k=1}^{n} A_k \, \hat{\sigma}_k$. Experimental demonstration of steering for mixed entangled states [Saunders et al., 2010] that are Bell local has confirmed that steering is a weaker form of correlations compared to nonlocality.

4.5 The entropic steering inequality and its formulation

For the case of continuous variable systems, the Reid criterion is an indicator for steering. However, there exist several pure entangled continuous variable states which do not reveal steering through the Reid criterion. An example of such a state is provided in Ref. [Walborn et al., 2011]. Since entanglement is a weaker form of correlations compared to steering [Cavalcanti et al., 2009; Wiseman, Jones, and Doherty, 2007], it is clear that for such states the steering correlations do not appear up to second order (variances) that may be checked by the Reid criterion. The Reid criterion itself is derived using the Heisenberg uncertainty relation involving product of variances of noncommuting observables. On the other hand, more stronger uncertainty relation will give more stronger steering inequality. A more general form of the uncertainty relation of, for example, the position and momentum distributions of a quantum system is provided by the entropic uncertainty relation [Bialynicki-Birula and Mycielski, 1975] given by

$$h_Q(X) + h_Q(P) \geq \ln \pi e, \tag{4.14}$$

which is lower bounded by $\ln \pi e$. Here, h_Q is the Shannon entropy for the measurement of observables i, where $i \in \{X, P\}$. As the entropic function contains correlations of all orders, the entropic uncertainty relation is stronger than the Heisenberg uncertainty relation.

4.5.1 Formulation of the entropic steering inequality

Walborn et al. [Walborn et al., 2011] have derived an entropic steering inequality on the basis of the stronger entropic uncertainty relation. They have considered a joint probability distribution of two parties, Alice and Bob, corresponding to a nonsteerable state for which there exists a local hidden state (LHS) description, given by

$$\mathcal{P}(r_A, r_B) = \sum_\lambda \mathcal{P}(\lambda)\,\mathcal{P}(r_A \,|\, \lambda)\,\mathcal{P}_Q(r_B \,|\, \lambda), \qquad (4.15)$$

where r_A and r_B are the outcomes of measurements of the observables R_A and R_B respectively; λ's are hidden variables that specify an ensemble of states; $\mathcal{P}$ are general probability distributions; and $\mathcal{P}_Q$ are probability distributions corresponding to the quantum state possessed by Bob, and specified by λ. Now, using a rule for conditional probabilities $P(a, b \,|\, c) = P(b \,|\, c)\,P(a \,|\, b)$ which holds when $\{b\} \in \{c\}$, i.e., there exists a local hidden state of Bob predetermined by Alice, it follows that the conditional probability $\mathcal{P}(r_B \,|\, r_A)$ becomes

$$\mathcal{P}(r_B \,|\, r_A) = \sum_\lambda \mathcal{P}(r_B, \lambda \,|\, r_A) \qquad (4.16)$$

with $P(r_B, \lambda \,|\, r_A) = P(\lambda \,|\, r_A)\,P_Q(r_B \,|\, \lambda)$. It is clear that (4.15) and (4.16) are equivalent conditions for nonsteerability. Next, we consider the relative entropy for two distributions $p(X)$ and $q(X)$ defined as

$$\mathcal{H}(p(X) \,||\, q(X)) = \sum_x p_x \ln(p_x/q_x). \qquad (4.17)$$

So, the positivity of the relative entropy between the probability distributions $\mathcal{P}(r_B, \lambda \,|\, r_A)$ and $\mathcal{P}(\lambda \,|\, r_A)\,\mathcal{P}(r_B \,|\, r_A)$ gives that

$$\sum_\lambda \int dr_B\, \mathcal{P}(r_B, \lambda \,|\, r_A) \ln \frac{\mathcal{P}(r_B, \lambda \,|\, r_A)}{\mathcal{P}(\lambda \,|\, r_A)\,\mathcal{P}(r_B \,|\, r_A)} \geq 0. \qquad (4.18)$$

Using the nonsteering condition (4.16), the definition of conditional entropy which is given by

$$h(X \,|\, Y) = -\sum_{x,y} p(x, y) \ln p(x \,|\, y), \qquad (4.19)$$

and averaging over all measurement outcomes r_A, it follows that the conditional entropy $h(R_B \mid R_A)$ satisfies

$$h(R_B \mid R_A) \geq \sum_\lambda \mathcal{P}(\lambda) \, h_Q(R_B \mid \lambda). \tag{4.20}$$

Considering a pair of variables S_A, S_B conjugate to R_A, R_B respectively, a similar bound on the conditional entropy may be written as

$$h(S_B \mid S_A) \geq \sum_\lambda \mathcal{P}(\lambda) \, h_Q(S_B \mid \lambda). \tag{4.21}$$

For the LHS model for Bob, it is clear that the entropic uncertainty relation (4.14) holds for each state marked by λ. Averaging over all hidden variables, it follows that

$$\sum_\lambda \mathcal{P}(\lambda) \left[h_Q(R_B \mid \lambda) + h_Q(S_B \mid \lambda) \right] \geq \ln \pi e. \tag{4.22}$$

Now, using the bounds (4.20) and (4.21) in the relation (4.22), one gets the entropic steering inequality given by

$$h(R_B \mid R_A) + h(S_B \mid S_A) \geq \ln \pi e. \tag{4.23}$$

The violation of the inequality (4.23) for a given state will give the demonstration of steerability of that state. Using the relation between information entropy and variance, it has been further shown by Walborn et al. [Walborn et al., 2011] that the Reid criterion follows in the limiting case of the entropic steering relation (4.23). So, the entropic steering inequality should be stronger than the Reid criterion for steering.

4.5.2 An example of steering

Walborn et al. [Walborn et al., 2011] have presented an example of the state given by (up to a suitable normalization)

$$\phi_n(x_A, x_B) = \mathcal{H}_n \left(\frac{x_A + x_B}{\sqrt{2}\,\sigma_+} \right) e^{-(x_A+x_B)^2/4\sigma_+^2} \, e^{-(x_A-x_B)^2/4\sigma_-^2}, \tag{4.24}$$

where $\mathcal{H}_n$ is the nth-order Hermite polynomial, which does not reveal steering using the Reid criterion when $\sigma_\pm / \sigma_\mp < 1 + 1.5\sqrt{n}$, whereas the entropic steering criterion (4.23) is able to show steering except when the state is separable, i.e., for $n = 0$, and $\sigma_+ = \sigma_-$. In the following section, we will use the entropic steering inequality for demonstrating steering by several continuous variable non-Gaussian states.

4.6 Steering and nonlocality for non-Gaussian states

Now, we shall study steering and nonlocality for several non-Gaussian states. First, we shall study the steering and nonlocal properties of the entangled states constructed using the eigenstates of the two-dimensional harmonic oscillator, i.e., Laguerre-Gaussian (LG) beams. Then, we shall discuss some properties for non-Gaussian states obtained by subtracting single and two photons from two-mode squeezed vacuum states. The steerability of these states will be tested through both the Reid criterion and the entropic steering criterion. Also, we shall compare the strength of steering with the degree of nonlocality, i.e., the amount of Bell violation for such states. Finally, we investigate the nonlocal and steering properties of another class of non-Gaussian states, viz. NOON states.

4.6.1 Non-Gaussian entangled states of a two-dimensional harmonic oscillator

The importance of the two-dimensional harmonic oscillator cannot be overemphasized in the context of quantum mechanics. The historical development of radiation theory started with the correspondence of the two modes of the radiation field. The classic problem of the charged particle in an electromagnetic field leading to the existence of Landau levels was developed using the same machinery.

4.6.1.1 The Laguerre-Gaussian (LG) wave function and the corresponding Wigner function

The energy eigenfunctions of the two-dimensional harmonic oscillator may be expressed in terms of Hermite-Gaussian (HG) functions given by

$$
u_{nm}(x,y) = \sqrt{\frac{2}{\pi}} \left(\frac{1}{2^{n+m} \, w^2 \, n! \, m!} \right)^{1/2} H_n \left(\frac{\sqrt{2} \, x}{w} \right) H_m \left(\frac{\sqrt{2} \, y}{w} \right) e^{-(x^2+y^2)/w^2} ,
\tag{4.25}
$$

and this is normalized, i.e., $\int | \, u_{nm}(x,y) \, |^2 \, dx \, dy = 1$. Superpositions of HG wave functions [Beigersbergen et al., 1993; Danakas and Aravind, 1992] may construct entangled states as follows

$$
\Phi_{nm}(\rho,\theta) = \sum_{k=0}^{n+m} u_{n+m-k,k} \, (x,y) \, \frac{f_k^{(n,m)}}{k!} \left(\sqrt{-1} \right)^k \sqrt{\frac{k! \, (n+m-k)!}{n! \, m! \, 2^{n+m}}} ,
\tag{4.26}
$$

$$
f_k^{(n,m)} = \frac{d^k}{dt^k} [(1-t)^n (1+t)^m]|_{t=0} ,
\tag{4.27}
$$

where $\Phi_{nm}(\rho,\theta)$ are the well-known Laguerre-Gaussian functions. The LG beams are physically realizable field configurations [Fickler et al., 2012; Molina-Terriza, Torres, and Torner, 2007] containing optical vortices with interesting topological [Nye and Berry, 1974] and coherence [Agarwal and Banerji, 2002; Simon and Agarwal, 2000] properties. Using the Eq. (4.25), the LG beam can be rewritten as [Agarwal, 2013]

$$
\Phi_{nm}(\rho,\theta) = e^{i \, (n-m) \, \theta} e^{-\rho^2/w^2} \, (-1)^{\min(n,m)} \left(\frac{\rho \sqrt{2}}{w} \right)^{|n-m|}
$$

$$
\times \sqrt{\frac{2}{\pi \, n! \, m! \, w^2}} \, L_{\min(n,m)}^{|n-m|} \left(\frac{2 \, \rho^2}{w^2} \right) [\min(n,m)]!
\tag{4.28}
$$

with $\int | \, \Phi_{nm}(\rho,\theta) \, |^2 \, dx \, dy = 1$, where w is the beam waist, $l = |n-m|$ is the angular momentum and $L_p^l(x)$ is the generalized Laguerre polynomial. As the superposition (4.26) is like a Schmidt decomposition, which plays a key role in

defining the quantum entanglement, the Schmidt form (4.26) signifies the entanglement of the LG wave functions. In the special case

$$
\begin{aligned}
\Phi_{10} &= \frac{2}{\sqrt{\pi}\,w^2}\,(x + i\,y)\,e^{-(x^2+y^2)/w^2}, \\
\Phi_{01} &= \frac{2}{\sqrt{\pi}\,w^2}\,(x - i\,y)\,e^{-(x^2+y^2)/w^2}.
\end{aligned}
\tag{4.29}
$$

It is henceforth convenient to work with the pair of dimensionless quadratures $\{X,\ P_X\}$ and $\{Y,\ P_Y\}$, given by

$$
x\,(y) \to \frac{w}{\sqrt{2}}\ X\,(Y), \qquad p_x\,(p_y) \to \frac{\sqrt{2}\,\hbar}{w}\ P_X\,(P_Y).
\tag{4.30}
$$

The canonical commutation relations are $[\hat{X}, \hat{P}_X] = i$, $[\hat{Y}, \hat{P}_Y] = i$, and the operator $\hat{P}_X$ and $\hat{P}_Y$ are given by $\hat{P}_X = -i\frac{\partial}{\partial X}$ and $\hat{P}_Y = -i\frac{\partial}{\partial Y}$, respectively. The Wigner function corresponding to the LG wave function in terms of the scaled variables is given by

$$
\begin{aligned}
W_{nm}(X, P_X; Y, P_Y) &= \frac{(-1)^{n+m}}{\pi^2}\,L_n\left[4\,(Q_0 + Q_2)\right] \\
&\quad \times L_m\left[4\,(Q_0 - Q_2)\right]\,\exp\left(-4\,Q_0\right),
\end{aligned}
\tag{4.31}
$$

where

$$
\begin{aligned}
Q_0 &= \frac{1}{4}\left[X^2 + Y^2 + P_X^2 + P_Y^2\right], \tag{4.32}\\
Q_2 &= \frac{X\,P_Y - Y\,P_X}{2}. \tag{4.33}
\end{aligned}
$$

The Wigner function is one of the important quasiprobabilities and the reason behind using it here is that we can get easily the marginal probabilities from the Wigner function. From the form of Q_2, we may state that LG beams have $\langle X\,P_Y \rangle \neq 0$ type correlations between two different light modes. In next sections, we shall use this Wigner function to detect steering and Bell nonlocality of the state.

4.6.1.2   The steerability of LG beams

Now, we shall analysis the quantum correlations present in the LG wave functions for the purpose of demonstrating steering.

Steerability through the Reid criterion :

Let us now check how the Reid criterion applies to the case of LG wave functions. In order to do so, we shall estimate the product of uncertainties of the values of inferred observables $(\Delta_{\text{inf}} X_{\theta_1})^2 (\Delta_{\text{inf}} X_{\theta_2})^2$. This is performed by maximizing the correlation function C_{θ_1, ϕ_1} and C_{θ_2, ϕ_2}. Using Eqs. (4.7) and (4.8), it follows that

$$(\Delta_{\text{inf}} X_\theta)^2 = \langle X_\theta^2 \rangle \left[1 - \left(C_{\theta,\phi}^{\max} \right)^2 \right] . \tag{4.34}$$

The maximum correlation strength $|C_{\theta,\phi}^{\max}| = \frac{1}{2}$ occurs for $\phi - \theta = \frac{k\pi}{2}$, where k is an odd integer. For arbitrary values of n and m, it can be shown that the expression of the maximum correlation function is given by

$$C_{0,\pi/2}^{\max} = \frac{\langle \hat{X} \hat{P}_Y \rangle}{\sqrt{\langle \hat{X}^2 \rangle \langle \hat{P}_Y^2 \rangle}} , \qquad C_{\pi/2,\pi}^{\max} = -\frac{\langle \hat{P}_X \hat{Y} \rangle}{\sqrt{\langle \hat{P}_X^2 \rangle \langle \hat{Y}^2 \rangle}} . \tag{4.35}$$

In Fig. 4.1, we have plotted the product of uncertainties $(\Delta_{\text{inf}} X_{\theta_1})^2 (\Delta_{\text{inf}} X_{\theta_2})^2$ versus the angular momentum n. It is seen that for each n, $(\Delta_{\text{inf}} X_{\theta_1})^2 (\Delta_{\text{inf}} X_{\theta_2})^2 \geq 1/4$ [Chowdhury et al., 2014]. Therefore, the Reid criterion given by Eq. (4.9) is not satisfied for any value of n. Hence, it is not possible to demonstrate steering by entangled LG modes using the Reid criterion.

Steerability through the entropic steering criterion :

We now apply the entropic steering criterion to the case of the LG wave functions. In the entropic steering inequality given by the Eq. (4.23), the observables have to be chosen such that there exist correlations between R_A and R_B (S_A and S_B). For the case of the LG wave functions, we shall use the nonvanishing $\langle X P_Y \rangle$ type correlations, as evident from the Wigner function (4.33). Thus, in terms of the conjugate pairs of dimensionless quadratures, the inequality (4.23) becomes

$$h(\mathcal{X} | \mathcal{P_Y}) + h(\mathcal{P_X} | \mathcal{Y}) \geq \ln \pi e , \tag{4.36}$$

where X, Y, P_X, and P_Y are the outcomes of measurements $\mathcal{X}$, $\mathcal{Y}$, $\mathcal{P_X}$, and $\mathcal{P_Y}$ respectively. Here, the conditional entropies $h(\mathcal{X} | \mathcal{P_Y})$ and $h(\mathcal{P_X} | \mathcal{Y})$ are given
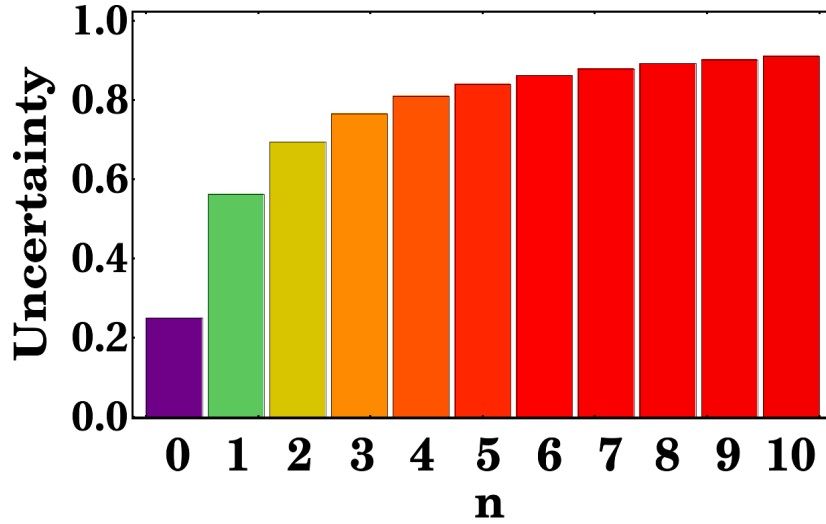
FIGURE 4.1: The product of uncertainties $(\Delta_{\inf} X_{\theta_1})^2 (\Delta_{\inf} X_{\theta_2})^2$ is plotted versus n for $m = 0$. The figure shows that the LG beam does not demonstrate steering through the Reid criterion.

by

$$
\begin{aligned}
h\left(\mathcal{X} \mid \mathcal{P}_{\mathcal{Y}}\right) &= h\left(\mathcal{X}, \mathcal{P}_{\mathcal{Y}}\right) - h\left(\mathcal{P}_{\mathcal{Y}}\right), \\
h\left(\mathcal{P}_{\mathcal{X}} \mid \mathcal{Y}\right) &= h\left(\mathcal{P}_{\mathcal{X}}, \mathcal{Y}\right) - h\left(\mathcal{Y}\right),
\end{aligned}
\tag{4.37}
$$

with

$$
\begin{aligned}
h\left(\mathcal{X}, \mathcal{P}_{\mathcal{Y}}\right) &= -\int_{-\infty}^{\infty} \mathcal{P}(X, P_Y) \ln \mathcal{P}(X, P_Y) \, dX \, dP_Y, \\
h\left(\mathcal{P}_{\mathcal{Y}}\right) &= -\int_{-\infty}^{\infty} \mathcal{P}(P_Y) \ln \mathcal{P}(P_Y) \, dP_Y,
\end{aligned}
\tag{4.38}
$$

and similarly for $h\left(\mathcal{P}_{\mathcal{X}}, \mathcal{Y}\right)$ and $h\left(\mathcal{Y}\right)$. The marginal probability distributions are obtained using the Wigner function (4.33) for the LG wave function.

For $n = 0$ and $m = 0$, the LG wave function becomes a separable state with the corresponding Wigner function given by

$$
W_{00}(X, P_X; Y, P_Y) = \frac{e^{-X^2 - Y^2 - P_X^2 - P_Y^2}}{\pi^2}.
\tag{4.39}
$$

In this case the relevant entropies are given by

$$h\left(\mathcal{X}, \mathcal{P_Y}\right) = h\left(\mathcal{P_X}, \mathcal{Y}\right) = \ln \pi e\,,$$

$$h\left(\mathcal{Y}\right) = h\left(\mathcal{P_Y}\right) = \frac{1}{2}\ln \pi e\,, \tag{4.40}$$

and hence, the entropic steering inequality becomes saturated, i.e.,

$$h(\mathcal{X}\,|\,\mathcal{P_Y}) + h(\mathcal{P_X}\,|\,\mathcal{Y}) = \ln \pi e\,. \tag{4.41}$$

For $n = 1$ and $m = 0$, the Wigner function has the form

$$W_{10}(X, P_X; Y, P_Y) = e^{-X^2 - Y^2 - P_X^2 - P_Y^2}\,\frac{(P_X - Y)^2 + (P_Y + X)^2 - 1}{\pi^2} \tag{4.42}$$

and the relevant entropies turn out to be

$$h\left(\mathcal{X}, \mathcal{P_Y}\right) = h\left(\mathcal{P_X}, \mathcal{Y}\right) \approx 2.41509\,,$$

$$h\left(\mathcal{Y}\right) = h\left(\mathcal{P_Y}\right) \approx 1.38774\,. \tag{4.43}$$

Hence, the entropic steering relation in this case becomes

$$h\left(\mathcal{X}\,|\,\mathcal{P_Y}\right) + h\left(\mathcal{P_X}\,|\,\mathcal{Y}\right) \approx 2.05471\,<\,\ln \pi e\,, \tag{4.44}$$

thus indicating the demonstration of steering of LG beam for $n = 1$ and $m = 0$. The non-Gaussian nature of the Wigner function for $n \geq 1$ enables demonstration of steering through the entropic criterion [Chowdhury et al., 2014]. For higher values of angular momentum, we have plotted the left-hand side of the entropic steering relation in Fig. 4.2. We can see that violation of the inequality becomes stronger for higher values of n [Chowdhury et al., 2014].

4.6.1.3   The Bell nonlocality of LG beams

Next, we want to study the Bell violation [Bell, 1964] of the LG wave function. In order to do so, here we use the Wigner transform $\Pi_{nm}(X, P_X; Y, P_Y)$ $[= \pi^2\,W_{nm}(X, P_X; Y, P_Y)$, where $W_{nm}(X, P_X; Y, P_Y)$ is given by Eq. (4.31)]
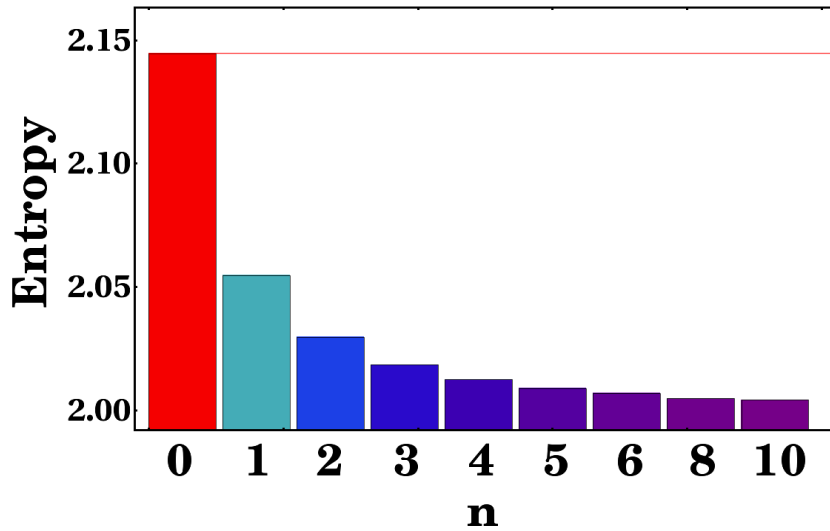
FIGURE 4.2: The figure shows the violation of the entropic steering inequality (4.36) for different values of n (except $n = 0$) of the LG wave function, keeping $m = 0$.

[Zhang et al., 2007]. In continuous variable systems, the Bell-Clauser-Horne-Shimony-Holt (Bell-CSHS) inequality can be written in terms of the Wigner transform as [Jeong et al., 2003]

$$
\begin{aligned}
|\mathcal{I}_\mathcal{B}| \;=\; & |\,\Pi_{n,m}(X_1, P_{X_1}; Y_1, P_{Y_1}) + \Pi_{n,m}(X_2, P_{X_2}; Y_1, P_{Y_1}) \\
& + \Pi_{n,m}(X_1, P_{X_1}; Y_2, P_{Y_2}) - \Pi_{n,m}(X_2, P_{X_2}; Y_2, P_{Y_2})\,| \;<\; 2\,. \quad (4.45)
\end{aligned}
$$

For $n = 0$ and $m = 0$, $|\mathcal{I}_\mathcal{B}| = 2$ and for $n > 1$, the amount of Bell violation increases with n, keeping $m = 0$. The Bell violation asymptotically reaches the maximum value $2\sqrt{2}$ of quantum mechanics when $n \to \infty$, as discussed in the previous chapter [Chowdhury, Majumdar, and Agarwal, 2013].

4.6.1.4 Comparison between the steerability and the nonlocality

Now, we shall make a comparison between the strength of steering and the degree of nonlocality of LG wave function, where the strength of steering is measured by the amount of violation of the steering inequality and the degree of nonlocality is measured by the amount of violation of the Bell's inequality. In the Table 4.1, we make comparison among the Bell violation, the entropic EPR steering, and the Reid EPR steering for different values of n keeping $m = 0$ [Chowdhury

n	$\frac{|\mathcal{I}_{\mathcal{B}_{\max}}|}{2}$	$\frac{\ln \pi e}{h(\mathcal{X}\,|\,\mathcal{P}_{\mathcal{Y}})+h(\mathcal{P}_{\mathcal{X}}\,|\,\mathcal{Y})}$	$4\,(\Delta_{\inf}\hat{X}_{\theta_1})^2\,(\Delta_{\inf}\hat{X}_{\theta_2})^2$
0	1	1	1
1	1.11934	1.04381	2.25
2	1.17437	1.0567	2.77778
3	1.20128	1.06256	3.0625
4	1.21738	1.06572	3.24
5	1.22813	1.06758	3.36111
6	1.23584	1.0687	3.44898
7	1.24165	1.06939	3.51563
8	1.24618	1.0698	3.5679
9	1.24982	1.07002	3.61
10	1.25281	1.07011	3.64463

TABLE 4.1: Comparison among the Bell violation, the entropic EPR steering, and the Reid EPR steering for different values of n with $m = 0$.

et al., 2014]. Here, $\frac{|\mathcal{I}_{\mathcal{B}_{\max}}|}{2} > 1$ signifies Bell violation, $\frac{\ln \pi e}{h(\mathcal{X}\,|\,\mathcal{P}_{\mathcal{Y}})+h(\mathcal{P}_{\mathcal{X}}\,|\,\mathcal{Y})} > 1$ signifies steering by the entropic steering criterion, and $4\,(\Delta_{\inf}\hat{X}_{\theta_1})^2\,(\Delta_{\inf}\hat{X}_{\theta_2})^2 < 1$ signifies steering through the Reid EPR steering criterion. From the first two columns of the table, one can note that both the maximum Bell violation and the steering through entropic criterion increase monotonically with n. On the other hand the last column provides values of the products of inferred variances, showing that the Reid criterion is unable to identify steering for any value of n in this case.

4.6.2 Photon-subtracted squeezed vacuum states

Non-Gaussian states can be prepared by the addition or subtraction of photons to or from the Gaussian states respectively. Here, we consider the particular class of non-Gaussian states obtained only by the subtraction of photons from the two mode entangled Gaussian state, i.e., NOPA state.

4.6.2.1 Formulation of photon-subtracted squeezed vacuum state and the corresponding Wigner function

First, we consider the two mode squeezed vacuum state, i.e., NOPA state given by the Eq. (4.10). This state is an entangled Gaussian state. The Wigner function associated with the state (4.10) is given by [Agarwal, 2013]

$$
W_{|\xi\rangle}(\alpha, \beta) = \frac{4}{\pi^2} \exp[-2\,|\,\alpha\,\cosh(r) - \beta^*\sinh(r)\,e^{i\phi}\,|^2 \\
- 2\,|-\alpha^*\sinh(r)\,e^{i\phi} + \beta\,\cosh(r)\,|^2\,], \qquad (4.46)
$$

which is normalized, i.e.,

$$
\int\int W_{|\xi\rangle}(\alpha, \beta)\, d^2\alpha\, d^2\beta = 1. \qquad (4.47)
$$

Here, α and β represent complex phase space displacements, and $\{x, k_x\}$, $\{y, k_y\}$ are conjugate quadrature observables. In terms of dimensionless quadratures $(X, P_X, Y,$ and $P_Y)$, α and β can be written as $\alpha = \frac{X + i\,P_X}{\sqrt{2}}$ and $\beta = \frac{Y + i\,P_Y}{\sqrt{2}}$, and with $\phi = 0$ the Wigner function becomes

$$
W_\xi(X, P_X; Y, P_Y) = \frac{1}{\pi^2} \exp[-2\,(P_X\,P_Y - X\,Y)\,\sinh 2r \\
- (X^2 + Y^2 + P_X^2 + P_Y^2)\,\cosh 2r\,]. \qquad (4.48)
$$

Here, it is clear that the correlations exist between X and Y, and P_X and P_Y. $\{X,\ P_X\}$ and $\{Y,\ P_Y\}$ are conjugate pairs of dimensionless quadratures.

Now, the subtraction of n photons from the state $|\xi\rangle$ (4.10) may be represented as

$$
|\xi_n\rangle = [\,a \otimes I + (-1)^k\,I \otimes b\,]^n\,|\xi\rangle, \qquad (4.49)
$$

where $k \in \{0, 1\}$, and it is assumed that one does not know from which mode the photon is subtracted. After proper normalization the state becomes $\sqrt{N_n}\,|\xi_n\rangle$, where the normalization constant N_n is given by $(N_n)^{-1} = \langle\xi_n\,|\,\xi_n\rangle$. The state $|\xi_n\rangle$ is the photon-subtracted squeezed vacuum state and it is a non-Gaussian state. The Wigner function of the state $|\xi_n\rangle$ is related to the Wigner function of the state $|\xi_{(n-1)}\rangle$ by

$$
W_n(\alpha, \beta) = \hat{\Lambda}(\alpha, \beta)\,W_{(n-1)}(\alpha, \beta), \qquad (4.50)
$$

where the operator $\hat{\Lambda}(\alpha, \beta)$ is given by

$$
\begin{aligned}
\hat{\Lambda}(\alpha, \beta) &= \left[\left(\alpha^* + \frac{1}{2}\frac{\partial}{\partial\alpha}\right)\left(\alpha + \frac{1}{2}\frac{\partial}{\partial\alpha^*}\right) + \left(\alpha^* + \frac{1}{2}\frac{\partial}{\partial\alpha}\right)\left(\beta + \frac{1}{2}\frac{\partial}{\partial\beta^*}\right)\right.\\
&\quad\left. + \left(\alpha + \frac{1}{2}\frac{\partial}{\partial\alpha^*}\right)\left(\beta^* + \frac{1}{2}\frac{\partial}{\partial\beta}\right) + \left(\beta^* + \frac{1}{2}\frac{\partial}{\partial\beta}\right)\left(\beta + \frac{1}{2}\frac{\partial}{\partial\beta^*}\right)\right].
\end{aligned}
$$

$$(4.51)$$

The Wigner function $W_n(\alpha, \beta)$ is obtained from $W(\alpha, \beta)$ given by the Eq. (4.46) by applying n times the operator $\hat{\Lambda}(\alpha, \beta)$, i.e.,

$$
W_n(\alpha, \beta) = \hat{\Lambda}^n(\alpha, \beta)\, W(\alpha, \beta), \tag{4.52}
$$

and normalizing suitably [$\int W_n(\alpha, \beta)\, \mathrm{d}^2\alpha\, \mathrm{d}^2\beta = 1$].

Now, if we consider that only single photon is reduced from each mode, i.e., by applying the operator $a \otimes I + (-1)^k I \otimes b$ on the state $|\xi\rangle$, the state (4.49) becomes

$$
|\xi_1\rangle = \sqrt{1 - \lambda^2}\, \sum \lambda^n\, \sqrt{n}\, \left[\,|n-1, n\rangle + (-1)^k\, |n, n-1\rangle\right] \tag{4.53}
$$

with the normalization constant $N_1 = \frac{1}{2\sinh^2(r)}$. The Wigner function for the above state is given by

$$
\begin{aligned}
W_1(\alpha, \beta) &= \frac{4}{\pi^2}\exp\left[2\left(\alpha\beta + \alpha^*\beta^*\right)\sinh(2r) - 2\left(|\alpha|^2 + |\beta|^2\right)\cosh(2r)\right]\\
&\quad\times\left[-\left\{2\left(\alpha\beta + \alpha^*\beta^*\right) + (-1)^k\left(\alpha^2 + \alpha^{*2} + \beta^2 + \beta^{*2}\right)\right\}\sinh(2r)\right.\\
&\quad\left. + 2\left\{|\alpha|^2 + |\beta|^2 + (-1)^k\left(\alpha\beta^* + \alpha^*\beta\right)\right\}\cosh(2r) - 1\right].
\end{aligned}
$$

$$(4.54)$$

In terms of the dimensionless quadratures $X, P_X, Y,$ and P_Y, the Wigner function for the single-photon-subtracted squeezed vacuum state becomes

$$
\begin{aligned}
W_1(X, P_X; Y, P_Y) &= \frac{1}{\pi^2}\exp\left[2\sinh(2r)\left(XY - P_X P_Y\right)\right.\\
&\quad\left. - \cosh(2r)\left(X^2 + Y^2 + P_X^2 + P_Y^2\right)\right]\\
&\quad\times\left[-\sinh(2r)\left\{P_X^2 - 2P_X P_Y + P_Y^2 - (X - Y)^2\right\}\right.\\
&\quad\left. + \cosh(2r)\left\{P_X^2 - 2P_X P_Y + P_Y^2 + (X - Y)^2\right\} - 1\right].
\end{aligned}
$$

$$(4.55)$$

It is clear from the form of the Wigner function that the state $|\xi_1\rangle$ is non-Gaussian in nature and there exist $\langle X Y \rangle \neq 0$ type correlations between the two modes. The Wigner function given above can be used to show the steerability and the nonlocality of this non-Gaussian state.

4.6.2.2 The steerability of the state $|\xi_1\rangle$

Now, we shall check the steerability of the single-photon-subtracted state through both the Reid criterion and the entropic steering criterion.

Steerability through the Reid criterion :

We have seen earlier that the Reid criterion is able to bring out the steering property of two mode squeezed vacuum state. Let us now see whether it is possible to demonstrate steering for single-photon-annihilated state (4.53) using the Reid criterion. The uncertainty for the inferred observables is in this case given by

$$
\begin{aligned}
(\Delta_{\text{inf}} X_\theta)^2 &= \cosh(2r) - \sinh(r)\cosh(r)\cos(2\theta) \\
&\quad - \frac{[\cosh(2r)\cos(\theta - \phi) - 2\sinh(2r)\cos(\theta + \phi)]^2}{4[\cosh(2r) - \sinh(r)\cosh(r)\cos(2\phi)]}. \quad (4.56)
\end{aligned}
$$

Calculating the minimum value of $(\Delta_{\text{inf}} X_\theta)^2$ for two different values of θ, i.e., for $\theta_1 = 0$ and $\theta_2 = \pi/2$, the product of uncertainties turns out to be

$$
(\Delta_{\text{inf}} X_{\theta_1})^2 (\Delta_{\text{inf}} X_{\theta_2})^2 = \frac{9}{2[3\cosh(4r) + 5]}, \quad (4.57)
$$

which goes to 0 for $r \to \infty$. But for $r \to 0$, the value of the product of uncertainties will be greater than $1/4$. In the Fig. 4.3(a), we have compared the amount of steerability of the NOPA state and the single-photon-annihilated NOPA state through the Reid criterion. We can see that the Reid criterion fails in the latter case for smaller values of the squeezing parameter r [Chowdhury et al., 2014].

Steerability through the entropic steering criterion :

Next, we shall use the entropic steering inequality to demonstrate the steerability of both the NOPA state and the photon-subtracted squeezed vacuum state. Considering the measurements corresponding to either position $(r = x)$ or momentum $(s = p)$, there exist nonvanishing $\langle X Y \rangle \neq 0$ type correlations for both of the state. So in terms of the dimensionless variables $(X, P_X, Y, \text{and } P_Y)$, the entropic
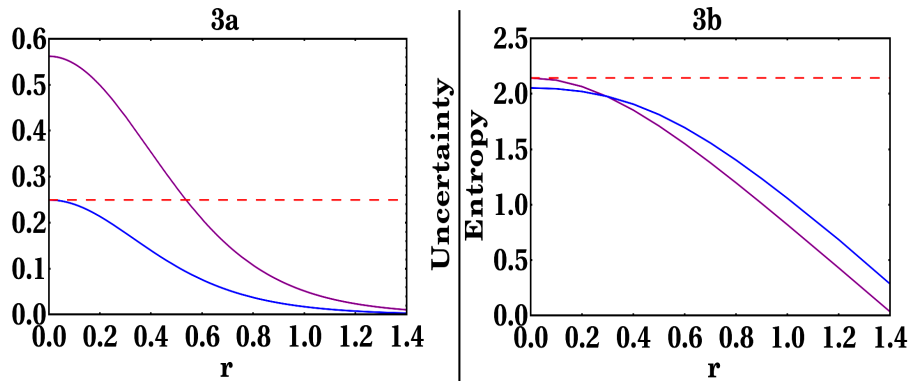
FIGURE 4.3: (a) The horizontal line represents the uncertainty bound below which steering is signified. The lower curve represents the product of inferred uncertainties for the two-mode squeezed vacuum state. Steering is demonstrated for all values of r through the Reid criterion. The upper curve represents the product of uncertainties for the photon-subtracted state. Clearly, the Reid criterion fails to show steering for smaller values of r in the latter case. (b) The horizontal line represents the bound $\ln \pi e$. The purple and blue curves represent the left-hand side of the entropic steering inequality for the squeezed state and the single-photon-subtracted squeezed state, respectively.

steering inequality (4.23) becomes

$$h\left(\mathcal{Y}\,|\,\mathcal{X}\right) + h\left(\mathcal{P}_{\mathcal{Y}}\,|\,\mathcal{P}_{\mathcal{X}}\right) \;\geq\; \ln \pi e \,, \tag{4.58}$$

where X, Y, P_X, and P_Y are the outcomes of measurements $\mathcal{X}$, $\mathcal{Y}$, $\mathcal{P}_{\mathcal{X}}$, and $\mathcal{P}_{\mathcal{Y}}$ respectively. Here, the conditional entropies $h\left(\mathcal{Y}\,|\,\mathcal{X}\right)$ and $h\left(\mathcal{P}_{\mathcal{Y}}\,|\,\mathcal{P}_{\mathcal{X}}\right)$ are given by

$$
\begin{aligned}
h\left(\mathcal{Y}\,|\,\mathcal{X}\right) &= h\left(\mathcal{X}, \mathcal{Y}\right) - h\left(\mathcal{X}\right), \\
h\left(\mathcal{P}_{\mathcal{Y}}\,|\,\mathcal{P}_{\mathcal{X}}\right) &= h\left(\mathcal{P}_{\mathcal{X}}, \mathcal{P}_{\mathcal{Y}}\right) - h\left(\mathcal{P}_{\mathcal{X}}\right),
\end{aligned} \tag{4.59}
$$

and calculated using the marginal probability distributions obtained from the corresponding Wigner functions [Eq. (4.48) and Eq. (4.55)]. One can thus calculate the left-hand side of the inequality (4.58) for the single-photon-subtracted state and the NOPA state for any value of the squeezing parameter $r > 0$. In Fig. 4.3(b), we have plotted the left-hand side of the entropic steering inequality versus r for the squeezed vacuum state as well as the single-photon-subtracted state. The figure shows that the violation of the steering inequality increases with r for each of these two states. Hence, it is clear from the Fig. 4.3 that the entropic

steering criterion is stronger than the Reid steering criterion [Chowdhury et al., 2014], as for smaller values r, the entropic criterion demonstrates the steerability of the single-photon-subtracted NOPA state, a feature which remains unable to be captured by the Reid criterion.

4.6.2.3 The Bell nonlocality of the state $|\xi_1\rangle$

First, we consider the Bell violation by the NOPA state, which has been studied earlier [Banaszek and Wodkiewicz, 1998]. In terms of the Wigner transform $\Pi(\alpha, \beta)$ $[= \frac{\pi^2}{4} W_{|\xi\rangle}(\alpha, \beta)]$ the Bell sum is given by [Banaszek and Wodkiewicz, 1998]

$$
\begin{aligned}
\mathcal{I}_\mathcal{B} &= \Pi(\alpha = 0, \beta = 0) + \Pi(\alpha = \sqrt{J}, \beta = 0) + \Pi(\alpha = 0, \beta = -\sqrt{J}) \\
&\quad - \Pi(\alpha = \sqrt{J}, \beta = -\sqrt{J}) \\
&= 1 + 2 \exp[-2J \cosh(2r)] \\
&\quad - \exp[-4J\{\cosh^2(r) - 2\cos(\phi)\cosh(r)\sinh(r) + \sinh^2(r)\}],
\end{aligned}
\tag{4.60}
$$

where J represents amount of displacement in the phase space. Here, we choose $\phi = 0$. By considering $r \to \infty$ [Banaszek and Wodkiewicz, 1998], the above expression becomes

$$
\mathcal{I}_\mathcal{B}(J, r) = 1 - \exp[-4J e^{2r}] + 2\exp[-J e^{2r}].
\tag{4.61}
$$

Particularly for the above choice of settings, $\mathcal{I}_\mathcal{B}$ will be maximum with the value 2.19055 [Banaszek and Wodkiewicz, 1998], which occurs for the constraints

$$
J \exp[2r] = \frac{1}{3} \ln 2,
\tag{4.62}
$$

where $J << 1$. For example, $\mathcal{I}_{\mathcal{B}\text{max}}$ $(= 2.19055)$ occurs for the choice of parameters $J = 0.00009467$ and $r = 3.9$. Next, we consider a more general choice of settings [Jeong et al., 2003; Olivares and Paris, 2004], where Alice measures either at α_1 or at α_2, and Bob measures either at β_1 or at β_2. For this general case, the Bell sum can be written as

$$
\mathcal{I}_\mathcal{B} = \Pi(\alpha_1, \beta_1) + \Pi(\alpha_1, \beta_2) + \Pi(\alpha_2, \beta_1) - \Pi(\alpha_2, \beta_2),
\tag{4.63}
$$

which leads to the maximum Bell violation $\mathcal{I}_{\mathcal{B}\mathrm{max}} = 2.32449$ for the choice of parameters $\alpha_1 = 0.0036990$, $\alpha_2 = -0.0115244$, $\beta_1 = -0.0039127$, $\beta_2 = 0.0113108$, and $r = 3.8853675$.

Now, to evaluate the Bell violation of the photon-subtracted squeezed vacuum states, we use the Wigner transform $\Pi_n(\alpha, \beta)$ $[= \frac{\pi^2}{4} W_n(\alpha, \beta)]$. Considering the more general choice of measurement settings given in the Eq. (4.63), the Bell sum using the above Wigner transform may be expressed as

$$\mathcal{I}_{\mathcal{B}n} = \Pi_n(\alpha_1, \beta_1) + \Pi_n(\alpha_1, \beta_2) + \Pi_n(\alpha_2, \beta_1) - \Pi_n(\alpha_2, \beta_2). \qquad (4.64)$$

We are interested to see whether the maximum Bell violation for this non-Gaussian state exceeds the maximum value obtained for the Gaussian state. So, to obtain the maximum Bell violation, one maximizes $\mathcal{I}_{\mathcal{B}n}$ over α_1, α_2, β_1, β_2, and r for a given value of n.

Considering single photon reduction from each mode, i.e., for $n = 1$, the corresponding single-photon-subtracted NOPA state and the corresponding Wigner function are given by the Eq. (4.53) and Eq. (4.54), respectively. For this case, the maximum Bell violation, i.e., $(\mathcal{I}_{\mathcal{B}1})_{\mathrm{max}} = -2.5444$ [Chowdhury et al., 2014] occurs for the choices $\alpha_1 = -0.0067$, $\alpha_2 = 0.0201$, $\beta_1 = 0.0067$, $\beta_2 = -0.0201$, $r = 3.0$, and $k = 1$. Now, comparing with the two-mode squeezed state where the Bell violation is -2.3245 [Jeong et al., 2003], it is seen that by photon annihilation, the maximum Bell violation increases. For the case of two photon subtraction from each mode $([a \otimes I + (-1)^k I \otimes b]^2)$, we can similarly obtain the maximum Bell violation, which turns out to be $(\mathcal{I}_{\mathcal{B}2})_{\mathrm{max}} = 2.6305$ [Chowdhury et al., 2014] for the choices $\alpha_1 = -0.1338$, $\alpha_2 = -0.1392$, $\beta_1 = -0.1365$, $\beta_2 = -0.1311$, $r = 4.4015$, and $k = 1$. We thus see that the maximum Bell violation increases further.

4.6.2.4   Comparison between the steerability and the nonlocality

In order to compare two types of correlations, we make the following table. In Table 4.2, Bell violation and the entropic EPR steering of both the NOPA state and the single-photon-subtracted NOPA state are compared for different values of r. Here, $\frac{|\mathcal{I}_{\mathcal{B}\mathrm{max}}|}{2} > 1$ signifies Bell violation, and $\frac{\ln \pi e}{h(\mathcal{Y}|\mathcal{X}) + h(\mathcal{P}_{\mathcal{Y}}|\mathcal{P}_{\mathcal{X}})} > 1$ identifies

State	r	Bell violation $(= \frac{|\mathcal{I}_{\mathcal{B}\max}|}{2})$	Entropic EPR steering criterion $(= \frac{\ln \pi e}{h(\mathcal{Y}|\mathcal{X}) + h(\mathcal{P_Y}|\mathcal{P_X})})$
$|\xi\rangle$	0	1.0	1.0
$|\xi\rangle$	0.2	1.040	1.038
$|\xi\rangle$	0.4	1.091	1.157
$|\xi\rangle$	0.6	1.125	1.383
$|\xi\rangle$	0.8	1.144	1.790
$|\xi\rangle$	1	1.153	2.616
$|\xi\rangle$	1.2	1.159	4.991
$|\xi\rangle$	1.4	1.160	62.737
$|\xi_1\rangle$	0	1.120	1.044
$|\xi_1\rangle$	0.2	1.189	1.061
$|\xi_1\rangle$	0.4	1.229	1.124
$|\xi_1\rangle$	0.6	1.252	1.264
$|\xi_1\rangle$	0.8	1.263	1.529
$|\xi_1\rangle$	1	1.267	2.027
$|\xi_1\rangle$	1.2	1.271	3.132
$|\xi_1\rangle$	1.4	1.271	7.531

TABLE 4.2: Comparison of the Bell violation with the entropic EPR steering for the NOPA state and the single-photon-annihilated NOPA state.

steering. One sees that although the magnitude of Bell violation reaches a maximum for a certain value of the squeezing parameter r, and subsequently decreases gradually, the strength of steering increases monotonically with r. Hence, it would be much easier to observe steering compared to Bell violation for higher values of r [Chowdhury et al., 2014].

4.6.3 NOON states

The maximally path-entangled number states have the form given by

$$|\psi\rangle = \frac{1}{\sqrt{2}} \left(|N\rangle_a |0\rangle_b + e^{i\phi}|0\rangle_a |N\rangle_b \right) . \qquad (4.65)$$

This is an example of a two-mode entangled state such that N photons can be found either in the mode a or in the mode b, and is referred to as a NOON state

[Lee, Kok, and Dowling, 2002]. The utility of NOON states in making precise interferometric measurements is of much importance in quantum metrology. Such states have been recently experimentally realized up to $N = 5$ [Afek, Ambar, and Silberberg, 2010]. The entanglement of NOON states is obtained in terms of the logarithmic negativity, viz. $E_N = 1$ [Agarwal, 2013], a value that remains constant with N.

The Wigner distribution function for the NOON states is given by [Wildfeuer, Lund, and Dowling, 2007]

$$W(\alpha, \beta) = \frac{2}{\pi^2} e^{-2|\alpha|^2 - 2|\beta|^2} \left[(-1)^N \left\{ L_N \left(4|\alpha|^2 \right) + L_N \left(4|\beta|^2 \right) \right\} \right.$$
$$\left. - \frac{2^{2N}}{N!} \left(\alpha^{*N} \beta^N + \alpha^N \beta^{*N} \right) \right], \qquad (4.66)$$

where for simplicity we choose $\phi = \pi$ and $L_N(x)$ is the Laguerre polynomial. In terms of the dimensionless quadratures $\{X, P_X\}$ and $\{Y, P_Y\}$ the Wigner function becomes

$$W(X, P_X; Y, P_Y) = \frac{1}{2\pi^2 N!} e^{-\left(X^2 + Y^2 + P_X^2 + P_Y^2 \right)}$$
$$\times \left[-2^N \left\{ (X + iP_X)^N (Y - iP_Y)^N \right. \right.$$
$$\left. + (X - iP_X)^N (Y + iP_Y)^N \right\}$$
$$+ (-1)^N N! \left\{ L_N \left[2 \left(X^2 + P_X^2 \right) \right] \right.$$
$$\left. \left. + L_N \left[2 \left(Y^2 + P_Y^2 \right) \right] \right\} \right].$$
$$(4.67)$$

The Bell-CHSH inequality

$$|\mathcal{I}_\mathcal{B}| = \Pi(\alpha, \beta) + \Pi(\alpha', \beta) + \Pi(\alpha, \beta') - \Pi(\alpha', \beta') \leq 2 \qquad (4.68)$$

is maximally violated with $\mathcal{I}_{\mathcal{B}\max} = -2.2387$, which occurs for $N = 1$, and the corresponding settings are $\alpha = -\beta = 0.0610285$, $\alpha' = -\beta' = -0.339053$. States with larger N do not violate the inequality (4.68). However, there are some other Bell-type inequalities [Wildfeuer, Lund, and Dowling, 2007] for six correlated events for which NOON states show the violation for any N.

From the expression of the Wigner function (4.67) for the NOON states, it is clear

that the nonvanishing correlations of the type $\langle XY \rangle \neq 0$ are present between the two modes of the entangled states and it is also clear about the non-Gaussian nature of the states. Using such correlations, the entropic steering inequality for the NOON states may be written as

$$h\left(\mathcal{Y} \,|\, \mathcal{X}\right) + h\left(\mathcal{P_Y} \,|\, \mathcal{P_X}\right) \;\geq\; \ln \pi e \,. \tag{4.69}$$

The conditional entropies $h\left(\mathcal{Y} \,|\, \mathcal{X}\right)$ and $h\left(\mathcal{P_Y} \,|\, \mathcal{P_X}\right)$ can be calculated with the help of the marginal probabilities obtained through the Wigner function (4.67), using which the left-hand side of the inequality (4.69) may be obtained for different values of N. It turns out that for $N = 1$, one gets

$$h\left(\mathcal{Y} \,|\, \mathcal{X}\right) + h\left(\mathcal{P_Y} \,|\, \mathcal{P_X}\right) \approx 2.05 \;<\; \ln \pi e \,, \tag{4.70}$$

thus violating the steering inequality. However, for $N = 2$, one gets $h\left(\mathcal{Y} \,|\, \mathcal{X}\right) + h\left(\mathcal{P_Y} \,|\, \mathcal{P_X}\right) \approx 2.25 > \ln \pi e$. Larger values of N will lead to further higher values of $h\left(\mathcal{Y} \,|\, \mathcal{X}\right) + h\left(\mathcal{P_Y} \,|\, \mathcal{P_X}\right)$, and hence, no steering is possible for $N > 1$, using the entropic steering relation.

In Fig. 4.4, we have plotted the joint probability $P(X, Y)$ for two different values of N, viz. $N = 1$ and $N = 4$, respectively. The higher peak of the $N = 1$ curve indicates stronger $\langle X, Y \rangle$ correlations responsible for steering in this case. The correlations weaken for larger values of N as is indicated by the lower peak value of the $N = 4$ curve, and are not sufficient for revealing steering through the entropic inequality. Thus, NOON states with $N = 1$ violate the entropic steering inequality, but for $N \geq 1$, these states are not steerable [Chowdhury et al., 2014]. This feature is similar to Bell violation for NOON states, which is revealed for $N = 1$, but the violation of the standard Bell-CHSH inequality does not occur for $N \geq 1$.

4.7 Limitations of the entropic steering inequality

To overcome the drawbacks of the Reid criterion for EPR-steering, the entropic steering inequality has been proposed by Walborn et al. [Walborn et al., 2011]. This criterion is able to demonstrate steering for many states having correlation
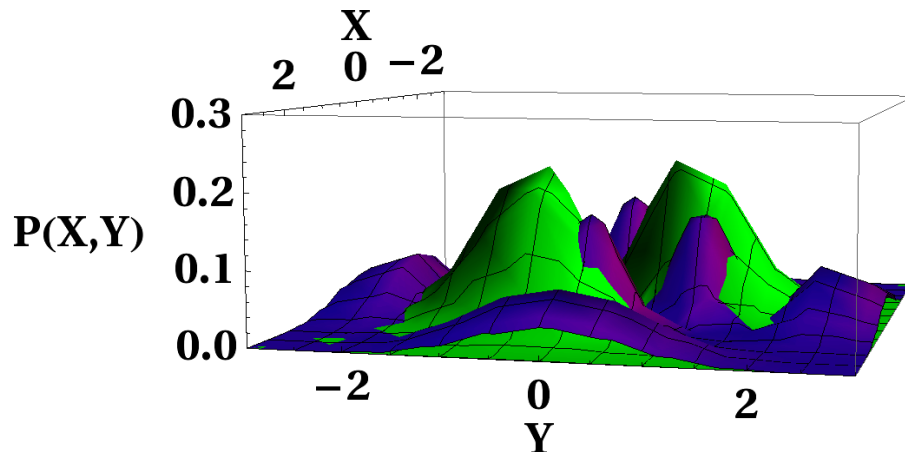
FIGURE 4.4: Correlations of the type $\langle X, Y \rangle$ responsible for steering using the entropic steering inequality are revealed through the joint probability distributions $P(X, Y)$. The figure shows that such correlations are sufficiently strong to admit steering for $N = 1$, but are significantly weakened for larger N.

higher than the second order. But it has also some limitations. As for example, it has the limitation to show steering of the NOON states only for $N = 1$. For $N > 1$, it is unable to detect steerability of the states [Chowdhury et al., 2014], whereas NOON states violate some Bell-type inequalities for any N. As the Bell violation certifies the steerability of the states, NOON states should be steerable for all N.

4.8 Summary

In this chapter, we have studied EPR steering by non-Gaussian continuous variable entangled states. Here, we have considered several examples of such systems, i.e., the two-dimensional harmonic oscillator, the photon-subtracted squeezed vacuum state, and the NOON states. Although such states are entangled pure states, we have shown that they fail to reveal steering through the Reid criterion for wide ranges of parameters. Steering with such states is demonstrated using the entropic steering inequality in terms of conditional entropies, indicating that it is a stronger criterion than that given by Reid. We have computed the relevant conditional entropies using the Wigner function, whose non-Gaussian nature plays an important role in demonstrating steering. For all the above examples, we have

performed a quantitative study of the strength of steering (determined by the magnitude of violation of the entropic steering inequality) as a function of the state parameters. This leads to some interesting observations, especially in comparison with the magnitude of Bell nonlocality demonstrated by these states.

For the LG modes, one sees that the steering strength increases with the increase of the angular momentum n, a feature that is also common to the Bell violation. However, for both the two-mode squeezed vacuum state and the single-photon-subtracted state derived from it, we have shown that the behaviours of the maximum Bell violation and steering strength versus the squeezing parameter are not similar. This is evident from the fact that although the maximum Bell violation peaks for a certain value of r, the steering strength rises monotonically with increasing r. This feature clearly establishes the fact that although Bell violation guarantees steerability, the two types of quantum correlation are distinct from each other. Moreover, the presence of quantum correlations in such class of states may be more easily detected through the violation of the entropic steering inequality compared to the violation of the Bell inequality for higher values of squeezing. Finally, we have studied steering by NOON states. Here, steering through the entropic criterion is revealed only for $N = 1$, although the entanglement of such states remains independent of N. This shows that entanglement is a different correlation compared to steering, as it is also different compared to Bell nonlocality. The above results should be useful for detecting and manipulating correlations in non-Gaussian states for practical purposes in different arenas such as information processing, quantum metrology, and Bose condensates. Further work on the issue of the recently proposed symmetric steering framework [Schneeloch et al., 2013] may be of interest using non-Gaussian resources.

Chapter 5

Stronger steerability criterion in continuous-variable systems

The uncertainty principle introduces a sharp distinction between quantum and classical physics. The presence of uncertainty relations endows quantum mechanics with significant advantages over classical mechanics for performing different information processing tasks such as teleportation, dense coding, etc. Uncertainty relations are linked directly to the ability of quantum states to enable steering. The phenomenon of quantum steering [Schrödinger, 1935, 1936] emerges from the EPR paradox [Einstein, Podolsky, and Rosen, 1935] that was first formulated for experimental realization [Reid, 1989] based on the Heisenberg uncertainty relation. Subsequently, a number of improved uncertainty relations [Bialynicki-Birula and Mycielski, 1975; Maassen and Uffink, 1988; Oppenheim and Wehner, 2010; Robertson, 1929; Schrödinger, 1930; Wehner and Winter, 2010] introduce various kinds of stronger steering criteria. Nonetheless, there exist states such as the NOON states which fail to display steering using the existing steering criteria for higher values of N in spite of violating Bell-type inequalities [Bell, 1964; Clauser et al., 1969]. Such a feature calls for further improved steerability conditions since steering lies between entanglement and nonlocality in the hierarchy [Wiseman, Jones, and Doherty, 2007] of quantum correlations.

The tightest steering inequality in discrete-variable systems is obtained [Pramanik, Kaplan, and Majumdar, 2014] through the application of the fine-grained uncertainty relation (FUR) [Oppenheim and Wehner, 2010]. Fine-graining makes it

possible to distinguish the uncertainty inherent in obtaining any particular combination of outcomes for different measurements. In this Chapter, we shall derive the fine-grained uncertainty relation, the corresponding steering inequality, and security of continuous-variable systems.

5.1   Wigner function

Wigner function can be used for computing various probabilities associated with continuous variables in phase space. There exists an analogy between the measurement of spin-1/2 projectors and the parity operator, since the measurement outcomes for both are dichotomic. It is well known [Banaszek and Wodkiewicz, 1998, 1999] that the Wigner function, expressed as an expectation value of a product of displaced parity operators, can be used to derive Bell-CHSH inequalities [Bell, 1964; Clauser et al., 1969] for continuous variables. In this chapter, we shall use the Wigner function formalism [Banaszek and Wodkiewicz, 1998, 1999] to derive a steering inequality for continuous variables.

5.2   Choice of appropriate observables for continuous-variable systems

To derive fine-grained steering inequality, it is necessary to choose observables, which will be appropriate for continuous-variable states. For this, here we choose displaced parity observables and the usefulness of these observables in deriving steering inequality and the ability to show steering of non-Gaussian entangled states will be shown later. Here, we label the outcome of even parity measurement by "0". The corresponding projection operator is given by

$$\Pi^+(\beta) \;\; = \;\; \mathcal{D}(\beta) \left(\sum_{n=0}^{\infty} |2n\rangle \langle 2n| \right) \mathcal{D}^\dagger(\beta) \,, \tag{5.1}$$

where $\mathcal{D}(\beta)$ ($= \exp\{ \beta \, \hat{b}^\dagger - \beta^* \, \hat{b} \}$), is the displacement operator with coherent displacement β, and $\hat{b}$ and $\hat{b}^\dagger$ are the annihilation and creation operators, respectively. Similarly, the projection operator corresponding to the odd parity measurement

outcome labeled by "1" is given by

$$\Pi^-(\beta) \;=\; \mathcal{D}(\beta)\left(\sum_{n=0}^{\infty}|2n+1\rangle\,\langle 2n+1|\right)\mathcal{D}^\dagger(\beta). \qquad (5.2)$$

The observable associated with the Wigner function is given by $\hat{\mathcal{W}}(\beta) = \Pi^+(\beta) - \Pi^-(\beta)$ which can be realized using detectors with the capability of distinguishing the number of absorbed photons [Banaszek and Wodkiewicz, 1998, 1999]. We will take β's to be real displacements in the rest of this chapter.

5.3 Example of fine-grained uncertainty relation in discrete-variable systems

The concept of fine-graining in uncertainty relations was first introduced by Oppenheim and Wehner [Oppenheim and Wehner, 2010] to explain the failure of quantum theory to exhibit the full non-local strength allowed by no-signaling theory. They bound an event (which is defined by the outcomes chosen using imposed restrictions or conditions) by its minimum possible uncertainty, or maximum possible certainty, for two incompatible observables. For single qubit system, fine-grained uncertainty relation (FUR) can be explained by the following game [Oppenheim and Wehner, 2010]. A binary question $q \in \{0, 1\}$ is received by a player, say, Bob randomly. According to the question $q = 0$ (1), he measures σ_z (σ_x) observable on his system B, which is prepared in the state ρ_B. Here, the average uncertainty of getting a particular outcome, say, spin up outcome (labeled by "$b = 0$") irrespective of the given question (or indeed, the average certainty) where the average is taken over all possible choice of measurements, is bounded by

$$\frac{1}{2} - \frac{1}{2\sqrt{2}} \;\leq\; \frac{1}{2}\left[\,P(b_{\sigma_z}=0) + P(b_{\sigma_x}=0)\,\right] \;\leq\; \frac{1}{2} + \frac{1}{2\sqrt{2}}, \qquad (5.3)$$

where the equalities occur for maximally certain states. Here they are the eigenstates of the observables $(\sigma_z + \sigma_x)/\sqrt{2}$ and $(\sigma_z - \sigma_x)/\sqrt{2}$ for the upper and lower bounds, respectively. The bounds remain the same for the spin down outcome ("$b = 1$").

5.4   Formulation of the fine-grained uncertainty relation in continuous-variable systems

In continuous-variable systems, Bell's inequality is shown to be violated using the Wigner function formalism [Banaszek and Wodkiewicz, 1998, 1999]. Fine-graining connects uncertainty with nonlocality, and hence for a given Bell-CHSH inequality one can formulate a FUR for a bipartite system [Oppenheim and Wehner, 2010]. Similar considerations hold true for single particle quantum systems, thus making it possible to construct a FUR for single systems using the Wigner distribution representing the average of displaced parity measurement.

The average certainty of the parity measurement outcome b over displacements α and β is given by $\frac{1}{2}[P(b_\alpha) + P(b_\beta)]$. Similar to the case of discrete variables, the average certainty is bounded by the minimum uncertainty states. In continuous variable systems it is well known that the coherent states

$$|\gamma\rangle = \exp[-\frac{|\gamma|^2}{2}] \sum_{m=0}^{\infty} \frac{\gamma^m}{\sqrt{m!}} |m\rangle \tag{5.4}$$

correspond to the minimum uncertainty states in phase-space. Therefore, we obtain the fine-grained bounds on $\frac{1}{2}[P(b_\alpha) + P(b_\beta)]$ using the coherent states.

For even parity measurement $(b = 0)$ at the displacement chosen from $\{\alpha, \beta\}$, the average certainty becomes

$$
\begin{aligned}
\frac{1}{2}[P(b_\alpha = 0) + P(b_\beta = 0)] &= \langle\gamma| \frac{\Pi^+(\alpha) + \Pi^+(\beta)}{2} |\gamma\rangle \\
&= \frac{1}{2}\big(\exp[-|\gamma-\alpha|^2]\cosh[|\gamma-\alpha|^2] \\
&\quad + \exp[-|\gamma-\beta|^2]\cosh[|\gamma-\beta|^2]\big), \tag{5.5}
\end{aligned}
$$

where, similar to the displacements α and β, we choose γ also to be real. Here, the condition $\alpha = \beta \to \gamma$ needs to be excluded in order to ensure that the average certainty of getting even parity for the zero photon state does not always stay close to 1, which is similar to getting, say, spin up outcome in discrete variables for spin measurements along directions $\hat{i}$ and $\hat{j}$ when $\hat{i} \to \hat{j}$. For simplification we henceforth set $\alpha = -\beta$, and compute the probability distribution $[P(b_\beta = 0) + P(b_{-\beta} = 0)]$. The probability distribution $[P(b_\beta = 0) + P(b_{-\beta} = 0)]$ is bounded by $[\frac{1}{2}, \frac{3}{4}]$, where the maximum occurs for $\beta = \gamma$. Similarly, the average

certainty of odd parity measurements for the displacements β and $-\beta$ is bounded by

$$
\begin{aligned}
\frac{1}{2}\left[P(b_\beta = 1) + P(b_{-\beta} = 1)\right] &= \langle\gamma|\frac{\Pi^-(\beta) + \Pi^-(-\beta)}{2}|\gamma\rangle \\
&= \frac{1}{2}\left(\exp[-|\gamma - \beta|^2]\sinh[|\gamma - \beta|^2]\right. \\
&\quad \left. + \exp[-|\gamma + \beta|^2]\sinh[|\gamma + \beta|^2]\right). \text{ (5.6)}
\end{aligned}
$$

Hence, one gets $\frac{1}{4} \leq \frac{1}{2}\left[P(b_\beta = 1) + P(b_{-\beta} = 1)\right] \leq \frac{1}{2}$, except at $\gamma \to 0$ and $\beta \to 0$ for which the probability of getting odd counts for the zero photon state approaches zero as shown in the Fig. (5.1).

Combining the cases of odd and even parities, one finds that the FUR bounds the certainty for the measurement of two incompatible continuous-variable observables by

$$
\frac{1}{4} \leq \frac{1}{2}\left[P(b_\beta) + P(b_{-\beta})\right] \leq \frac{3}{4}. \tag{5.7}
$$

In the Fig. (5.1), we have plotted the infimum value of $\frac{1}{2}\left[P(b_\beta) + P(b_{-\beta})\right]$ with γ. When $\beta \to 0$, the FUR (5.7) remains valid for $|\gamma^2| \geq 1$, i.e., for a source with at least a single average photon number. Here, we only need to avoid the situation when $\gamma \to 0$ and $\beta \to 0$ simultaneously. It is clear that the range of certainty in discrete-variable systems given by Eq. (5.3) [Pramanik, Kaplan, and Majumdar, 2014] is higher than that in continuous-variable systems [Chowdhury, Pramanik, and Majumdar, 2015]. This feature, reflecting more uncertainty, helps to improve the secret key rate, since higher uncertainty enables less information to the eavesdropper.

5.5 Fine-grained steering criterion through the violation of local hidden state model

Before going to the derivation of the fine-grained steering criterion for continuous-variable systems, let us first begin with a brief description of EPR-steering by considering the following game [Wiseman, Jones, and Doherty, 2007] between two parties, say, one is Alice and the other is Bob. Alice prepares two systems A and B in the state ρ_{AB} and sends the system B to Bob. Alice's task is to convince
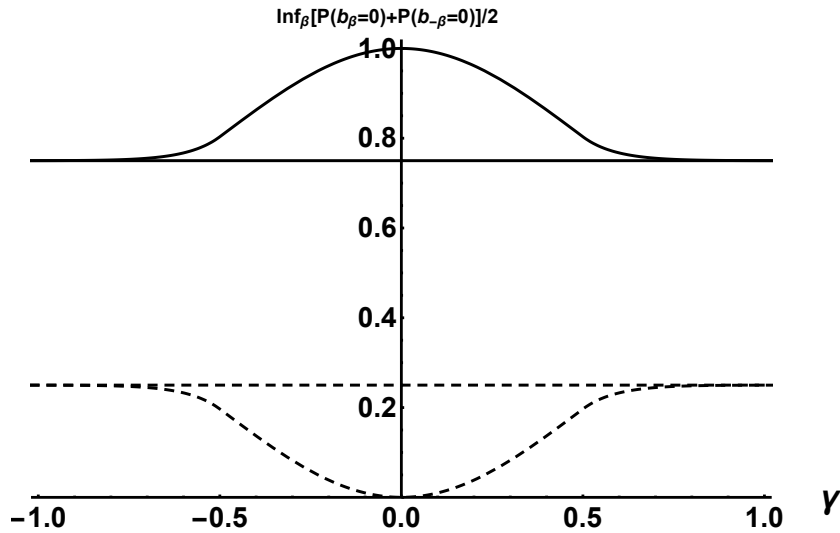
FIGURE 5.1: Plot of $\frac{1}{2}\inf_\beta[P(b_\beta = 0) + P(b_{-\beta} = 0)]$ with γ. The solid curve is for $\frac{1}{2}\max_\beta[P(b_\beta = 0) + P(b_{-\beta} = 0)]$, and the dashed curve is for $\frac{1}{2}\min_\beta[P(b_\beta = 1) + P(b_{-\beta} = 1)]$. The solid and dashed lines correspond, respectively, to the upper and lower bounds of certainty in regions of validity of the FUR (5.7).

Bob that the prepared state ρ_{AB} is entangled. Bob does not trust Alice, but he trusts that he receives a quantum system B. He is convinced only when the correlation between his outcome b for the measurement chosen randomly from the set $\mathcal{B} \in \{\beta_1, \beta_2\}$ and Alice's outcome a for the measurement chosen randomly from the set $\mathcal{A} \in \{\alpha_1, \alpha_2\}$ can not be explained by a local hidden state (LHS) model, i.e., the joint probability $P(a_\mathcal{A}, b_\mathcal{B})$ can not be written as the following form

$$P(a_\mathcal{A}, b_\mathcal{B}) \;=\; \sum_\lambda P(\lambda)\, P(a_\mathcal{A} \,|\, \lambda)\, P_Q(b_\mathcal{B} \,|\, \lambda)\,, \tag{5.8}$$

where $P(\lambda)$ is a positive valued distribution over a set of hidden variables λ with $\sum_\lambda P(\lambda) = 1$, and P_Q denotes probability of an outcome obtained from a quantum measurement. We assume here that Alice knows about Bob's set of observables.

Now, from Eq. (5.8) it is easy to derive the relation

$$P(b_\mathcal{B} \,|\, a_\mathcal{A}) \;\leq\; \max_\lambda\left[\, P_Q(b_\mathcal{B} \,|\, \lambda)\,\right] \;=\; P_Q(b_\mathcal{B} \,|\, \lambda_{\max}) \tag{5.9}$$

using $\sum_i x_i y_i \leq \max_i[x_i] \sum_i y_i \, \forall \, \{x_i, y_i\} \geq 0$. Next, using $\sum_i x_i y_i \geq \min_i[x_i] \sum_i y_i$ $\forall \, \{x_i, \, y_i\} \geq 0$, we get

$$P(b_{\mathcal{B}} \,|\, a_{\mathcal{A}}) \;\geq\; \min_{\lambda} \left[\, P_Q(b_{\mathcal{B}} \,|\, \lambda) \, \right] \;=\; P_Q(b_{\mathcal{B}} \,|\, \lambda_{\min}) \;. \tag{5.10}$$

Combining the relations (5.9) and (5.10), the sum of conditional probability distributions according to the LHS model is bounded by

$$
\begin{aligned}
\min_{\beta_1, \beta_2} \left[\, P_Q(b_{\beta_1} \,|\, \lambda_{\min}) + P_Q(b_{\beta_2} \,|\, \lambda_{\min}) \, \right] \;&\leq\; P(b_{\beta_1} \,|\, a_{\alpha_1}) + P(b_{\beta_2} \,|\, a_{\alpha_2}) \\
&\leq\; \max_{\beta_1, \beta_2} \left[\, P_Q(b_{\beta_1} \,|\, \lambda_{\max}) + P_Q(b_{\beta_2} \,|\, \lambda_{\max}) \, \right].
\end{aligned}
\tag{5.11}
$$

In order to obtain the bounds of the algebraic inequality (5.11), we shall use the new uncertainty relation, just formulated. The validity of the inequality (5.11) is ensured by avoiding the region where both $\beta \to 0$ and $\gamma \to 0$, as shown in the Fig. (5.1). In case of discrete-variable systems, using the uncertainty relation (5.3), the inequality (5.11) is bounded by $\left[1 - \frac{1}{\sqrt{2}}, 1 + \frac{1}{\sqrt{2}} \right]$. The bounds remains the same for spin down outcome ("$b = 1$") also. Hence, the shared state is steerable if the value of $\frac{1}{2} \left[P(b_{\sigma_z}) + P(b_{\sigma_x}) \right]$ lies outside the above range [Pramanik, Kaplan, and Majumdar, 2014], where Alice has prior knowledge of Bob's measurement settings.

Now, using the FUR (5.7), the steering inequality (5.11) for continuous-variable systems becomes

$$\frac{1}{4} \;\leq\; \frac{1}{2} \left[\, P(b_{\beta} \,|\, a_{\alpha_1}) + P(b_{-\beta} \,|\, a_{\alpha_2}) \, \right] \;\leq\; \frac{3}{4} \;. \tag{5.12}$$

The violation of the inequality (5.12) indicates that the measurement correlations are unable to be explained with the help of a LHS model, i.e., the given state is steerable [Chowdhury, Pramanik, and Majumdar, 2015]. In the next section, we shall provide an application of our derived steering inequality for NOON states.

5.6   Steerability of NOON states

NOON states [Lee, Kok, and Dowling, 2002] are regarded to be of high utility in quantum metrology for making precise interferometric measurements. Such a state is a maximally path-entangled two-mode number state of continuous variables,

given by [Agarwal, 2013]

$$| \text{N00N} \rangle = \frac{1}{\sqrt{2}} (| N, 0 \rangle - | 0, N \rangle), \tag{5.13}$$

where N is the number of photons either in the first or the second mode. These states have been experimentally realized up to $N = 5$ [Afek, Ambar, and Silberberg, 2010]. The entanglement of NOON states given in terms of their logarithmic negativity is independent of the value of N, and Bell's inequality is maximally violated for all N [Wildfeuer, Lund, and Dowling, 2007]. However, they do not violate the entropic steering inequality for $N \geq 2$ [Chowdhury et al., 2014]. Now, we can check whether such states are steerable for $N \geq 2$ using our derived steering inequality.

Considering the cases for N even and odd separately, we find that for the former the maximum violation of the inequality (5.12) on the upper side occurs when $\frac{1}{2} [P(b_\beta | a_{\alpha_1}) + P(b_{-\beta} | a_{\alpha_2})] = 1$ for the choices of the parameters given by $\{b = 0, a = 0\}$, $\{b = 0, a = 1\}$. Similarly, the maximum violation on the lower side occurs when $\frac{1}{2} [P(b_\beta | a_{\alpha_1}) + P(b_{-\beta} | a_{\alpha_2})] = 0$ for the choices of the parameters give by $\{b = 1, a = 0\}$, $\{b = 1, a = 1\}$. When N is odd, the maximum violations on the upper side are 1 for the choices $\{b = 0, a = 1\}$, $\{b = 1, a = 0\}$, and on the lower side they are 0 for the choices $\{b = 0, a = 0\}$, $\{b = 1, a = 1\}$.

In the Fig. (5.2), we have plotted the quantity $\frac{1}{2} [P(b_\beta = 0 | a_\alpha = 1) + P(b_{-\beta} = 0 | a_{-\alpha} = 1)]$ versus β and α for $N = 2$, 4, and 6. One sees that the violation of the steering inequality occurs maximally for $N \geq 2$ in the region $| \beta | \to 0$ [Chowdhury, Pramanik, and Majumdar, 2015]. The condition for the validity of our FUR, viz. $| \gamma | \geq 1$ when $\beta \to 0$, is ensured since the average photon number ($N/2$ here) is greater than 1.

5.7 Security of key generation

Steering finds direct applicability in demonstration of security of quantum key distribution (QKD). The goal of any QKD protocol is to generate a key string between two distant parties, say, Alice and Bob such that it remains secret from an eavesdropper, say, Charlie. In the first QKD protocol (BB84) proposed by Bennett and Brassard [Bennett and Brassard, 1984], security is based on the uncertainty
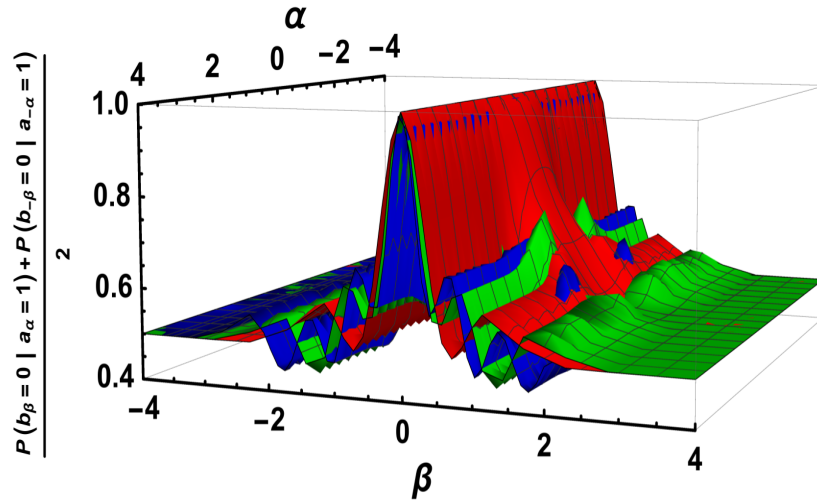
FIGURE 5.2: The variation of $\frac{1}{2}\left[P(b_\beta = 0 \,|\, a_\alpha = 1) + P(b_{-\beta} = 0 \,|\, a_{-\alpha} = 1)\right]$ with respect to β and α for three different values of N. (i) The red colored curve corresponds to the value $N = 2$; (ii) the green colored curve is for $N = 4$; (iii) and the blue colored curve is for $N = 6$.

of the outcome of incompatible spin measurements chosen randomly along x- and z-directions. The security of standard QKD protocols is based on certain idealistic assumptions [Gisin et al., 2002; Scarani et al., 2009] that may be minimized in the so-called device independent QKD (DIQKD) [Acin et al., 2007; Barrett, Hardy, and Kent, 2005; Gisin, Pironio, and Sangouard, 2010; Masanes, Pironio, and Acin, 2011; Mayers and Yao, 1998], where it is no longer required to fully trust the devices used by Alice and Bob. However, practical and loophole free implementations of DIQKD protocols are difficult since they require demonstration of nonlocality. On the other hand, 1s-DIQKD [Branciard et al., 2012; Tomamichel and Renner, 2011] protocols, which are intermediate between standard QKD and DIQKD protocols, rely on demonstration of quantum steering for their security. Continuous-variable 1s-DIQKD protocols have attracted attention in recent times since they are reasonably robust to losses and practically more feasible compared to their discrete-variable counterparts [Walk, Wiseman, and Ralph, 2014].

5.7.1   Derivation of monogamy relation associated with the new steering inequality

Monogamy of non-local correlations certifies the security of QKD [Barrett, Kent, and Pironio, 2006; Barrett et al., 2005; Masanes, Acin, and Gisin, 2006]. To develop a monogamy relation associated with the upper bound of our steering inequality (5.12), let us consider that three parties Alice, Bob, and Charlie share a tripartite state ρ_{ABC} for which the inequality

$$\frac{1}{2}\left(\Sigma_{BA} + \Sigma_{BC}\right) \;\leq\; \frac{3}{2} \tag{5.14}$$

is satisfied, where $\Sigma_{BA} = P(b_{\beta_1}\,|\,a_{\alpha_1}) + P(b_{\beta_2}\,|\,a_{\alpha_2})$ and $\Sigma_{BC} = P(b_{\beta_1}\,|\,c_{\gamma_1}) + P(b_{\beta_2}\,|\,c_{\gamma_2})$, and c is Charlie's outcome for the measurement chosen from the set $\{\gamma_1, \gamma_2\}$. The proof comes from contradiction. Let $\frac{1}{2}\left(\Sigma_{BA} + \Sigma_{BC}\right) > \frac{3}{2}$. The above sum can be written as the sum of $\left[\,P(b_{\beta_1}\,|\,a_{\alpha_1}) + P(b_{\beta_2}\,|\,c_{\gamma_2})\,\right]$ and $\left[\,P(b_{\beta_1}\,|\,c_{\gamma_1}) + P(b_{\beta_2}\,|\,a_{\alpha_2})\,\right]$. As the average of the above two terms is greater than $3/2$, one of the terms, say, the first, is greater than $3/2$. Then, it is possible to find a conditional Bob's state for which $\left[\,P(b_{\beta_1}) + P(b_{\beta_2})\,\right] > 3/2$, which contradicts the FUR given by the inequality (5.7). Similarly, using the lower bound of our steering inequality (5.12), one can obtain $\frac{1}{2}\left(\Sigma_{BA} + \Sigma_{BC}\right) \geq \frac{1}{2}$, which together with the relation (5.14) gives

$$\frac{1}{2} \;\leq\; \frac{1}{2}\left(\Sigma_{BA} + \Sigma_{BC}\right) \;\leq\; \frac{3}{2}. \tag{5.15}$$

Here, the upper bound of the monogamy relation $(3/2)$ [Chowdhury, Pramanik, and Majumdar, 2015] is useful for calculation of the lower bound of the secret key rate as will be shown in the next section.

5.7.2   Lower bound of the secret key rate

The monogamy relation (5.14) is used to bound the secret key rate in a 1s-DIQKD protocol. The lower bound of the secret key rate under individual attack is given by [Csiszàr and Körner, 1978]

$$r \;\geq\; \mathcal{I}(B:A) - \mathcal{I}(B:C)\,, \tag{5.16}$$

where $\mathcal{I}$ is the mutual information. Suppose that the upper bound of the steering inequality (5.12) is violated by an amount δ, i.e., $\frac{1}{2} \left[P(b_{\beta_1} \,|\, a_{\alpha_1}) + P(b_{\beta_2} \,|\, a_{\alpha_2}) \right] = \frac{3}{4} + \delta$, where $0 < \delta \leq \frac{1}{4}$. Then, the monogamy relation (5.14) implies that $\frac{1}{2} \left[P(b_{\beta_1} \,|\, c_{\gamma_1}) + P(b_{\beta_2} \,|\, c_{\gamma_2}) \right] \leq 0.75 - \delta$. Hence, the lower bound of the key rate becomes

$$ r \;\; \geq \;\; \log_2 \left[\frac{0.75 + \delta}{0.75 - \delta} \right], \tag{5.17} $$

where the logarithm of base 2 is taken since the secret key rate is expressed in the units of bits per shared state. For the maximally entangled NOON states for which $\delta = 1/4$, the steering inequality (5.12) is maximally violated, making the lower bound of the secret key rate unity [Chowdhury, Pramanik, and Majumdar, 2015]. One may note here that in comparison the lower bound for discrete variables is 1/2 [Pramanik, Kaplan, and Majumdar, 2014]. Hence, the use of continuous-variable systems in QKD offers more security in principle.

5.8 Summary

To summarize, in this chapter first we have derived a fine-grained uncertainty relation (FUR) for continuous-variable systems with the help of an operational interpretation of the Wigner function [Banaszek and Wodkiewicz, 1998, 1999]. The FUR provides a manifestation of higher uncertainty in continuous-variable systems than in discrete-variable systems. The increment of uncertainty in continuous-variable systems restricts the amount of information leakage to the eavesdropper, making them more secure in principle, than discrete-variable systems. Bob is convinced of the prepared state being entangled only when the average of the conditional probabilities is larger than $1/2 + 1/(2\sqrt{2})$ [Pramanik, Kaplan, and Majumdar, 2014] for discrete-variable systems, whereas, in continuous-variable systems it is 3/4. Hence, our steering inequality is also stronger than that of discrete-variable systems. Further, we have shown that our steering inequality is capable of detecting maximal steerability by NOON states for $N \geq 2$, thereby circumventing a drawback of the entropic steering inequality which is not violated by the NOON states for $N \geq 2$ [Chowdhury et al., 2014].

With the help of the derived monogamy relation corresponding to our steering inequality, we have bounded the key rate in the 1s-DIQKD protocol secured under

individual attacks. The relation of the Wigner function with displaced parity operators [Banaszek and Wodkiewicz, 1998, 1999] facilitates comparison of the key rates in continuous and discrete variables. The lower bound of the secret key rate is unity for the shared maximally entangled state of continuous variables, which is double that for discrete variables [Pramanik, Kaplan, and Majumdar, 2014] even when Alice knows Bob's set of observables before preparation of the state. Knowing Bob's set of observables does not help Alice to cheat here, whereas it is indeed helpful in discrete-variable systems [Pramanik, Kaplan, and Majumdar, 2014]. The quasi-probability distributions contained in our steering inequality may be reconstructed experimentally by homodyne detection techniques that are currently realizable with high efficiency [Wakui et al., 2007]. Recent experiments [D'Angelo et al., 2006; Jeong et al., 2003; Kuzmich, Walmsley, and Mandel, 2000] have indeed confirmed Bell violation in continuous-variable systems using similar techniques. It should thus be feasible to experimentally verify our steering inequality. Further analysis of more general security attacks, as well as consideration of decoherence effects would be needed to assess the practical viability of such key generation protocols.

Chapter 6

Conclusions and future directions

The practical realization of non-Gaussian states are easier rather than that of perfect Gaussian states. These non-Gaussian states are more efficient in studying different quantum mechanical properties. In this thesis, nonlocality of non-Gaussian states which is higher compared to the Gaussian states has been studied. In this chapter, we have briefly summarized the important results obtained in this thesis and discussed some possible future directions.

In the second chapter, we have examined the weak equivalence principle of gravity at the quantum level. We have provided two ways of examination using a non-Gaussian wave packet controlled by a tunable parameter. First, the position detection probabilities of particles described by our tunable non-Gaussian wave-packet projected upwards against gravity around the classical turning point and also around the point of initial projection are calculated. These probabilities exhibit mass dependence at both these points, thereby reflecting the quantum violation of the weak equivalence principle [Chowdhury et al., 2012]. Secondly, we have calculated the mean arrival time of freely falling particles using the quantum probability current, which also turns out to be mass dependent [Chowdhury et al., 2012]. Such a mass dependence is shown to be enhanced by increasing the non-Gaussianity parameter of the wave packet, thus signifying a stronger violation of the weak equivalence principle [Chowdhury et al., 2012] through a greater departure from Gaussianity of the initial wave packet. The mass dependence of both the position detection probabilities and the mean arrival time vanish in the limit of large mass. Thus, compatibility between the weak equivalence principle and quantum mechanics is recovered in the macroscopic limit of the latter. We

have also exhibited a selection of Bohm trajectories to illustrate these features in the free fall case using our non-Gaussian wave packet [Chowdhury et al., 2012]. It should be noted that the validity of this work is confined to non-relativistic quantum mechanics. The use of our special kind of non-Gaussian wave packet can facilitate the experimental verification of the violation of WEQ and can also verify the quantitative departure of the violation of WEQ from that obtained using Gaussian nature of the wave packet.

In the third chapter, we have provided an example of non-locality in classical optics. Here, we have considered optical beams with topological singularities which possess Schmidt decomposition and shown that such classical beams share many features of two mode entanglement in quantum optics. We have demonstrated the coherence properties of such beams through the violations of Bell inequality for continuous variables using the Wigner function. This violation is a consequence of correlations between the (x, p_x) and (y, p_y) spaces which mathematically play the same role as nonlocality in quantum mechanics. The Bell violation for the Laguerre-Gaussian beams is shown to increase with higher orbital angular momenta l of the vortex beam [Chowdhury, Majumdar, and Agarwal, 2013]. This increase is reminiscent of enhancement of nonlocality for many particle Greenberger-Horne-Zeilinger states or for higher spins. The states with large l can be easily produced using spatial light modulators. The increase of nonlocality is again proved by the corresponding increase of the quadrature correlation function [Chowdhury, Majumdar, and Agarwal, 2013]. It is possible to experimentally realize the predicted values of the correlation function as a function of the beam parameters. As two-point correlation functions are used in our Bell's inequality, shear Sagnac interferometry [Iaconis and Walmsley, 1996; Singh et al., 2006; Zhang and Mukamel, 2007] may be used to verify experimentally our predicted Bell violation and its enhancement for vortex beams with higher angular momentum.

Non-Gaussian states have correlations higher than second order and to detect that correlation, one needs some detection criterion that contains higher order terms. As an example of this and in view of the increasing importance of non-Gaussian entangled states in quantum information protocols like teleportation and violations of Bell's inequalities, the steering of continuous-variable non-Gaussian entangled states is investigated in the fourth chapter. The EPR steering for Gaussian states may be demonstrated through the violation of the Reid inequality

[Einstein, Podolsky, and Rosen, 1935] involving products of the inferred variances of non-commuting observables. However, for arbitrary states the Reid inequality is not always sufficient because of the higher order correlations in such states [Chowdhury et al., 2014]. One then needs to use the entropic steering inequality [Walborn et al., 2011]. We have examined several classes of currently important non-Gaussian entangled states, such as the two-dimensional harmonic oscillator, the photon subtracted two mode squeezed vacuum, and the NOON states, with the motivation to investigate EPR-steering of such states [Chowdhury et al., 2014]. This should stimulate steering experiments using non-Gaussian states. We have presented a comparative study of the violation of the Bell-inequality and steering strength for these states. Both the Bell violation and steering strength increase with the angular momentum of LG modes. For both the two-mode squeezed vacuum state and the single-photon-subtracted two-mode squeezed vacuum state, we have shown that steering strength can detect better the inherent entanglement than Bell violation. NOON states are steerable for $N = 1$ only using the entropic steering relation, whereas the entanglement of such states is same for all N. This again shows that entanglement, steering, and Bell nonlocal correlations are different from each other [Chowdhury et al., 2014]. The above results should be useful for detecting and manipulating correlations in non-Gaussian states for practical purposes in different arenas such as information processing, quantum metrology, and Bose condensates. Further work on the issue of the recently proposed symmetric steering framework [Schneeloch et al., 2013] may be of interest using non-Gaussian resources.

In the fifth chapter, we have described how a stronger uncertainty relation will provide a correspondingly stronger steering inequality. Here, we have derived a fine-grained uncertainty relation for the measurement of two incompatible observables on a single quantum system of continuous variables using the operational definition of Wigner function, and have shown that continuous-variable systems are more uncertain than discrete-variable systems [Chowdhury, Pramanik, and Majumdar, 2015]. Using the derived fine-grained uncertainty relation, we have formulated a new steering criterion for continuous-variable systems and have given an application of this for NOON states. Entropic steering criterion is able to demonstrate steerability of NOON states for $N = 1$ only [Chowdhury et al., 2014]. But using our derived steering criterion, we are able to reveal the steerability of NOON states for all $N > 1$ that has hitherto not been possible using other criteria [Chowdhury, Pramanik, and Majumdar, 2015]. Therefore, our fine-grained steering criterion is

stronger than previously existing ones. We further obtain a monogamy relation for our steering inequality which leads to an, in principle, improved lower bound on the secret key rate of a one-sided device independent quantum key distribution protocol for continuous variables under individual attacks. By considering Alice's knowledge about Bob's set of observables, we have calculated the lower bound of the secret key rate as unity [Chowdhury, Pramanik, and Majumdar, 2015] for the shared maximally entangled state of continuous variables, whereas the lower bound is just half for discrete variables. We have used the Wigner function as quasiprobability distribution, which can be experimentally reconstructed by homodyne detection techniques that are currently realizable with high efficiency [Wakui et al., 2007]. Recently, experimental Bell violation is also confirmed [D'Angelo et al., 2006; Jeong et al., 2003; Kuzmich, Walmsley, and Mandel, 2000] using similar techniques for continuous-variable systems. Therefore, this should facilitate the experimental verification of our steering criterion. Further analysis of more general security attacks, as well as consideration of decoherence effects would be needed to assess the practical viability of such key generation protocols.

Bibliography

Acin, A., Brunner, N., Gisin, N., Massar, S., Pironio, S. and Scarani, V., Phys. Rev. Lett. **98**, 230501 (2007).

Adunas, G. Z., Milla, E. R. and Ahluwalia, D. V., Gen. Rel. Grav. **33**, 183 (2001).

Afek, I., Ambar, O. and Silberberg, Y., Science **328**, 879 (2010).

Agarwal, G. S., *Quantum optics* (Cambridge University Press, Cambridge, 2013).

Agarwal, G. S. and Banerji, J., Opt. Lett. **27**, 800 (2002).

Aiello, A. and Woerdman, J. P., Phys. Rev. Lett. **94**, 090406 (2005).

Ali, M. A., Majumdar, A. S., Home, D. and Pan, A. K., Class. Quantum Grav. **23**, 6493 (2006).

Aspect, A., Dalibard, J. and Roger, G., Phys. Rev. Lett. **49**, 1804 (1982).

Aspect, A., Grangier, P. and Roger, G., Phys. Rev. Lett. **47**, 460 (1981).

Aspect, A., Grangier, P. and Roger, G., Phys. Rev. Lett. **49**, 91 (1982).

Banaszek, K. and Wódkiewicz, K., Phys. Rev. A **58**, 4345 (1998).

Banaszek, K. and Wódkiewicz, K., Phys. Rev. Lett. **82**, 2009 (1999).

Bandres, M. A. and Gutierrez-Vega, J. C., Opt. Express **16**, 21087 (2008).

Barrett, J., Hardy, L. and Kent, A., Phys. Rev. Lett. **95**, 010503 (2005).

Barrett, J, Kent, A. and Pironio, S., Phys. Rev. Lett. **97**, 170409 (2006).

Barrett, J., Linden, N., Massar, S., Pironio, S., Popescu, S. and Roberts, D., Phys. Rev. A **71**, 022101 (2005).

Beigersbergen, M. W., et al., Opt. Commun. **96**, 123 (1993).

Bell, J. S., Physics (Long Island City, N.Y.) **1**, 195 (1964).

Bennett, C. H. and Brassard, G., in : Proceedings of IEEE International Conference on Computers, Systems and Signal Processing, Bangalore, India, pp. 175-179 (1984).

Bennett, C. H., Brassard, G., Crépeau, C. and Maurer, U.M., in : IEEE Trans. Information th., **41**, 1915 (1995).

Berta, M., Christandl, M., Colbeck, R., Renes, J. M. and Renner, R., Nat. Phys. **6**, 659 (2010).

Bialynicki-Birula, I. and Mycielski, J., Commun. Math. Phys. **44**, 129 (1975).

Biswas, A. and Agarwal, G. S., New. J. Phys. **7**, 211 (2005).

Bohm, D., Phys. Rev. **85**, 166 (1952); **85**, 180 (1952).

Bohm, D., Phys. Rev. **89**, 458 (1953).

Bonse, U. and Wroblewski, T., Phys. Rev. Lett. **51**, 1401 (1983).

Borges, C. V. S., Hor-Meyll, M., Huguenin, J. A. O. and Khoury, A. Z., Phys. Rev. A **82**, 033833 (2010).

Branciard, C., Cavalcanti, E. G., Walborn, S. P., Scarani, V. and Wiseman, H. M., Phys. Rev. A **85**, 010301(R) (2012).

Braunstein, S. L. and Loock, P. van, Rev. Mod. Phys. **77**, 513 (2005).

Cavalcanti, E. G., Jones, S. J., Wiseman, H. M. and Reid, M. D., Phys. Rev. A **80**, 032112 (2009).

Chowdhury, P., Home, D., Majumdar, A. S., Mousavi, S. V., Mozaffari, M. R. and Sinha, S., Class. Quantum Grav. **29** 025010 (2012).

Chowdhury, P., Majumdar, A. S. and Agarwal, G. S., Phys. Rev. A **88**, 013830 (2013).

Chowdhury, P., Pramanik, T. and Majumdar, A. S., Phys. Rev. A **92**, 042317 (2015).

Chowdhury, P., Pramanik, T., Majumdar, A. S. and Agarwal, G. S., Phys. Rev. A **89**, 012104 (2014).

Clauser, J.F., Horne, M.A., Shimony, A. and Holt, R. A., Phys. Rev. Lett. **23** 880 (1969).

Cohen, L., *Time-frequency analysis: theory and applications* (Prentice-Hall, Upper Saddle River, NJ, 1995).

Colella, R., Overhauser, A. W. and Werner, S. A., Phys. Rev. Lett. **34**, 1472 (1975).

Csiszàr, I. and Körner, J., IEEE Trans. Inf. Theory **24**, 339 (1978).

Damborenea, J. A., Egusquiza, I. L. and Muga, J. G., Am. J. Phys. **70**, 738 (2002).

Danakas, S. and Aravind, P. K., Phys. Rev. A **45**, 1973 (1992).

D'Angelo, M., Zavatta, A., Parigi, V. and Bellini, M., Phys. Rev. A **74**, 052114, (2006).

Das, S. K. and Sengupta, S., Curr. Sci. **83**, 1234 (2002).

Davies, P. C. W., Class. Quantum Grav. **21**, 2761 (2004).

Deutsch, D., Phys. Rev. Lett. **50**, 631 (1983).

Deutsch, D., Ekert, A., Jozsa, R., Macchiavello, C., Popescu, S. and Sanpera, A., Phys. Rev. Lett. **77**, 2818 (1996).

Devetak, I. and Winter, A., Proc. R. Soc. A **461**, 207 (2005).

Dey, A., Pramanik, T. and Majumdar, A. S., Phys. Rev. A **87**, 012120 (2013).

Drummond, P. D. and Reid, M. D., Phys. Rev. A **41**, 3930 (1990).

Dumont, R. S. and Marchioro, T. L. II, Phys. Rev. A **47**, 85 (1993).

Durnin, J., Miceli, Jr., J. J. and Eberly, J. H., Phys. Rev. Lett. **58**, 1499 (1987).

Einstein, A., Podolsky, B. and Rosen, N., Phys. Rev. **47**, 777 (1935).

Ekert, A. K., Phys. Rev. Lett. **67**, 661 (1991).

Eötvös, R. V., Math. Nat. Ber. Ungarn. **8**, 65 (1890).

Eötvös, R. V., Pekar, V. and Fekete, E., Ann. Phys. (NY) **68**, 11 (1922).

Evans, D. A., Cavalcanti, E. G. and Wiseman, H. M., Phys. Rev. A **88**, 022106 (2013).

Everett, H., *The theory of the universal wavefunction* (Princeton University Press, Princeton, 1973).

Fickler, R., et al., Science **338**, 640 (2012).

Ford, G. W. and O'Connell, R. F., Am. J. Phys. **70**, 319 (2002).

Furrer, F., Franz, T., Berta, M., Leverrier, A., Scholz, V. B., Tomamichel, M. and Werner, R. F., Phys. Rev. Lett. **109**, 100502 (2012).

Gago, A. M., Nunokawa, H. and Funchal, R. Z., Phys. Rev. Lett. **84**, 4035 (2000).

Galilei, G., *Discorsi Intorno a due Nuove Scienze*(Elsevier, Leiden, 1638) [English translation edited by Crew, H. and Salvio, A. de, (Macmillan, New York, 1914) pp. 212-213].

Garces-Chavez, V., et al., Nature (London) **419**, 145 (2002).

Gasperini, M., Phys. Rev. D **38**, 2635 (1988).

Ghose, P. and Mukherjee, A., Rev. Theor. Sci. **2**, 274-288 (2014).

Gillet, J., Bastin, T. and Agarwal, G. S., Phys. Rev. A **78**, 052317 (2008).

Gisin, N. and Peres, A., Phys. Lett. A **162**, 15 (1992).

Gisin, N., Pironio, S. and Sangouard, N., Phys. Rev. Lett. **105**, 070501 (2010).

Gisin, N., Ribordy, G., Tittel, W. and Zbinden, H., Rev. Mod. Phys. **74**, 145 (2002).

Greenberger, D. M., Ann. Phys. **47**, 116 (1968).

Greenberger, D. M., Rev. Mod. Phys. **55**, 875 (1983).

Greenberger, D. M. and Overhauser, A. W., Rev. Mod. Phys. **51**, 43 (1979).

Grobe, R., Rzazewski, K. and Eberly, J. H., J. Phys. B **27**, L503 (1994).

Grosshans, F. and Grangier, P., Phys. Rev. Lett. **88**, 057902 (2002).

Hahne, G. E., J. Phys. A: Math. Gen. **36**, 7149 (2003).

Halprin, A. and Leung, C. N., Phys. Rev. D **53**, 5365 (1996).

He, Q. Y., Drummond, P. D., Olsen, M. K. and Reid, M. D., Phys. Rev. A **86**, 023626 (2012).

He, Q. Y., Reid, M. D., Vaughan, T. G., Gross, C., Oberthaler, M. and Drummond, P. D., Phys. Rev. Lett. **106**, 120405 (2011).

Heisenberg, W., Z. Phys. **43**, 172 (1927).

Holland, P., *The Quantum Theory of Motion* (Cambridge University Press, London, 1993), pp. 259-266.

Home, D. and Majumdar, A. S., Phys. Rev. A **52**, 4959 (1995).

Horodecki, R., Horodecki, P., Horodecki, M. and Horodecki, K., Rev. Mod. Phys. **81**, 865 (2009).

Iaconis, C. and Walmsley, I. A., Opt. Lett. **21**, 1783 (1996).

Ivan, J. Solomon, et al., Phys. Rev. A **83**, 032118 (2011).

Jeong, H., Son, W., Kim, M. S., Ahn, D. and Brukner, C., Phys. Rev. A **67**, 012106 (2003).

Jha, A. K., Agarwal, G. S. and Boyd, R. W., Phys. Rev. A **84**, 063847 (2011).

Jones, S. J., Wiseman, H. M. and Doherty, A. C., Phys. Rev. A **76**, 052116 (2007).

Kagalwala, K. H., et al., Nat. Photonics **7**, 72 (2013).

Kennard, E. H., Z. Phys. **44**, 326 (1927).

Kraus, K., Phys. Rev. D **35**, 3070 (1987).

Krauss, L. M. and Tremaine, S., Phys. Rev. Lett. **60**, 176 (1988).

Kuzmich, A., Walmsley, I. A., and Mandel, L., Phys. Rev. Lett. **85**, 1349 (2000).

Law, C. K., Walmsley, I. A. and Eberly, J. H., Phys. Rev. Lett. **84**, 5304 (2000).

Leach, J., et al., Science **329**, 662 (2010).

Leavens, C. R., Phys. Lett. A **178**, 27 (1993).

Leavens, C. R., The tunneling-time problem for electrons *Bohmian Mechanics and Quantum Theory: An Appraisal* ed Cushing, J., Fine, A. and Goldstein, S., (Kluwer, Dordrecht, 1996), pp. 111.

Leavens, C. R., Phys. Rev. A **58**, 840 (1998).

Leavens, C. R., *Bohm Trajectory Approach to Timing Electrons Time in Quantum Mechanics* ed Muga, J. G., Sala, R. and Egusquiza, I. L., (Springer, Berlin, 2002).

Lee, H., Kok, P. and Dowling, J. P., J. Mod. Opt. **49**, 2325 (2002).

Lee, N., et al., Science **332**, 330 (2011).

Li, C., Xu, J., Xu, X., Li, K. and Guo, G.-C., Nat. Phys. **7**, 752 (2011).

Lloyd, S. and Braunstein, S. L., Phys. Rev. Lett. **82**, 1784 (1999).

Maassen, H. and Uffink, J. B. M., Phys. Rev. Lett. **60**, 1103 (1988).

Majumdar, A. S. and Nayak, N., Phys. Rev. A **64**, 013821 (2001).

Mal, S., Pramanik, T. and Majumdar, A. S., Phys. Rev. A **87**, 012105 (2013).

Masanes, L., Acin, A. and Gisin, N., Phys. Rev. A. **73**, 012112 (2006).

Masanes, L., Pironio, S. and Acin, A., Nat. Comm. **2**, 238 (2011).

Mayers, D. and Yao, A., in : Proceedings of the 39th IEEE Conference on Foundations of Computer Science, IEEE, Los Alamitos, pp. 503 (1998).

McMorran, B. J., et al., Science **331**, 192 (2011).

Mermin, N. D., Phys. Rev. Lett. **65**, 1838 (1990).

Mitri, F. G., Ann. Phys. (N.Y.) **323**, 1604 (2008).

Molina-Terriza, G., Torres, J. P. and Torner, L., Nat. Phys. **3**, 305 (2007).

Mureika, J. R., Phys. Rev. D **56**, 2408 (1997).

Nha, H., Phys. Rev. A **76**, 014305 (2007).

Nielsen, M. A. and Chuang, I. L., *Quantum Computation and Information* (Cambridge University Press, Cambridge, 2000).

Nye, J. F. and Berry, M. V., Proc. R. Soc. London A **336**, 165 (1974).

Olivares, S. and Paris, M. G. A., Phys. Rev. A **70**, 032112 (2004).

Olsen, M. K. and Corney, J. F., Phys. Rev. A **87**, 033839 (2013).

Opanchuk, B., He, Q. Y., Reid, M. D. and Drummond, P. D., Phys. Rev. A **86**, 023625 (2012).

Opatrny, T., Kurizki, G. and Welsch, D.-G., Phys. Rev. A **61**, 032302 (2000).

Oppenheim, J. and Wehner, S., Science **330**, 1072 (2010).

Ou, Z. Y., Pereira, S. F., Kimble, H. J. and Peng, K. C., Phys. Rev. Lett. **68**, 3663 (1992).

Padmanabhan, H. and Padmanabhan, T., Phys. Rev. D **84**, 085018 (2011).

Peres, A., Am. J. Phys. **48**, 552 (1980).

Peters, A., Chung, K. Y. and Chu, S., Nature **400**, 849 (1999).

Pramanik, T., Chowdhury, P. and Majumdar, A. S., Phys. Rev. Lett. **110**, 020402 (2013).

Pramanik, T., Kaplan, M. and Majumdar, A. S., Phys. Rev. A **90**, 050305(R) (2014).

Pramanik, T. and Majumdar, A. S., Phys. Rev. A **85**, 024103 (2012).

Prevedel, R., Hamel, D. R., Colbeck, R., Fisher, K. and Resch, K. J., Nat. Phys. **7**, 757 (2011).

Qian, X-F., Broadbent, C. J. and Eberly, J. H., New J. Phys. **16**, 013033 (2014).

Qian, X-F. and Eberly, J. H., Opt. Lett. **36**, 4110 (2011).

Reid, M. D., Phys. Rev. A **40**, 913 (1989).

Renes, J. M. and Boileau, J. C., Phys. Rev. Lett. **103**, 020402 (2009).

Robertson, H. P., Phys. Rev. **34**, 163 (1929).

Robinett, R. W., Doncheski, M. A. and Bassett, L. C., Found. Phys. Lett. **18**, 455 (2005).

Roncaglia, M., Montorsi, A. and Genovese, M., Phys. Rev. A **90**, 062303 (2014).

Roy, S. M. and Singh, V., Phys. Rev. Lett. **67**, 2761 (1991).

Saleh, B. E. A. and Teich, M. C., *Fundamentals of Photonics* (Wiley, New Jersey, 2007), pp. 48.

Saunders, D. J., Jones, S. J., Wiseman, H. M. and Pryde, G. J., Nat. Phys. **6**, 845 (2010).

Scarani, V., Bechmann-Pasquinucci, H., Cerf, N. J., Dusek, M., Lutkenhaus, N. and Peev, M., Rev. Mod. Phys. **81**, 1301 (2009).

Schneeloch, J., Broadbent, C. J. and Howell, J. C., Phys. Lett. A **378**, 766 (2014).

Schneeloch, J., Broadbent, C. J., Walborn, S. P., Cavalcanti, E. G. and Howell, J. C., Phys. Rev. A **87**, 062103 (2013).

Schrödinger, E., Proc. Cambridge Philos. Soc. **31**, 553 (1935).

Schrödinger, E., Proc. Cambridge Philos. Soc. **32**, 446 (1936).

Schrödinger, E., Sitzungsber. Preuss. Akad. Wiss., Phys. Math. Kl. **14**, 296 (1930).

Seshadreesan, K. P., Dowling, J. P. and Agarwal, G. S., Phys. Scr. **90**, 074029 (2015).

Simon, B. N., Simon, S., Gori, F., Santarsiero, M., Borghi, R., Mukunda, N. and Simon, R., Phys. Rev. Lett. **104**, 023901 (2010).

Simon, R., Phys. Rev. Lett. **84**, 2726 (2000).

Simon, R. and Agarwal, G. S., Opt. Lett. **25**, 1313 (2000).

Singh, R. P., et al., J. Mod. Opt. **53**, 1803 (2006).

Sperling, J. and Vogel, V., Phys. Scr. **83**, 045002 (2011).

Sperling, J. and Vogel, W., Phys. Rev. A **79**, 042337 (2009).

Spreeuw, R. J. C., Found. Phys. **28**, 361 (1998).

Steinlechner, S., Bauchrowitz, J., Eberle, T. and Schnabel, R., Phys. Rev. A **87**, 022104 (2013).

Takahashi, H., et al., Nature Photonics **4**, 178 (2010).

Tara, K. and Agarwal, G. S., Phys. Rev. A **50**, 2870 (1994).

Tatarskii, V. I., Sov. Phys. Usp. **26**, 311 (1983).

Tomamichel, M. and Renner, R., Phys. Rev. Lett. **106**, 110506 (2011).

Verbeeck, J., Tian, H. and Schattschneider, P., Nature (London) **467**, 301 (2010).

Verrier, N., et al., JOSA A **25**, 1459 (2008).

Viola, L. and Onofrio, R., Phys. Rev. D **55**, 455 (1997).

Wakui, K., Takahashi, H., Furusawa, A. and Sasaki, M., Optics Express **15**, 3568 (2007).

Walborn, S. P., Salles, A., Gomes, R. M., Toscano, F. and Ribeiro, P. H. Souto, Phys. Rev. Lett. **106**, 130402 (2011).

Walk, N., Wiseman, H. M. and Ralph, T. C., arXix: 1405.6593 [quant-ph] (2014).

Weedbrook, C., et al., Rev. Mod. Phys. **84**, 621 (2012).

Wehner, S. and Winter, A., New J. Phys. **12**, 025009 (2010).

Weyl, H., *Gruppentheorie und Quantenmechanik* (Hirzel, Leipzig, 1928).

Wigner, E.P., Phys. Rev. **40**, 749 (1932).

Wildfeuer, C. F., Lund, A. P. and Dowling, J. P., Phys. Rev. A **76**, 052101 (2007).

Wiseman, H. M., Jones, S. J. and Doherty, A. C., Phys. Rev. Lett. **98**, 140402 (2007).

Zhang, L., Mukamel, E., Walmsley, I. A., Silberhorn, Ch., U'Ren, A. B. and Banaszek, K., in *Quantum Information with Continuous Variables of Atoms and Light*, edited by Serf, N. J., Leuchs, G. and Polzik, E. S. (Imperial College Press, London, 2007), pp. 375.

Zhang, L., et al., J. Mod. Opt. **54**, 707 (2007).